AD_____

Award Number: DAMD17-99-1-9010

TITLE: Angiostatic Therapy: A New Treatment Modality for Prostate Cancer

PRINCIPAL INVESTIGATOR: Per Borgstrom

CONTRACTING ORGANIZATION: Sidney Kimmel Cancer Center
San Diego, California 92126

REPORT DATE: July 2001

TYPE OF REPORT: Final

PREPARED FOR: U.S. Army Medical Research and Materiel Command
Fort Detrick, Maryland 21702-5012

DISTRIBUTION STATEMENT: Approved for Public Release;
Distribution Unlimited

The views, opinions and/or findings contained in this report are those of the author(s) and should not be construed as an official Department of the Army position, policy or decision unless so designated by other documentation.

REPORT DOCUMENTATION PAGE

Form Approved
OMB No. 074-0188

1. AGENCY USE ONLY (Leave blank)	2. REPORT DATE	3. REPORT TYPE AND DATES COVERED
	July 2001	Final (1 Jan 99 - 30 Jun 01)

4. TITLE AND SUBTITLE
Angiostatic Therapy: A New Treatment Modality for Prostate Cancer

5. FUNDING NUMBERS
DAMD17-99-1-9010

6. AUTHOR(S)
Per Borgstrom

7. PERFORMING ORGANIZATION NAME(S) AND ADDRESS(ES)
Sidney Kimmel Cancer Center
San Diego, California 92126

E-Mail: pborgstrom@skcc.org

8. PERFORMING ORGANIZATION REPORT NUMBER

9. SPONSORING / MONITORING AGENCY NAME(S) AND ADDRESS(ES)
U.S. Army Medical Research and Materiel Command
Fort Detrick, Maryland 21702-5012

10. SPONSORING / MONITORING AGENCY REPORT NUMBER

11. SUPPLEMENTARY NOTES
Report contains color

12a. DISTRIBUTION / AVAILABILITY STATEMENT
Approved for Public Release; Distribution Unlimited

12b. DISTRIBUTION CODE

13. Abstract *(Maximum 200 Words)* *(abstract should contain no proprietary or confidential information)*

The overall goal of this project is to investigate if blockade of vascular endothelial growth factor combined with conventional cytotoxic agents could be a **new innovative treatment regimen** for hormone-refractory prostate cancer. This was to be achieved with human prostate cancer tissue and established cell lines in a xenograft chamber model. Using soluble-flt and chemotherapy regimens, combinatorial strategies for prostate cancer were to be examined. During the first 18-month period, the growth and angiogenesis of three human prostate tumor cell lines transduced with a Histone H2B GFP fusion protein (DU145, PC3, and LnCAP) were evaluated using an intravital microscopic system in nude mice. Unlike other human carcinoma cell lines, the human prostate carcinoma cell lines regressed rapidly in the chamber model, with poor angiogenesis, massive apoptosis and little mitotic activity. Tumorigenic potential could only be be rescued with prostate stroma and diversion of the innate immune system. The goals of our proposed SOW could not be achieved with this artificial model. A pseudo-orthotopic syngeneic system was therefore developed using the TRAMP-C2 H2BGFP model with anterior murine prostate tissue in the chamber model. These hybrid tumorspheroids became fully vascularized and grew progressively over a 4-week period, with low mitotic indices, low cell death and a highly invasive phenotype. Using this model we identified surgical castration, COX-2 inhibition and dendritic cell based immunotherapy as effective mono and combined therapies for prostate carcinoma.

14. SUBJECT TERMS

15. NUMBER OF PAGES
133

16. PRICE CODE

17. SECURITY CLASSIFICATION OF REPORT	18. SECURITY CLASSIFICATION OF THIS PAGE	19. SECURITY CLASSIFICATION OF ABSTRACT	20. LIMITATION OF ABSTRACT
Unclassified	Unclassified	Unclassified	Unlimited

Table of Contents

INTRODUCTION

The overall goal of this project was to investigate if blockade of vascular endothelial growth factor (VEGF) in combination with conventional cytotoxic agents could be a new innovative treatment regimen for hormone-refractory prostate cancer. We had proposed to evaluate the angiogenic potential of tumor tissues derived from human prostate cancer thin needle biopsies and compare with established prostate cancer cell lines. Examine the capacity of a soluble VEGF receptor fusion protein (flt-IgG) to inhibit angiogenesis and growth, using our *in vivo* model designed for quantitative studies of the microvascular changes associated with the implantation of micro tumors. We also had proposed to evaluate combination treatments, combining the flt-IgG with Estramustine phosphate and Taxol to assess effective curative strategies for prostate cancer biopsy xenografts.

BODY

KEY RESEARCH ACCOMPLISHMENTS: In our original application we had proposed to develop new human prostate cell lines from primary tumors, and compare the characteristics of these cell lines with established cell lines (LNCAP, PC3, and DU145). In that application we had proposed to label tumor cells with a rhodamine based in vivo dye (CMTMR). However, we found that the CMTMR labeling did at most last for two weeks, and also, we found that macrophages which had engulfed tumor cells became fluorescent, and thus it was very difficult to assess the true tumor area.

Green fluorescent protein, GFP, is a spontaneously fluorescent protein isolated from coelenterates, such as the Pacific jellyfish, Aequoria victoria ([i]). Kanda et al. ([ii]) developed a highly sensitive method for observing chromosome dynamics in living cells. They fused the human histone H2B gene to the gene encoding the (GFP). We have generated the histone H2B-GFP fusion protein in a retroviral construct, and introduced this fusion protein into a number of human prostate cancer cell lines (LNCAP, PC3M, DU145), allowing us to evaluate not only tumor size, but also mitotic and apoptotic indices of the implanted tumor spheroids. After implantation of tumor spheroids using these cell lines we experienced very poor growth in our dorsal skinfold chamber model. The androgen dependent cell line, LNCAP regressed rapidly following implantation *in vivo*, with complete tumor cell death within 7 days. These micro-tumors were poorly angiogenic, and demonstrated rapid and massive apoptosis following implantation, with nearly undetactable mitotic indices. The androgen independent cell line, PC3 regressed at a slower rate than LNCAP cells, with a weak angiogenic response and a high apoptotic rate, though considerably lower than LNCAP. The DU145 spheroids regressed the slowest, demonstrating substantial angiogenic activity, considerably lower apoptotic rates, and measurable mitotic rates.

One plausible explanation for the poor growth of the implanted tumor cells could be the ectopic expression of H2B-GFP. GFP, is a spontaneously fluorescent protein isolated from coelenterates, such as the Pacific jellyfish, Aequoria victoria ([iii]). Even though the H2B-GFP fusion protein generated by Kanda et al. ([iv]) was shown not to

affect cell cycle progression, overexpression of the H2B GFP could have deleterious effects upon the tumor cell lines examined. To test this hypothesis, tumor spheroids obtained from the parental LNCAP cell lines labeled with the rhodamine based *in vivo* dye CMTMR, were implanted into the chamber model. The parental cell line without H2B-GFP also regressed rapidly, again demonstrating poor angiogenic activity, and massive apoptosis.

Evidence is accumulating that tumor-mesenchymal interactions are of great importance in prostate cancer. Many similarities exist between the stroma at sites of wound repair and reactive stroma in cancer. Common features include an elevated stromal cell proliferation, altered expression of matrix components, elevated expression of TGF beta-1, neovascularization, and expression of several common stromal markers ([v]).The presence of a stromal androgen receptor is required ([vi]), and humoral factors, such as keratinocyte growth factor (FGF-7) have been shown to be mediated in stromal epithelial paracrine fashion. The adult prostate is also under control of multiple steroid hormone and paracrine peptide factors, and there is evidence that the prostatic stroma plays a major role in mediation of androgen effects on prostatic epithelium, but androgens also increase VEGF transcription and secretion of biologically active VEGF from human prostatic stroma. Androgens, therefore, also enhance prostate growth via this up-regulation of VEGF from the surrounding stroma ([vii]). Thus, prostatic stromal cells are critically involved in growth and progression of prostate cancer, and the one possibility for the poor growth in our system could be the lack of mesenchymal-epithelial interactions and we decided to test this hypothesis. To achieve this goal, we excised murine prostate, minced it up and implanted small pieces (1-2 mm in diameter) into our chambers prior to implantation of the tumor spheroids.

An interesting finding from these experiments was that prostate tissue per se induced a very strong angiogenic reponse. This finding made it very difficult to do achieve the goals proposed under Aim #1. As the stroma itself was found to be the key player in prostate cancer angiogenesis, evaluation of angiogenesis of thin needle biopsies which contain their own stroma would not reveal the degree of malignancy of the biopsies.

Nevertheless, the introduction of murine prostatic stroma to our system which by it self induced strong angiogenesis, did not much enhance growth of the human prostate cell lines and we still experienced very low mitotic and very high apopototic indices. One plausible explanation could be that growth factors such as FGF-7, are species specific, and that the murine factors were not able to stimulate growth of the human prostate cell lines.

To test this hypothesis, we cultured human prostatic fibroblasts that we generated from a thin needle biopsy from a human prostate carcinoma. The fibroblasts were mixed (50/50%) with the prostate cancer cells prior to implantation in the dorsal skinfold chamber. The introduction of human fibroblasts did significantly improve the growth of the human cell lines. However introduction of fibroblasts which were labeled with CMTMR revealed that we had massive infiltration of macrophages (TAMS), and that the macrophages engulfed the fibroblasts, as evidenced from a large number of CMTMR labeled macrophages in the vicinity of the tumor spheroid. Consequently, the enhanced growth of the human prostate cells was only temporary and in less than seven days, when no live fibroblasts could be found at the tumor site, the response subsided.

The introduction of human fibroblasts obtained from prostate tissue thus did not solve our problems with poor growth in vivo of the human prostate cell lines.

Tumors are frequently infiltrated by numerous monocytes/macrophages (TAMs), which can be found within the tumor mass or surrounding the tumor. The TAMs excert diverse effects, including neovascularization, modulation of tumor growth rate and

stroma formation. Data currently available suggests that in solid syngeneic tumors the TAMs can induce immune suppression of host defenses in situ, through release of specific cytokines, prostanoids and other humoral mediators. However, TAMS can also participate in the innate antitumor defense mechanism through cytotoxic activities, such as direct cellular cytotoxicity and the release of cytokines and reactive oxegen species. In a recent study ([viii]) of human colorectal carcinoma, differential antibody staining of TAMs was used to identify the presence of different macrophage phenotypes, localized in different regions of the carcinoma. At the tumor-host interface, infiltrative, poorly demarcated and non-infiltrative, well bordered areas alternated. $27E10^{+}$, inflammatory macrophages were associated with the infiltrative areas at the interface. In contrast, $25F9^{+}$, mature, resident macrophages and $RM3/1^{+}$ macrophages, those cells associated with anti-inflammatory function, were associated with sharply bordered tumor areas dominating within the tumor stroma, particularly in carcinomas with marked desmoplastic stromal response. These findings suggest the possibility that phenotypically distinct macrophage subsets may have different effects on the tumor cells. Recent data suggest that macrophage-derived metalloelastase is responsible for the generation of angiostatin in the Lewis lung carcinoma model ([ix]), and more interestingly, those data suggest that tumor derived GM-CSF increased the production of elastase in a dose-dependent manner, whereas CSF-1 inhibited it ([x]). Nowicki, et al, showed that the growth and angiogenesis of Lewis lung cell carcinoma cells implanted in op/op-mice was significantly inhibited, but that normal growth was restored after systemic administration of CSF-1 ([xi]).

Thus, complex interactions between tumor cells and TAMs are pivotal in tumor biology, but a fundamental question was how these complex interactions are perturbed when "foreign" human tumor cells are implanted in immunodeficient mice.

Bucana et al., ([xii]) studied the distribution pattern of TAMs in murine and human neoplasms growing subcutaneously in nude mice. The TAMs were studied immunohistochemically by the use of several antibodies, including the macrophage-specific F4/80. The pattern of TAM distribution differed between mouse and human tumors. Regardless of histologic classification, TAMs were uniformly distributed throughout all the murine neoplasms growing in syngeneic or nude mice. In the human neoplasms, TAMs were found on the periphery of the lesions and in association with fibrous septae.

Lapis et al. ([xiii]) studied the effect of macrophages on tumor progression using human colorectal tumors transplanted in immune-suppressed mice and metastasizing Lewis lung carcinoma. Their results indicated that the activity of macrophages influences markedly the tumor progression--even in hosts with damaged T cell population.

Our data also demonstrates

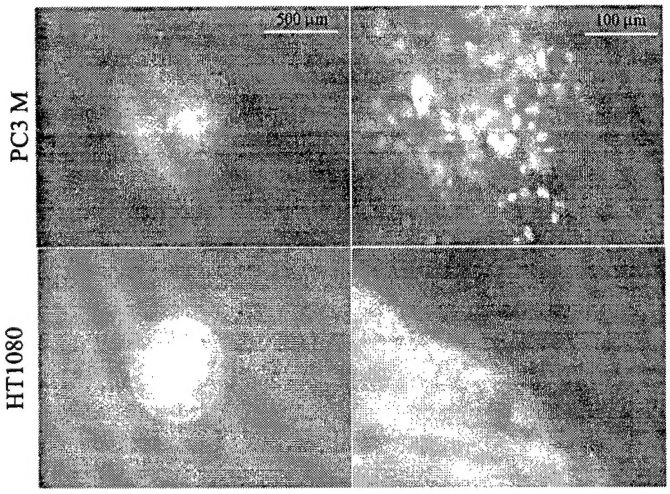

Figure 0 A common feature of the three human prostate carcinoma cell lines investigated in the present study was very poor encapsulation, with the fasted regressing cell line displaying the least encapsulation. Other human cell lines which grow well in the dorsal skinfold chamber have one thing

large differences in macrophage behavior in immuno-suppressed mice implanted with human tumors compared to syngeneic implants. Our data indicates that the TAMs become programmed to participate in the innate antitumor defense mechanism rather than immune suppression of host defenses. Thus, we found numerous apoptotic cells in the periphery of the prostate tumors, while mitotic figures still were found in the center. The tumors were dying from the outside in.

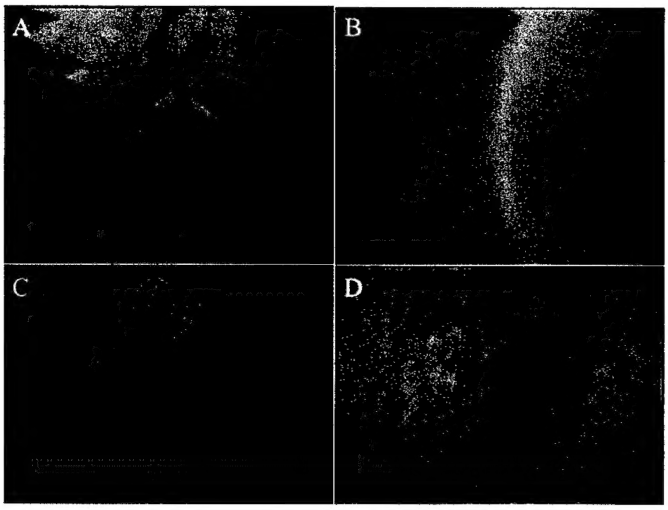

Figure 2 Beige nude mice which were transplanted with bone marrow from GFP+ mice, illustrate effective encapsulation of human tumors (HT1080) implanted in mice preventing infiltration of macrophages (upper panels). The lower panels illustrate infiltration of macrophages in syngeneic tumors (LLC).

In the past, we have successfully grown various other human cell lines in our system (HT1080, A673, MDA231). One common characteristic of these cell lines is that they become tightly encapsulated (FIG. 1), effectively excluding infiltration of macrophages. A characteristic of all human prostate cell lines we have tested was that they were very invasive, and their encapsulation was extremely poor. Thus, they were exposed to infiltrating macrophages which may have been programmed to engulf the slowly dividing prostate cancer cells.

In a subsequent series of experiments, we transplanted bone marrow from GFP+ mice into beige nude mice. The mice were fitted with dorsal skinfold chambers and one group of mice were implanted with tumor spheroids obtained from the human fibrosarcoma cell line HT1080 (xenograph), and a second group were implanted with tumor spheroids obtained from Lewis Lung Carcinoma cells (syngeneic). Figure 2 shows photomicrographs obtained from these experiments. The upper panels (HT1080) demonstrate again demonstrate that these cells grow in well encapsulated, and that the bone marrow derived cells are excluded from the tumor. Interestingly, the capsule formed around the xenograph is composed of bone marrow derived cells. The lower panels illustrate the growth characteristics of a syngeneic tumor. The tumor cells attracts bone marrow derived cells, and numorous macrophages can be seen at the tumor site.

In an attempt to test our hypothesis that the human prostate tumor cells failed to grow in our chamber system because of the tumorcidal TAMSs, we pretreated the mice with dextran. The mice received 200 µl dextran for two days prior to implantation, 200 µl at the day of implantation, followed by 10 daily injections of 100 µl all given i.v.

We have previously shown that following iv injections of dextran, phagosytosis by macrophages is severely hampered. In these series of experiments, we had two groups of untreated nude mice (controls). The first group was implanted with tumor spheroids obtained from H2B GFP PC3 cells, and the second group was implanted with tumor spheroids obtained from a mixture of the PC3 cells and cultured human prostate fibroblasts. A third group of mice were implanted with the PC3 fibroblast mixture, and treated with dextran as described above. Figure 3 illustrates the pronounced effect of

pretreatment with dextran on tumor growth, whereas the addition of fibroblasts only marginally and transiently enhances tumor growth. Panel B depicts mitotic and apoptotic indices obtained from these experiments 5 and 10 days after implantation, illustrating significantly lower apoptotic as well as significantly higher mitotic indices in tumors of dextran treated mice.

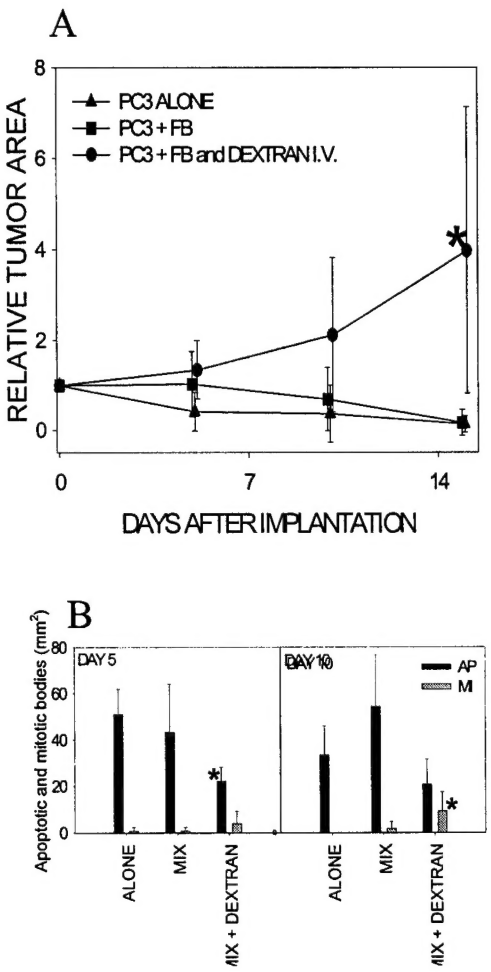

Figure 3 Pre-treatment with dextran i.v. prior to implanation effectively prevents macrophages from engulfing the human tumor cells.

Our findings suggest that due to the unique tumor-mesenchymal interactions in prostate, and the fact that TAMs become reprogrammed to participate in the innate antitumor defense, experimental xenograph models do not provide a relevant system to study prostate cancer progression, and thus the goals of our proposed SOW could not be achieved. After multiple failed attempts to grow human prostate cancer cell lines in our system under different conditions, we decided to develop a syngeneic mouse prostate system to study the role of VEGF in prostate cancer progression.

Recently, Greenberg et al. created a transgenic mouse model, TRAMP (Transgenic Adenocarcinoma Mouse Prostate), in which mice develop spontaneous prostate tumors ([xiv]). Greenberg derived and characterized three epithelial cell lines from a heterogeneous 32-week old spontaneous tumor. Two of these three cell lines are tumorigenic in immune competent syngeneic C57BL/6 hosts: TRAMP-C1 and TRAMP-C2 ([xv]). TRAMP-C1 and TRAMP-C2 cells do not express *in vitro* and *in vivo* the T antigen oncoprotein, and are thus able to grow in non-transgenic, syngeneic C57BL/6 hosts ([xvi]). The establishment of syngeneic cell lines from the TRAMP transgenic mice provides a complete animal model system in which preclinical testing of new therapeutic approaches for prostate cancer can be investigated. The fact that the disease in TRAMP mice recapitulates closely the evolution of disease in humans offers a unique opportunity to test alternative approaches for the treatment of prostate cancer.

Development of syngeneic "pseudo-orthotopic" in vivo model of prostate cancer. Thus we set out to develop a syngeneic intravital microscopy prostate cancer model. Our intention was to breed GFP+ mice to be donors of prostate tissue, and to make an RFP H2B retroviral construct. Considerable time was spent trying to transfect the TRAMP-C2 cells with the RFP-H2B, but failed.

While we were able to generate an RFP-H2B retroviral construct and could produce high titer virus pseudotyped with VSVG, cells transduced with this virus were not viable due apparent toxicity of the RFP fusion protein. Weak red fluorescence

localized to the nucleus could be found several days post transduction, but no clonal expansion of the fluorescent cells occurred. Following drug G418 selection, cells were unable to propagate with RFP and the only drug resistant colonies that emerged were not fluorescent. As the H2B RFP and Neo resistance genes were under the control of two separate promoters, and as the MLV 5'LTR is known to be silenced by hypermethylation, we examined the effects of 5' Aza cytidine and trichostatin A on RFP gene expression in the drug resistant colonies. Following treatment with demethylating agents, bright fluorescence could be found but was followed by massive apoptosis. While this could be due to the toxicity of the demethylating agents, removal of demethylating agents resulted in propagation of cells which were again non-fluorescent. Aside from HEK 293 cells, we were also unable to generate parental RFP expressing cells using plasmid or retroviral constructs. Recent reports by Clontech (Palo Alto, CA) of the toxicity of their dsRed construct due to oligomerization, further supports the failure of our group and two other research laboratories at SKCC to generate RFP or H2BRFP expressing cell lines.

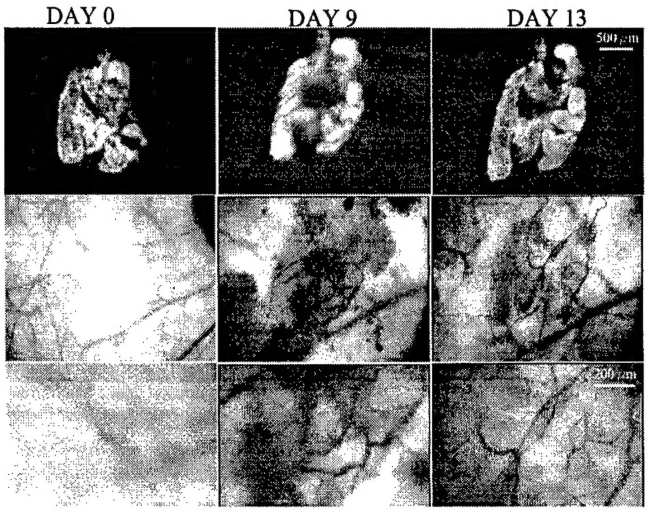

Figure 4 Anterior prostate tissue induces a strong angiogenic response and the prostate graft is fully re-vascularized within 7-10 days.

Since the RFP-GFP construct did not work, we introduced the histone H2B-GFP fusion protein it into the TRAMP-C2 cell line by retroviral transduction. Our recent findings that tumor-mesenchymal interactions are of great importance in prostate cancer, suggested that it could be beneficial to introduce an orthotopic milieu to our system. In a first series of experiments, we implanted prostate tissue derived from GFP+ mice. Figure 4 illustrates graphting of pieces of anterior prostate obtained from GFP+ mice implanted in dorsal skinfold chambers of C57BL6 mice. The prostate tissue induced

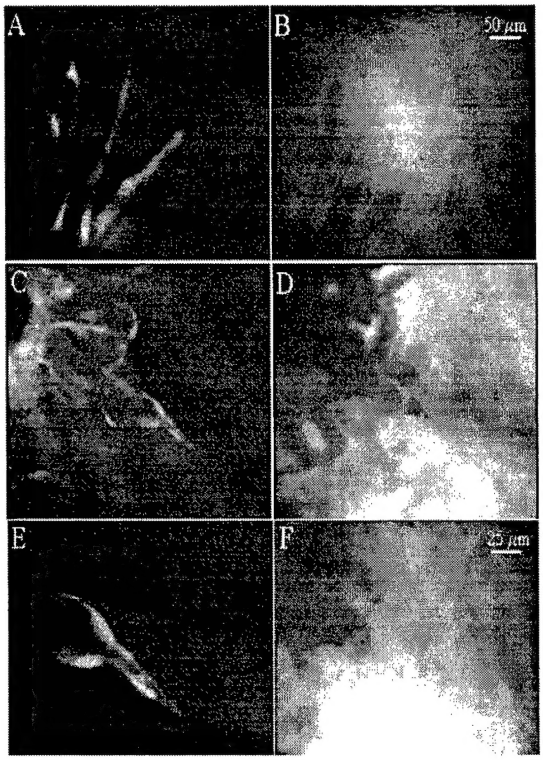

Figure 5 Photomicrographs illustrating budding of GFP labeled endothelial cells from prostate tissue

rapid re-organization of GFP labeled endothelial cells within the prostate. After three to four days, and the endothelial cells formed sprouts that could be seen re-connecting with pre-excisting vessels outside the grapht. In about 7 to 10 days, the prostate tissue was fully re-vascularized.

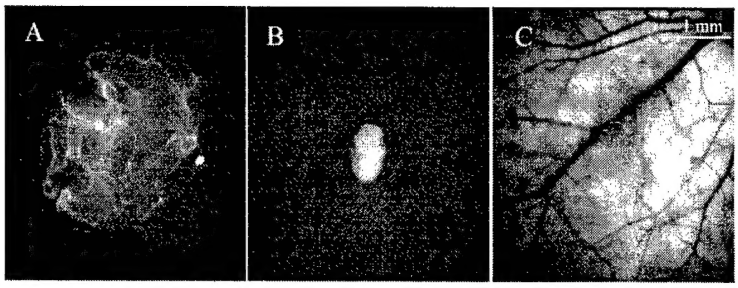

Figure 6 Illustration of "pseudo-orthotopic" implantation of TRAMP-C2 tumor cells

In a second series of experiments we compared growth characteristics of tumor spheroids obtained from TRAMP-C2 cells alone and the hybrid anterior prostate/ TRAMP-C2 prostate carcinoma cells spheroids. A small piece of anterior prostate tissue was excised from a C57BL6 mouse, labeled with a rhodamine based dye (CMTMR). It was carefully placed in a chamber of another C57BL6 mouse, and a tumor spheroid obtained from TRAMP-C2 H2B GFP cells were caryfully placed ontop of the prostate tissue (Fig 6). Figure 7 shows representative photo micrographs from these experiments. The two upper panels are from chambers implanted with hybrid spheroids, and the lower ones from TRAMP-C2 alone. This figure illustrates the high angiogenic activity induced by the hybrid spheroids. The prostate stroma induced re-vascularization rather than angiogenesis, and pre-existing unconnected vascular elements were seen to re-organize as early as 5 days post-implantation. Shortly after they became re-attached to the pre-existing vasculature underneath the spheroid. To our surprise prostate tissue alone induced a similar vascular response, whereas TRAMP-C2 tumor spheroids were less angiogenic. The hybrid spheroids were fully re-vascularized within 10 days after implantation.

Figure 7 illustrates more in detail the growth characteristics. Panel A demonstrates that for TRAMP-C2 spheroids, between day 0 and day 5, the tumor area increases by 80±26% however total intensity increases with only 41±16% implying that the increase in area is to a large degree due to migration of tumor cells, i.e., cell density is significantly lower at day 5 compared to at implantation. Hybrid spheroids actually showed an increase in area and a corresponding increase in intensity, reflecting true growth (panel B). Panels C and D depict mitotic and apoptotic indices. Both indices were found to be very low and mitotic and apoptotic bodies had to calculated over the entire tumor area. These values were expressed in relation to relative photointensity for each time point. Mitotic indices (number of telophase bodies) for TRAMP-C2 cells alone were in the order of 0.1-0.2 cell divisions per 1000 cells ($1\text{-}2 \times 10^{-4}$) and being in the order of 5 times higher for the hybrid spheroids. Apoptotic indices were very in the order of $1\text{-}2 \times 10^{-4}$ for tumor cells alone, and for the hybrid spheroids, there was a gradual decline from 5 to 0.5×10^{-4} during the 4 week observation period. Figure 9 depicting vascular parameters, demonstrates that the vascular area was 70% higher ($p=0.018$), average vessel diameter 50 % higher ($p=0.026$), and vascular density 13% higher (NS) for the TRAMP-C2 hybrid spheroids compared to the TRAMP-C2 spheroids.

Effects of surgical castration.

In order to evaluate the response of this model to a common therapy for prostate cancer patients, we performed surgical castration on the tumor bearing mice to examine the response of the hybrid spheroids to androgen ablation. Surgical castration was performed 9 days post-implantation of the tumor spheroids and prostate tissue. Representative photomicrographs from this group of animals are shown in Figure 9 within the same field pre and post castration. This figure illustrates the profound vascular regression seen 48 hours after surgical castration. Figure 10 illustrates more in detail, the consequences of surgical castration Panel A depicting tumor area and relative tumor intensity demonstrates that during the 18 day observation period after castration there was a significant reduction in tumor intensity, while there was no significant change in tumor area. No change could be see in mitotic indices, whrereas apoptotic indices increased slightly (Panel B). Panels C and D depicting vascular parameters, show significant reduction in both vascular area and vascular density.

Effects of COX-2 inhibition

Nonsteroidal anti-inflammatories (NSAID) are currently being evaluated clinically as chemopreventive drugs for major cancer targets because of their colon cancer chemopreventive effects in clinical

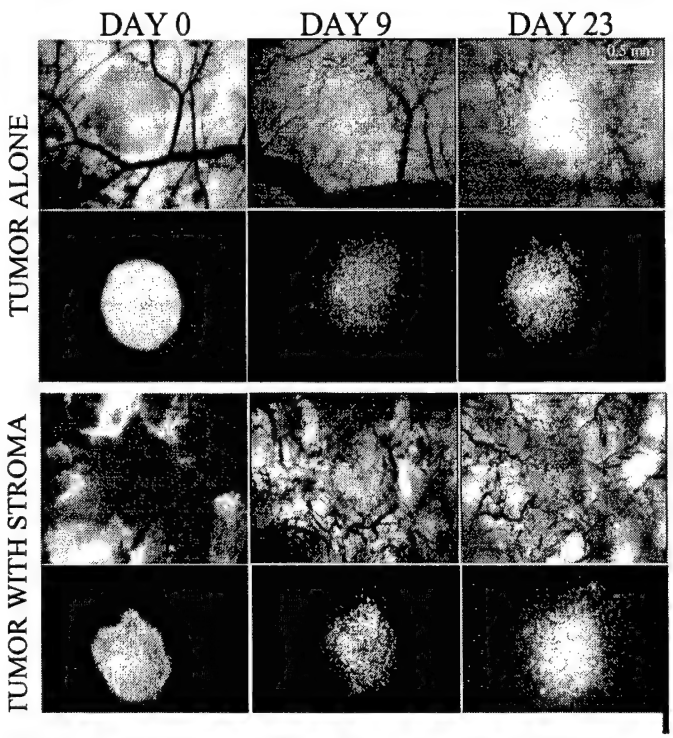

Figure 7 Illustration of the difference in growth characteristics of tumor spheroids obtained from TRAMP-C2 cells only (Without stroma)) and hybrid anterior prostate/ TRAMP-C2 prostate carcinoma cell spheroids (With Stroma).

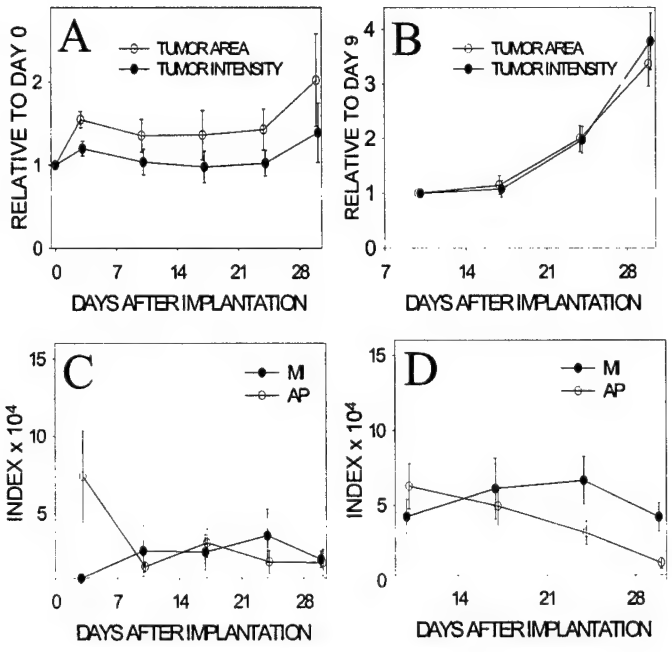

Figure 8 Growth curves and mitotic and apoptotic indices for TRAMP-C2 implanted with and without stroma.

intervention, epidemiological, and animal studies ([xvii]). NSAID was also shown recently to affect the prostate cancer progression TRAMP mouse prostate cancer model. NSAID treatment resulted in a significantly lower incidence of metastasis and a reduction in the primary tumor incidence, suggesting the use of NSAIDs as promising chemopreventive and treatment for human prostate cancer ([xviii]).

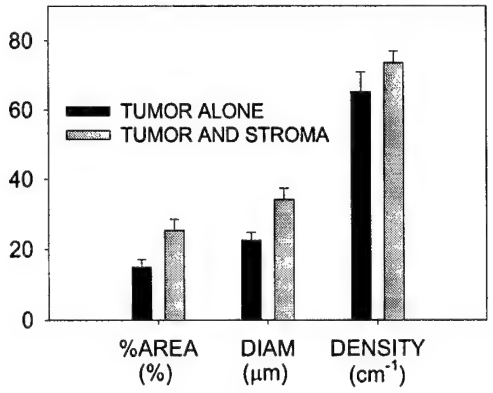

Figure 9 Bar graft illustrating higher angiogenic activity for hybrid spheroids.

Cyclooxygenase (COX), the key regulatory enzyme for prostaglandin synthesis is transcribed from two distinct genes. COX-1 is expressed constitutively in most tissues, and COX-2 is induced by a wide variety of stimuli and was initially identified as an immediate-early growth response gene. COX-2 expression is markedly increased in 85-90% of human colorectal adenocarcinomas, whereas COX-1 levels remain unchanged. Several epidemiological studies have reported a 40-50% reduction in the risk of developing colorectal cancer in persons who chronically take such nonsteroidal anti-inflammatory drugs (NSAIDs) as aspirin, which are classic inhibitors of cyclooxygenase. Genetic evidence also supports a role for COX-2, since mice null for COX-2 have an 86% reduction in tumor multiplicity ([xix]). An expanding body of evidence indicates that downregulation of the cyclooxygenases (COX-1 and COX-2) will be an important strategy for preventing cancer because cyclooxygenases catalyze the formation of prostaglandins (PGs), and PGs have multiple effects that favor tumorigenesis. PGs also are more abundant in cancers than in the normal tissues from which cancers arise ([xx]). The in vivo mechanism by which COX-2 affects tumor growth has not yet been fully determined. Recent data

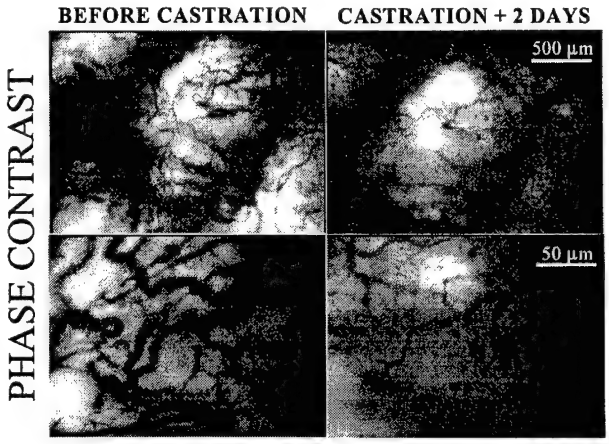

Figure 10 Illustration of the pronounced vascular regression following surgical castration

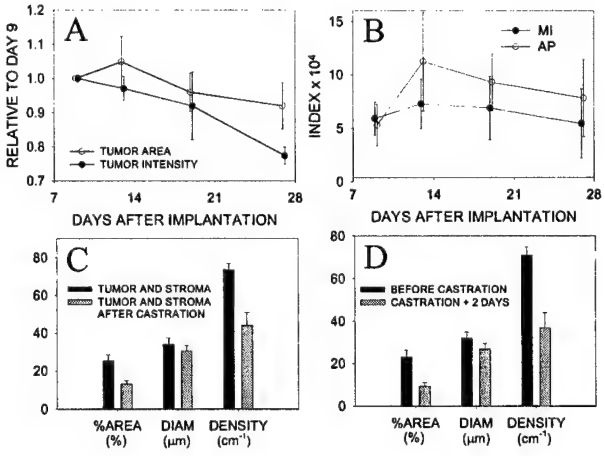

Figure 11 Compiled data illustrating significant reduction in tumor intensity, and the vascular regression following surical castration.

indicate that both tumor and stromally derived COX-2 could influence tumor immune function ([xxi]). COX-2 inhibitors have also been suggested to induce cell cycle arrest and apoptosis in colon cancer cell lines through aechanism that is fundamentally different from the apoptosis caused by cancer chemotherapeutic agents ([xxii]). The products of bcl-2 and p53 genes are involved in the regulation of apoptosis and a selective COX-2 inhibitor was recently shown to decrease the level of bcl-2 protein and to induce apoptosis also in the human prostate carcinoma cell line LNCaP

We believed that our system could be a valuabe tool to clarify the mechanisms behind COX-2 inibitors, and while constructing the sflt vectors, we performed a study where we administered celecoxib orally to mice (daily 250 mg/kg).

In a first series of experiments, we implanted tumor spheroids obtained from TRAMP-C2 cells alone. Figure 12 demonstrates that COX-2 inhibition did not significantly affect growth rate, and did not significantly alter apoptotic index, however, mitotic index increased significantly. In view of the unaltered growth rate, our interpretation of the increased mitosis was cyclic arrest.

In a second series of experiments, we implanted used our pseudo-orthotopic model. Figure 13 again illustrates the importance for stroma in prostate

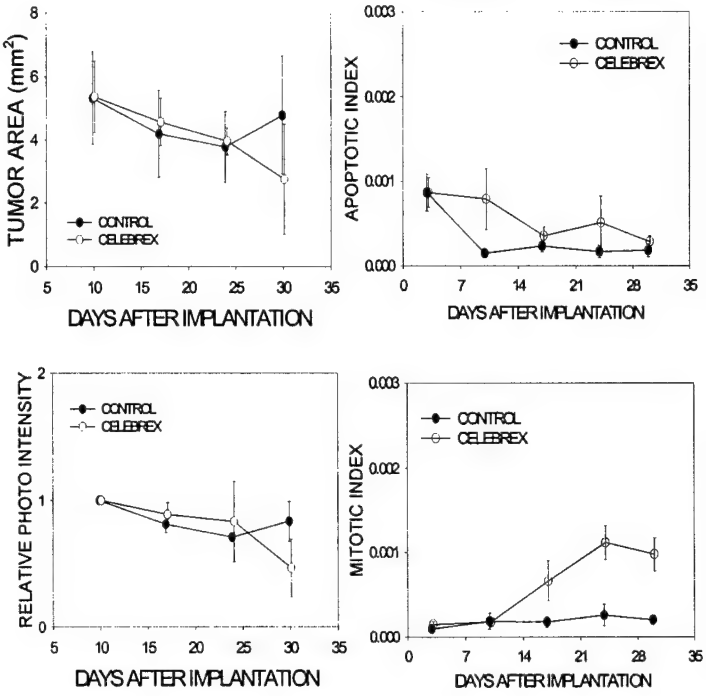

Figure 12 The only parameter which changed significantly in response to COX-2 inhibition was mitosis which increased by more than 600%.

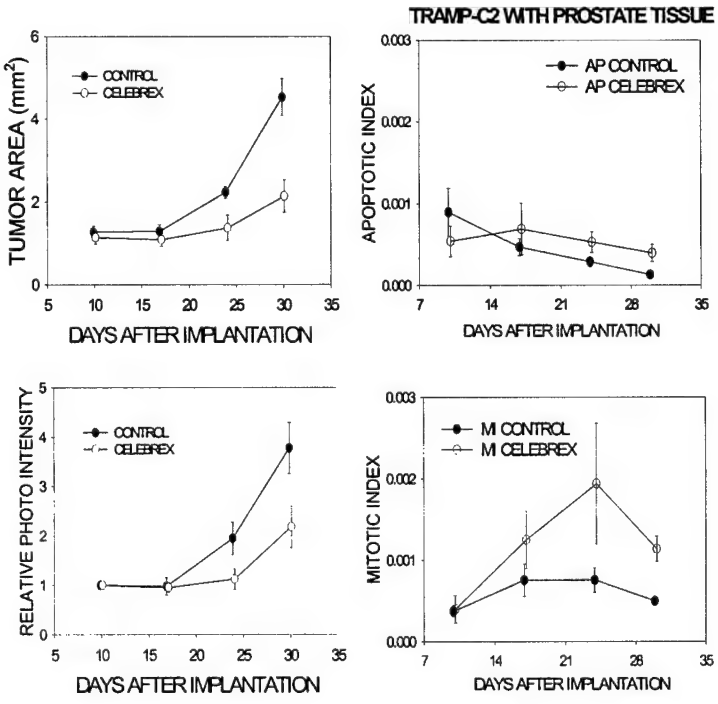

Figure 13 Using our pseudo orthotopic model, COX-2 inhibition significantly inhibited tumor growth, and significantly increased mitosis, whereas apoptosis was not affected.

cancer proliferation. Again, COX-2 inhibition hampered tumor growth, did not significantly change apoptotic index, but significantly increased mitotic index. Surprisingly, the vascular parameters from these series of experiments revealed that celecoxib did not possess any angiostatic activity.

Thus our pseudo orthotopic system demonstrated that surgical castration caused rapid vascular regression, a slight increase in apoptosis, and tumor growth inhibition. COX-2 inhibition on the other hand did not affect vascular parameters, but strongly affected the cell cycle (increased mitotic indices), resulting in quite strong growth inhibition.

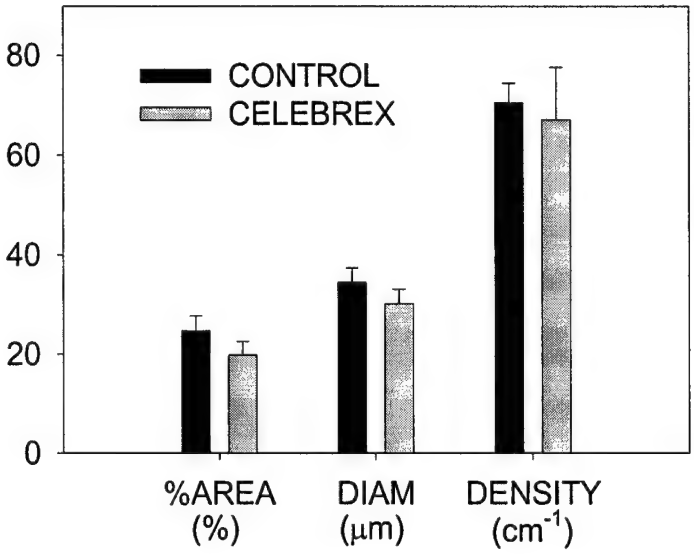

Figure 14 Surprisingly, we could not detect any changes in vascular parameters in response to COX-2 inhibition

In a third series of experiments we combined surgical castration with COX-2 inhibition figure 15 demonstrates that Surgical castration in combination with COX-2 inhibition had quite strong anti tumor activity, tumor photo intensity decreasing by 65%, compared to 20% after castration only. Apoptosis was not much affected, but again mitosis increased significantly. These series of experiments demonstrate that COX-2 inhibitors do not affect angiogenesis, nor do they increase apoptosis. The most important underlying mechanism is cell cycle arrest ([xxiii]). Our experiments also demonstrate that moderate

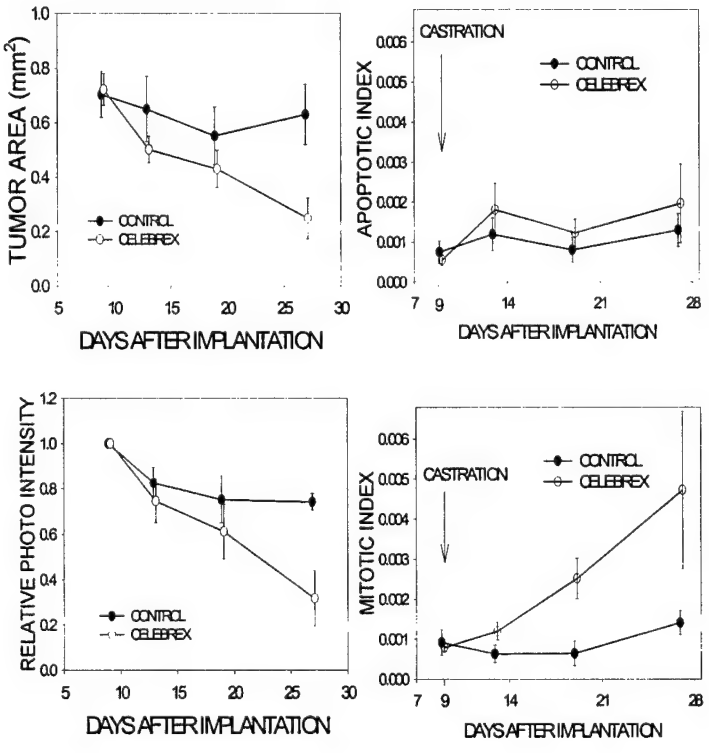

Figure 15 Surgical castration combined with COX-2 inhibition had quite strong anti tumor activity, underlying which we found a significantly increase mitotic index.

our newly developed syngeneic pseudo orthotopic model to study prostate cancer progression, is a very useful tool to investigate and clairify mechanisms underlying anti tumor activities for various therapeutic interventions, as well as to evaluate different combinatorial treatment regimens.

To summarize the key research accomplishments:

- Furthering of the understanding that macrophages in syngeneic tumors play a pivotal role and that innate anti-tumor defense mechanism in xenograft models is an artifact rather than being representative for normal tumor biology.
- Clarifying the importance of stroma in prostate tumor progression.
- Development of a syngeneic pseudo orthotopic in vivo model to study prostate tumor progression.
- Using our syngeneic pseudo orthotopic in vivo model to evaluate the effects of surgical castration on prostate cancer.
- Using our syngeneic pseudo orthotopic in vivo model to evaluate the effects of COX-2 inhibition alone and in combination with surgical castration.
- Generation of a retroviral construct for murine soluble flt receptor
- Using the chamber technique to demonstrate a profound angiostatic effect following DCs-based vaccination, suggesting, either that endothelial cells of tumor vasculature present tumor specific antigens, or that tumor vasculature is composed of a mosaic of tumor cells and endothelial cells.

REPORTABLE OUTCOMES: Three manuscripts describing the progress from research are included. Also a book chapter to be published in XXX is included

1. Frost G.I., Dudouet B., Lustgarten J., and Borgström P. The Roles Of Epithelial Mesynchymal Interactions And The Innate Immune Response On The Tumorgenicity Of Human Prostate Carcinoma Cell Lines Grown In Immuno-Compromised Mice

2. Frost G.I., Dudouet B., Lustgarten J., and Borgström P. The Vascular, Mitotic And Apoptotic Reponses to Androgen Ablation Revealed Through A Novel Syngeneic Pseudo-Orthotopic Prostate Cancer Model

3. Dudouet B., Frost G.I., Lustgaren J., and Borgström P. Dendritic Cells Pulsed With Apoptotic Prostate Tumor Cells Induces Protective and Therapeutic Prostate Tumor Rejection *In Vivo* (Submitted Prostate 2001).

CONCLUSIONS: We conclude that significant differences in macrophage behavior are found in immuno-suppressed mice implanted with human tumors xenografts than in syngeneic murine model systems. This innate anti-tumor defense mechanism is an artifact of xenograft models rather than normal tumor biology, such that large numbers of tumor cells need to be implanted for tumor take to occur. The combined requirements for tumor mesenchymal interactions and tumor encapsulation from the host innate immune response in human tumor xenografts demonstrated that the goals of our proposed SOW

could not be achieved and are in fact not a relevant model for studying therapeutic intervention in prostate cancer. Instead we have developed a novel syngeneic mouse prostate cancer model to study the role of VEGF in prostate cancer progression. We believe that our unique "pseudo-orthotopic" syngeneic in vivo model is a very powerful tool investigating the efficacy and modes of operation of combinatorial treatment regimens.

REFERENCES

[i] J. Cell Physiol. 77: 313-8. (1971)
[ii] Curr Biol 1998 Mar 26;8(7):377-85
[iii] Morin, J. and Hastings, J., 1971. Energy transfer in a bioluminescent system. J. Cell Physiol. 77: 313-8.

[iv] Kanda T, Sullivan KF, Wahl GM. Histone-GFP fusion protein enables sensitive analysis of chromosome dynamics in living mammalian cells. Curr Biol 1998 Mar 26;8(7):377-85

[v] Cancer Metastasis Rev 1998-99;17(4):411-9
[vi] Endocrinology 1998 Nov;139(11):4672-8
[vii]Endocrinology 1998 Nov;139(11):4672-8
[viii] Pathol Res Pract, 1994 Feb, 190:2, 159-67
[ix] Cell; 88(6):801-10 1997
[x] J Immunol; 157(11):5104-11 1996
[xi] Int J Cancer 65:112-119, 1996
[xii] Am J Pathol 1992 Nov;141(5):1225-36
[xiii] Arch Geschwulstforsch 1981;51(6):475-9
[xiv] Proc. Natl. Acad.Sci. USA 92:3439-3443, April 1995
[xv] Model Cancer Research, 57, 3325-3330, August 15, 1997
[xvi] Cancer Research, 57, 3325-3330, August 15, 1997
[xvii] Lawrence JA; Kopelovich L; Ali I; Viner JL; Sigman CC. Progress in cancer chemoprevention. Ann N Y Acad Sci 889:1-13 1999.

[xviii] Wechter WJ; Leipold DD; Murray ED Jr; Quiggle D; McCracken JD; Barrios RS; Greenberg NM. E-7869 (R-flurbiprofen) inhibits progression of prostate cancer in the TRAMP mouse. Cancer Res Apr 15;60(8):2203-8 2000.

[xix] Williams C; Shattuck Brandt RL; DuBois RN. The role of COX-2 in intestinal cancer. Ann N Y Acad Sci 889:72-83 1999.

[xx] Subbaramaiah K; Zakim D; Weksler BB; Dannenberg AJ. Inhibition of cyclooxygenase: a novel approach to cancer prevention. Proc Soc Exp Biol Med Nov; 216(2):201-10, 1997.

[xxi] Niiro H; Otsuka T; Tanabe T; Hara S; Kuga S; Nemoto Y; Tanaka Y; Nakashima H; Kitajima S; Abe M; et al. Inhibition by interleukin-10 of inducible cyclooxygenase expression in lipopolysaccharide-stimulated monocytes: its underlying mechanism in comparison with interleukin-4. Blood, Jun, 85:12, 3736-45, 1995.

[xxii] Ahnen DJ. Colon cancer prevention by NSAIDs: what is the mechanism of action? Eur J Surg Suppl (582):111-4, 1998.

[xxiii] Ahnen DJ. Colon cancer prevention by NSAIDs: what is the mechanism of action? Eur J Surg Suppl (582):111-4, 1998.

THE VASCULAR, MITOTIC AND APOPTOTIC RESPONSES TO ANDROGEN ABLATION REVEALED THROUGH A NOVEL SYNGENEIC PSEUDO-ORTHOTOPIC PROSTATE CANCER MODEL

Gregory I. Frost, Joseph Lustgarten, Brigitte Dudouet, Beryl Hartley-Asp and Per Borgström

Sidney Kimmel Cancer Center, 10835 Altman Row, San Diego, CA 92121

Phone: (858) 450 5990 ext 353, E-mail: pborgstrom@skcc.org, E-fax:

305-768-4602

Correspondence: Per Borgström, Sidney Kimmel Cancer Center, 10835 Altman Row, San Diego, CA 92121

ABSTRACT

In a recent study, we demonstrated that micro-tumors of human prostate carcinoma cell lines regressed rapidly following implantation *in vivo*. in immunodeficient mice. The cell lines were poorly angiogenic, and demonstrated rapid and massive apoptosis following implantation, with nearly undetactable mitotic indices. The inability to effectively exclude the innate immune system by encapsulation prevented the survival of the small prostate carcinoma micro-tumor xenografts preventing growth of human prostate tumor cells.

Due to the poor growth we experienced with human prostate cells in vivo, we set out to develop a syngeneic prostate carcinoma model. We used the murine prostate carcinoma cell line TRAMP-C2 which mimics closely the evolution of prostate cancer in humans. Our model is based on the dorsal skin fold chamber technique, utilizing fluorescence video-microscopy.

The "seed-soil" concept has been repeatedly explored in prostate cancer models, where direct tumor implantation into the prostate has resulted in a more accurate representation of the disease. To create a "pseudo-orthotopic milieu we implanted small pieces (10-15 mm^2) of anterior prostate tissue from donor mice, on top of which small tumor spheroids (25,000 cells) obtained from TRAMP-C2 were placed. These hybrid spheroids were implanted in dorsal skinfold chambers of syngeneic C57BL/6 hosts. To be able to evaluate not only tumor size, but also mitotic and apoptotic indices of the implanted tumor spheroids in real time, a histone H2B-GFP fusion protein was introduced into the TRAMP-C2 cell line. Tumor spheroids obtained from TRAMP-C2 cells alone were found to be poorly angiogenic and displayed very invasive growth

characteristics. Mitotic and apoptotic indices of the TRAMP-C2 cells were very low in the order $2x10^{-4}$ and no tumor growth could be detected. The hybrid spheroids on the other hand had mitotic and apoptotic indices in the order of $5x10^{-4}$ and were highly angiogenic, and fully vascularized in 7 to 10 days. During a four-week observation period tumor areas increase by more than 300%. The syngeneic "pseudo-orthotopic model was used to study in detail the effects of surgical castration. The most profound response was a dramatic and rapid vascular regression of the hybrid tumor vasculature. Also, castration caused a significant increase in the apoptotic rate, but no significant changes in mitosis was noted.

INTRODUCTION

Primary treatment in advanced prostate cancer normally includes some form of hormonal therapy to decrease the level of testosterone. Most prostate cancer responds initially to androgen ablation and the general concept is that the population of androgen-dependent cells undergoes rapid apoptosis upon androgen withdrawal. However, androgen ablation rarely cures patients, and most will experience recurrence due to takeover of the tumor mass by androgen-independent tumor cells. Castration has been believed to cause rapid apoptosis of androgen-dependent cells ([1]), however recent data ([2]) suggests that in fact castration does not cause massive apoptosis but rather results in a growth arrest where the cells persist in a dormant, androgen-responsive state for long periods of time, where-after spontaneous androgen-independent outgrowths develop.

Animal models are crucial to further our understanding of the mechanisms underlying the progression of prostate cancer, after castration, to an androgen-independent state. Unfortunately, the limited number of in vivo prostate tumor models has considerably hampered research. Various research groups have put significant effort into the development of human prostate tumor xenograft models ([3]).

In a recent study, we evaluated growth and angiogenesis of three human prostate tumor cell lines (DU145, PC3, and LnCAP) using an intravital microscopic system based on the dorsal skinfold chamber in nude mice ([4]). We experienced extremely poor growth (regression) of these cell lines in our system, and provided evidence that the poor growth in part was due to lack of appropriate tumor-mesenchymal interactions. However, our data also demonstrated that tumor associated macrophages TAMs participate in the immunologic antitumor defense mechanism, and the inability of the human prostatic cell

lines to effectively exclude the TAMs by encapsulation prevented the survival of the small micro-tumor xenografts. These findings thus question the use of xenograph model systems for the study of prostate cancer.

Recently, Greenberg et al. created a transgenic mouse model, TRAMP (Transgenic Adenocarcinoma Mouse Prostate), in which mice develop spontaneous prostate tumors ([5]). In these mice, expression of the SV40 large T-antigen is driven by the prostate-specific rat probasin promoter. TRAMP mice develop a distinct pathology in the dorso-lateral epithelium of the prostate by 10 weeks of age. By 12 weeks they have widespread infiltration of the prostate and by week 24, mice exhibit well-differentiated prostate tumors. By week 28, 100% of the animals have developed metastases in the lymph nodes and lungs ([6]). In parallel to human prostate patients, androgen ablation in TRAMP mice does not ultimately cure the disease due to the development of a hormone refractory state. Early castration in TRAMP model (12 weeks) ([7]) has a variable effect on progression of the disease and shows that prostate cancer is heterogeneous in this system. Although androgen ablation at 12 weeks can significantly decrease median primary prostate tumor burden, overall progression to poorly differentiated and metastatic prostate cancer is not ultimately delayed. Importantly, Greenberg has also derived and characterized three epithelial cell lines from a heterogeneous 32-week old spontaneous tumor. Two of these three cell lines are tumorigenic in immune competent syngeneic C57BL/6 hosts: TRAMP-C1 and TRAMP-C2 ([4]). TRAMP-C1 and TRAMP-C2 cells do not express *in vitro* and *in vivo* the T antigen oncoprotein, and are thus able to grow in non-transgenic, syngeneic C57BL/6 hosts ([8]). The establishment of syngeneic cell lines from the TRAMP transgenic mice provides a complete animal model system in which

preclinical testing of new therapeutic approaches for prostate cancer can be investigated. A metastatic prostate model with TRAMP-C2 cells transplanted into C57BL/6 mice has been developed by Kwon et al ([9]). In this system, the tumorigenic TRAMP-C2 cell line develops metastases in the lymph nodes and lung from the primary tumor. Following primary tumor removal, all mice relapse with metastases arising from micrometastases present at the time of the primary tumor resection. Interestingly, administration of immunotherapeutic treatment such as CTLA-4 blockade immediately after primary tumor resection can effectively prevent metastatic relapse.

The fact that the disease in TRAMP mice mimics closely the evolution of disease in humans offers a unique opportunity to test alternative approaches for the treatment of prostate cancer.

The purpose of the present study was a) to develop a syngeneic "pseudo-orthotopic model for castration, and b) examine the effects of castration using this model. We used TRAMP-C2 cells implanted in dorsal skinfold chambers in syngeneic C57BL/6 hosts. In order to evaluate not only tumor size but also mitotic and apoptotic indices of the implanted tumor spheroids, we generated a histone H2B-GFP fusion protein expressing variant of the TRAMP-C2 line by retroviral transduction.

Our recent study support the concept that tumor-mesenchymal interactions are of great importance in prostate cancer ([10]). With this in mind we suggested that it would be beneficial to introduce an orthotopic milieu to our system. To achieve this goal, we excised adult murine anterior prostate tissue from donor mice and generated hybrid anterior prostate/ TRAMP-C2 prostate carcinoma cell spheroids and implanted these hybrids into the chamber

Results from the present study suggest very different growth characteristics using a syngeneic system compared to human xenograft in immunodeficient mice. Our results also support the concept that the stroma is pivotal for angiogenic responses and that the stroma increases prostate tumor cell proliferation.

Our results do not support the concept that castration causes cyclic arrest but rather that it results in a moderate increase in apoptosis but more importantly it causes vascular regression. The most pronounced response seen after castration is a rapid vascular regression, followed by an increased migration of tumor cells away from the blood flow deprived tumor environment.

METHODS

Animal model and surgical techniques: The dorsal skinfold chamber in the mouse was prepared as described previously ([11]). Male mice (25-35 g body weight) were anesthetized (7.3 mg ketamine hydrochloride and 2.3 mg xylazine /100 g body weight, i.p.) and placed on a heating pad. Two symmetrical titanium frames were implanted into a dorsal skinfold, so as to sandwich the extended double layer of skin. A 15 mm full thickness layer was then excised. The underlying muscle (M. cutaneous max.) and subcutaneous tissues were covered with a glass cover slip incorporated in one of the frames. After a recovery period of 2-7 days, tumor spheroids were carefully placed in the chamber.

Surgical Castration Mice were anesthetized as described above in surgical techniques. A lateral incision across the scrotum was made and the testes were individually removed, ligated, excised and cauterized. The incision was then sutured and further sealed with Nexaband® acrylic.

Preparation of hybrid anterior prostate/ TRAMP-C2 prostate carcinoma cell spheroids. Tramp-C2 cells were transduced with a VSV pseudotyped LXRN virus encoding a Histone H2B-GFP fusion protein. The histone H2B-GFP cDNA was subcloned into the Sal-I/ Hpa-I sites in the LXRN vector (Clontech Palo Alto, CA) using Sal-I and blunted Not-I sites from the BOSH2BGFPN1 vector ([12]). LH2BGFPRN virus was VSV pseudotyped in GP-293 cells pelleted by centrifugation and frozen at -80C untill use. Transduced Tramp-C2 cells were FACs sorted to generate a homogeneously labeled population. Anterior prostate from a donor mouse was excised and minced into small pieces, followed by labeling with CMTMR for rhodamine counter-label for 15min

in serum free media. The labeled prostate was then washed and implanted in dorsal skinfold chabers in C57BL/6 mice Tumor spheroids were made using trypsinized TRAMP C2 H2BGFP cells (250,000 tumor cells/ml) which were dispersed (100ul/well) into 96 well round bottom plates coated with 1.0 % agarose for a liquid overlay. The spheroids were allowed to compact for 48 hours followed by washing in serum free media for implantation on top of the prostate tissue (FIG. 1).

Intravital microscopy : Fluorescence microscopy was performed using a Mikron Instrument Microscope (Mikron Instrument, San Diego, CA) equipped with epi-illuminator and video-triggered stroboscopic illumination from a xenon arc (MV-7600, EG&G, Salem, MA). A silicon intensified target camera (SIT68, Dage-MTI, Michigan City, IN) was attached to the microscope. A Hamamatsu image processor (Argus 20) with firmware version 2.50 (Hamamatsu Photonic System, USA) was used for image enhancement and to capture images to a computer. A Leitz PL1/0.04 objective was used to obtain an over-view of the chamber and for determination of tumor size. A Zeiss long distance objective 10/0.22 was used to capture images for calculation of vascular parameters. A Zeiss Achroplan 20X/0.5 W objective was used for capturing images for calculation of mitotic and apoptotic indices.

Image analysis: The tumor spheroid and vasculature was analyzed off-line from the video recording using a photodensitometric computer software (Image-Pro Plus, Media Cybernetics, MD). For each spheroid, video recordings were used to calculate tumor area, and relative photometric density of the tumor. To take into account heterogeneous tumor cell distribution (Fig. 2.) tumor area is defined as number of pixels with photo density above 75 (256 gray levels), i.e.,

$$A_T = \sum_{k=75}^{256} A_k,$$

and total intensity I_T is defined as,

$$I_T = \sum_{k=75}^{256} A_k * I_k,.$$

Relative intensity reflecting relative number of tumor cells at Day X is defined as;

$$(T_{REL})_{DAYX} = (I_T)_{DAYX} / (I_T)_{DAY0}$$

Length, area and vascular density of the neovasculature being induced by the implanted tumor spheroids were also calculated.

Mitotic and apoptotic indices: Mitotic and apoptotic indices were very low, and hence had to be counted over the whole tumor area. Relative indices were obtained by dividing the number of mitotic and apoptotic bodies with the relative intensity which was obtained as;

$$(I_{REL})_{DAY\ X} = (I_T)_{DAY\ X} / (I_T)_{DAY\ 0},$$

where $(I_T)_{DAY0,}$ and $(I_T)_{DAYX}$ are total intensities at DAY 0 and DAY X respectively. Mitotic figures in metaphase through telophase were included in the mitotic index. Apoptotic/Pyknotic nuclei were defined as H2BGFP labeled nuclei with a cross sectional area $>30um^2$. Nucelar karyorhexis, easily distinguishable by the vesicular nuclear condensation and brightness of H2BGFP, was included within this apoptotic index.

RESULTS

Development of syngeneic "pseudo-orthotopic" in vivo model of prostate cancer.

In a first series of experiments, we implanted prostate tissue derived from GFP+ mice. (Figs. 3-5)

In a second series of experiments we compared growth characteristics of tumor spheroids obtained from TRAMP-C2 cells alone and the hybrid anterior prostate/ TRAMP-C2 prostate carcinoma cells spheroids. Figure 6 shows representative photo micrographs from these experiments. The two upper panels are from chambers implanted with TRAMP-C2 spheroids alone, and the lower ones with hybrid spheroids. This figure illustrates the high angiogenic activity induced by the hybrid spheroids. The prostate stroma induced re-vascularization rather than angiogenesis, and pre-existing unconnected vascular elements were seen to re-organize as early as 5 days post-implantation. Shortly after they became re-attached to the pre-existing vasculature underneath the spheroid. To our surprise prostate tissue alone induced a similar vascular response, whereas TRAMP-C2 tumor spheroids were less angiogenic. The hybrid spheroids were fully re-vascularized within 10 days after implantation.

Figure 7 illustrates more in detail the growth characteristics. Panel A demonstrates that for TRAMP-C2 spheroids, between day 0 and day 3, the tumor area increases by 55∀10% however total intensity increases with only 20∀9% implying that the increase in area is to a large degree due to migration of tumor cells, i.e., cell density is significantly lower at day 3 compared to at implantation. Hybrid spheroids actually showed an increase in area and a corresponding increase in intensity, reflecting true growth (panel B). Panels C and D depict mitotic and apoptotic indices. Both indices

were found to be very low and mitotic and apoptotic bodies had to calculated over the entire tumor area. These values were expressed in relation to relative photointensity for each time point. Mitotic indices (number of telophase bodies) for TRAMP-C2 cells alone were in the order of 0.1-0.2 cell divisions per 1000 cells ($1\text{-}2 \times 10^{-4}$) and being in the order of 5 times higher for the hybrid spheroids. Apoptotic indices were very in the order of $1\text{-}2 \times 10^{-4}$ for tumor cells alone, and for the hybrid spheroids, there was a gradual decline in apoptotic indecis from 5 to 0.5×10^{-4} during the 4 week observation period whereas mitotic indices were in the order of 5×10^{-4}. Figure 8 depicting vascular parameters, demonstrates that the vascular area was 70% higher ($p=0.018$), average vessel diameter 50 % higher ($p=0.026$), and vascular density 13% higher (NS) for the TRAMP-C2 hybrid spheroids compared to the TRAMP-C2 spheroids.

Effects of surgical castration.

In order to evaluate the response of this model to a common therapy for prostate cancer patients, we performed surgical castration on the tumor bearing mice to examine the response of the hybrid spheroids to androgen ablation. Surgical castration was performed 9 days post-implantation of the tumor spheroids and prostate tissue. Representative photomicrographs from this group of animals are shown in Figure 9 within the same field pre and post castration. This figure illustrates the profound vascular regression seen 48 hours after surgical castration. Figure 10 illustrates more in detail, the consequences of surgical castration Panel A depicting tumor area and relative tumor intensity demonstrates that during the 18 day observation period after castration there was a significant reduction in tumor intensity, while there was no significant change in tumor

area. No change could be see in mitotic indices, whrereas apoptotic indices increased slightly (NS) (Panel B). Panel C depicting vascular parameters for castrated mice versus control mice (Day 17), and panel D depicting vascular parameters for castrated mice before and 48 h after castration both show significant reduction in both vascular area and vascular density.

DISCUSSION

In a recent study ([13]) we failed to grow human prostate carcinoma cell lines (LNCAP, DU145, and PC3) in dorsal skinfold chambers in nude mice. The poor growth was found to be due to very high apoptotic indices, especially in the periphery of the tumors, which we attributed to tumor cell killing by macrophages recognizing the foreign human cancer cells and being re-programmed to participate in the immunologic antitumor defense mechanism. A characteristic of the human prostate cell lines we tested in the chamber system was that they were very invasive, and never became encapsulated. The exposure of these slowly dividing non-encapsulated tumor spheroids to the tumor infiltrating macrophages may prevent them from effective growth within the system. We have successfully grown LNCAP, DU145, and PC3 cells sub-cutaneously but have had to inject in the order of 1-5 x 10^6 cells for tumor take, and it has been reported that human prostate tumors grown sub-cutaneously grow encapsulated ([14]). In the past, we successfully grew other human tumor cell lines in the dorsal skinfold chamber ([15]) and one common characteristic of these cell lines was their effective encapsulation, thereby excluding infiltration of macrophages. Our recent findings thus question the use of human tumor xenografts in prostate cancer research.

The recently developed TRAMP model in which mice develop spontaneous prostate tumors ([16]) is the first syngeneic animal model for prostate cancer, which mimics closely the evolution of disease in humans, thus offering a unique opportunity to test alternative approaches for the treatment of prostate cancer. We have implemented TRAMP-C2 in our in vivo system, and have generated histone H2B-GFP fusion protein expressing variants, allowing us to evaluate not only overall growth of tumors, but also

mitotic and apoptotic indices of the implanted tumor spheroids as well. Evidence is accumulating that tumor-mesenchymal interactions, are of great importance in prostate cancer. Many similarities exist between the stroma at sites of wound repair and reactive stroma in cancer. Common features include an elevated stromal cell proliferation, altered expression of matrix components, elevated expression of TGF beta-1, neovascularization, and expression of several common stromal markers ([17]).

Prostate development occurs via mesenchymal-epithelial interactions in which urogenital sinus mesenchyme induces epithelial morphogenesis, regulating epithelial proliferation and evoking the expression of epithelial androgen receptors and prostate-specific secretory proteins ([18],[19]). The presence of a stromal androgen receptor is required for this effect, and humoral factors, such as keratinocyte growth factor have been shown to mediate in stromal epiithelial paracrine fashion. The adult prostate is also under control of multiple steroid hormone and paracrine peptide factors, and there is evidence that the prostatic stroma plays a major role in mediation of androgen effects on prostatic epithelium. Thus, prostatic stromal cells seem to be critically involved in growth and progression of prostate cancer. Hence it is not surprising that a marginally tumorigenic cell line such as LNCaP cells acquires much higher tumorigenic and metastatic potential after orthotopic implantation into the prostate ([20]). In addition, hormone independent cell lines become much more tumorigenic and acquire a higher rate of lymph node metastasis after orthotopic rather than after subcutaneous implantation ([21]).

In an effort to develop an "orthotopic milieu" for prostate carcinoma cells in the dorsal skinfold chamber, we have successfully managed to re-establish normal adult murine prostate tissue in dors chambers of recipient mice. The implanted prostate tissue

evokes a dramatic angiogenic response, and 10-14 days after implantation the tissue is fully re-vascularized. In the present study we decided used a modification of this pseudo-orthotopic technique. To achieve this goal we excised adult murine anterior prostate tissue from donor mice and generated hybrid anterior prostate/ TRAMP-C2 prostate carcinoma cell spheroids and implanted these hybrids into the chamber.

Although primary treatment in advanced prostate cancer normally includes some form of hormonal therapy to decrease the level of testosterone, the exact effects brought about by castration are poorly understood. Most prostate cancer does respond initially to androgen ablation and the general belief is that the population of androgen-dependent cells undergo rapid apoptosis upon androgen withdrawal. However, androgen ablation rarely is curative, and most patients will experience recurrence due to takeover of the tumor mass by androgen-independent tumor cells. In contrast to the concept that castration causes rapid apoptosis of androgen-dependent cells ([22]), recent data ([2]) suggest that castration in fact does not cause massive apoptosis but rather results in growth arrest and the cells persist in a dormant, androgen-responsive state for long periods of time, where-after spontaneous androgen-independent outgrowths develop. We present data suggesting that castration in the TRAMP C2 model causes no demonstrable change in mitotic activity, and only a moderate increase in apoptosis. However, in response to castration, we find that TRAMP-C2 cells become highly invasive and migrate away from the tumor. Although it is possible that the downstream molecular genetic pathways being altered following inactivation of P53 and Rb by the large T Ag in the TRAMP system may make these cells less dependent upon stromal growth factors for survival than the

human disease, the apoptotic response of the TRAMP-C2 cells to androgen ablation *in vivo* supports an androgen dependence for survival.

The most pronounced response to castration seen in our model is the dramatic and very rapid vascular regression of the hybrid tumor prostate vasculature. The angiostatic response to castration is not surprising, in view of data demonstrating that androgens, indirectly enhance prostate growth via up-regulation of VEGF from the surrounding stroma ([23]). However, the increase in tumor cell migration from the primary tumor mass suggests that these tumors effectively evade the angiostatic response to castration by invading into non prostatic tissue where the androgen dependence for stromal angiogenesis is not present.

We believe that the ability of our newly developed pseudo-orthotopic prostate tumor model to measure the response of tumor cells to various therapies without animal necropsy and yet determine vascular, mitotic and apoptotic parameters makes this system a promising model to evaluate novel therapies for the treatment of this disease. The strengths of our system lies in the relative speed and mechanistic detail by which therapies can be evaluated for their effectiveness towards prostate tumor growth and survival while maintaining an orthotopic milieu that is needed for many indirect anti tumor regimens such as angiostatic therapy.

In conclusion, our results demonstrate very different growth characteristics for murine prostate cells grown in immuno-competent mice compared to human xenograft prostate cells implanted in immuno-deficient mice. Also our results demonstrate very different growth characteristics of murine prostate cells grown in the present of prostate stroma compared to murine cells grown alone. Furthermore, our results suggest that the

most pronounced response to castration is a dramatic and very rapid vascular regression of the tumor prostate vasculature, and our data thus don't support the concept that castration causes rapid apoptosis of androgen-dependent cells, as previously suggested.

LEGENDS

FIG. 1. photomicrographs illustrating implantation of CMTMR labeled prostate tissue (A), ontop of which a small tumor spheroid (25,000 cells TRAMP-C2), transduced with H2B-GFP (B) is placed.

FIG. 2. Due to the heterogeneous tumor cell distribution, H2B-GFP labeling tumor areas per se do not directly reflect tumor growth i.e., total number of tumor cells. To estimate growth, (relative increase of number of tumor cells), tumor area (A_T) is defined as the sum of pixels with intensity above than 75, and total intensity (I_T) reflecting total number of tumor cells, as the sum of the product of pixels and photo intensity for intensity levels above 75.

FIG. 3 Grafting of anterior prostate from a GFP transgenic mouse. Small tissue pieces of anterior prostate from eGFP transgenic mice were grafted into the chamber of recipient mice. Viability was confirmed by continued expression of eGFP.

FIG. 4 Revascularization of eGFP prostate grafts with prostate derived endothelium. EGFP positive vessels could be visualized to graft with existing unlabeled vessels in the chamber. The majority of eGFP positive vessels connected to existing vasculature as evidenced through blood filled (right panels) eGFP positive vessels (left panels) that were flowing with blood by 7 days postimplantation.

FIG. 5 Viability of prostate tissue post grafting. Viable GFP positive cells could be found 10 days post implantation of eGFP tissues.

FIG. 6. Photomicrographs illustrating the difference in growth characteristics of tumor spheroids obtained from TRAMP-C2 cells only (Tumor alone) and hybrid anterior prostate/ TRAMP-C2 prostate carcinoma cell spheroids (Tumor With Stroma) implanted in dorsal skinfold chambers in syngeneic C57BL/6 hosts.

Fig. 7. Panel A; Growth curves for pure and hybrid tumor spheroids. Between day 0 and day 3, the tumor area increased by 55∀10% however total intensity increased with only 20∀9%, implying that the increase in area is to a large degree due to migration of tumor cells, i.e., cell density is significantly lower at day 5 compared to at implantation. **Panel B**; The increase in tumor area of hybrid spheroids actually reflects true growth (relative intensity). There is a statisticaly significant increase in tumor area (278∀50%; paired t-test p=0.03) as well as in relative intensity (237∀40%; paired t-test p=0.03). **Panels C and D;** Relative mitotic and apoptotic indices. Since mitotic indices were found to be very lows, counting of mitotic and apoptotic bodies were calculated over the entire tumor area, and were adjusted for tumor intensity at each time point.

Fig. 8. Compiled data illustrating that hybrid spheroids were more vascularized than spheroids without stroma.

FIG. 9. Photomicrographs illustrating the profound vascular regression in response to castration, and the invasive growth characteristics seen after castration.

FIG. 10. Illustration of the response to surgical castration Panel A depicting tumor area and relative tumor intensity demonstrates that during the 18 day observation period after castration there was a significant reduction in tumor intensity, while there was no significant change in tumor area. No change could be see in mitotic indices, whrereas apoptotic indices increased slightly (NS) (Panel B). Panel C depicting vascular parameters for castrated mice versus control mice (Day 17), and panel D depicting vascular parameters for castrated mice before and 48 h after castration both show significant reduction in both vascular area and vascular density.

REFERENCES

[1] Porter AT, Target to apoptosis: a hopeful weapon for prostate cancer. Prostate 1997 Sep; 32(4):284-93

[2] Craft N, Chhor C, Tran C, Belldegrun A, DeKernion J, Witte ON, Said J, Reiter RE, Sawyers CL. Evidence for clonal outgrowth of androgen-independent prostate cancer cells from androgen-dependent tumors through a two-step process. Cancer Res 1999 Oct 1;59(19):5030-6

[3] van Weerden WM, Romijn JC. Use of nude mouse xenograft models in prostate cancer research. Prostate 2000 Jun 1;43(4):263-71

[4] Frost, GI; Dudouet B; Lustgarten J; Borgström P. The roles of epithelial mesynchymal interactions and the innate immune response on the tumorigenicity of human prostate carcinoma cell limes grown in immunocompromised mice. Cancer Research, Submitted, 2001.

[5] Greenberg NM; DeMayo F; Finegold MJ; Medina D; Tilley WD; Aspinall JO; Cunha GR; Donjacour AA; Matusik RJ; Rosen JM. Prostate cancer in a transgenic mouse Proc. Natl. Acad.Sci. USA 92:3439-3443, April 1995.

[6] Gingrich JR; Barrios RJ; Morton RA; Boyce BF; DeMayo FJ; Finegold MJ; Angelopoulou R; Rosen JM; Greenberg NM. Metastic Prostate Cancer in a Transgenic Mouse *Cancer Research* **56,** 4096-4102, September 15, 1996.

[7] Gingrich JR; Barrios RJ; Kattan MW; Nahm HS; Finegold MJ; Greenberg NM. Androgen-independent Prostate Cancer Progression in the TRAMP Model *Cancer Research* **57**, 4687-4691, November 1, 1997

[8] Foster BA; Gingrich JR; Kwon ED; Madias C; Greenberg NM. Characterization of Prostatic Epithelial Cell Lines Derived from Transgenic Adenocarcinoma of the Mouse Prostate (TRAMP) Model Cancer Research, 57, 3325-3330, August 15, 1997.

[9] Kwon ED; Foster BA; Hurwitz AA, Madias C, Allison JP, Greenberg N; Burg MB. Elimination of residual metastatic prostate cancer after surgery and adjunctive cytotoxic T lymphocyte- associated antigen (CTLA-4) blockade immunotherapy. PNAS, December 21,1999, vol.96, No26.

[10] Frost, GI; Dudouet B; Lustgarten J; Borgström P. The roles of epithelial mesynchymal interactions and the innate immune response on the tumorigenicity of human prostate carcinoma cell limes grown in immunocompromised mice. Cancer Research, Submitted, 2001.

[11] Lehr H; Leunig M; Menger MD; Messmer K. Dorsal skinfold chamber technique for intravital microscopy on striated muscle in nude mice. Am. J. Pathol. 143,1055-1062, 1993.

[12] Kanda T, et al; Histone-GFP fusion protein enables sensitive analysis of chromosome dynamics in living mammalian cells. Curr Biol, 1998 Mar,

[13] Frost G.I., Dudouet B., Lustgarten J., and Borgström P. The roles of epithelial mesynchymal interactions and the innate immune response on the tumorigenicity of human prostate carcinoma cell limes grown in immunocompromised mice. Cancer Research, Submitted, 2001.

[14] Bucana CD, Fabra A, Sanchez R, Fidler IJ. Different patterns of macrophage infiltration into allogeneic-murine and xenogeneic-human neoplasms growing in nude mice. Am J Pathol 1992 Nov;141(5):1225-36

[15]. Borgström, P., Hillan, K.J., Sriramarao, P. Ferrara, N. Complete inhibition of angiogenesis and growth of micro tumors by an anti-vascular endothelial growth factor neutralizing antibody: Novel concepts of angiostatic therapy from intravital videomicroscopy. Cancer Research, 56, 4032-39, 1996. XX and the combo paper

[16] Greenberg NM; DeMayo F; Finegold MJ; Medina D; Tilley WD; Aspinall JO; Cunha GR; Donjacour AA; Matusik RJ; Rosen JM. Prostate cancer in a transgenic mouse Proc. Natl. Acad.Sci. USA 92:3439-3443, April 1995.

[17] Rowley DR. What might a stromal response mean to prostate cancer progression? Cancer Metastasis Rev 1998-99;17(4):411-9

[18] Condon MS ; Bosland MC. The role of stromal cells in prostate cancer development and progression. In Vivo; 13(1):61-5 1999.

[19] Cunha GR. Role of mesenchymal-epithelial interactions in normal and abnormal development of the mammary gland and prostate. Cancer; 74(3 Suppl):1030-44 1994.

[21] Rembrink K ; Romijn JC ; van der Kwast TH ; Rubben H ; Schroder FH.Orthotopic implantation of human prostate cancer cell lines: a clinically relevant animal model for metastatic prostate cancer. Prostate; 31(3):168-74 1997.

[22] Porter AT, Target to apoptosis: a hopeful weapon for prostate cancer. Prostate 1997 Sep; 32(4):284-93

[23] Levine AC; Liu XH; Greenberg PD; Eliashvili M; Schiff JD; Aaronson SA; Holland JF; Kirschenbaum A. Androgens induce the expression of vascular endothelial growth factor in human fetal prostatic fibroblasts. Endocrinology, Nov, 139:11, 4672-8 1998.

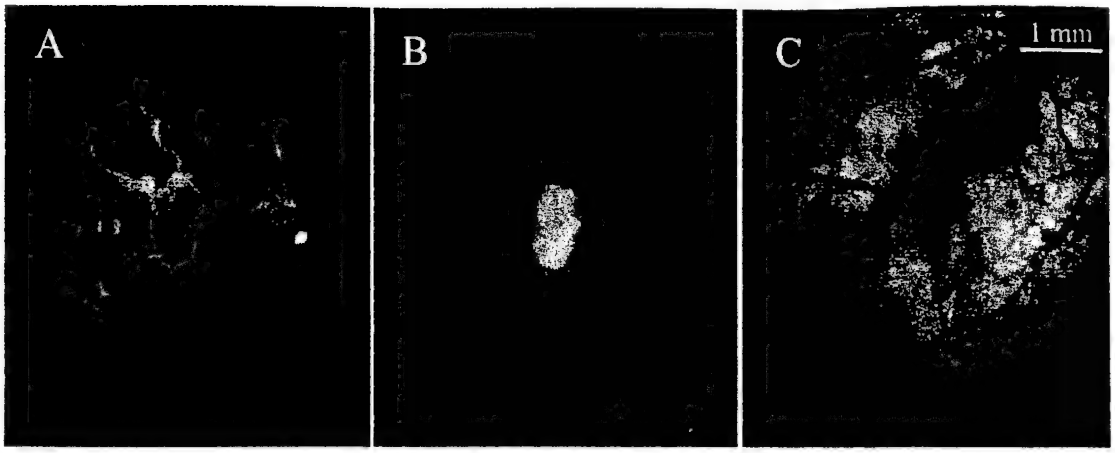

FIG. 1

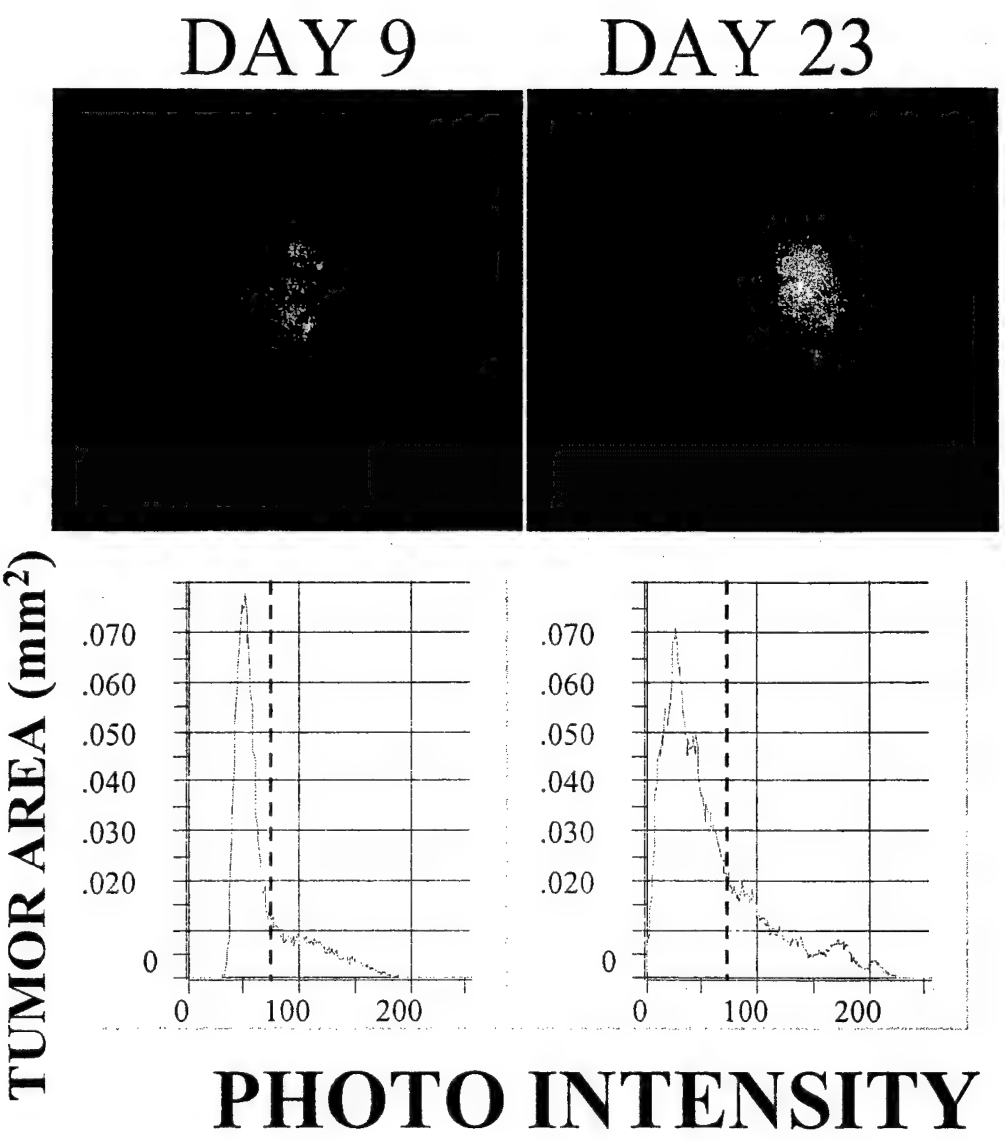
DAY 9
DAY 23
TUMOR AREA (mm²)
.070
.060
.050
.040
.030
.020
0
0
100
200
PHOTO INTENSITY

FIG. 2

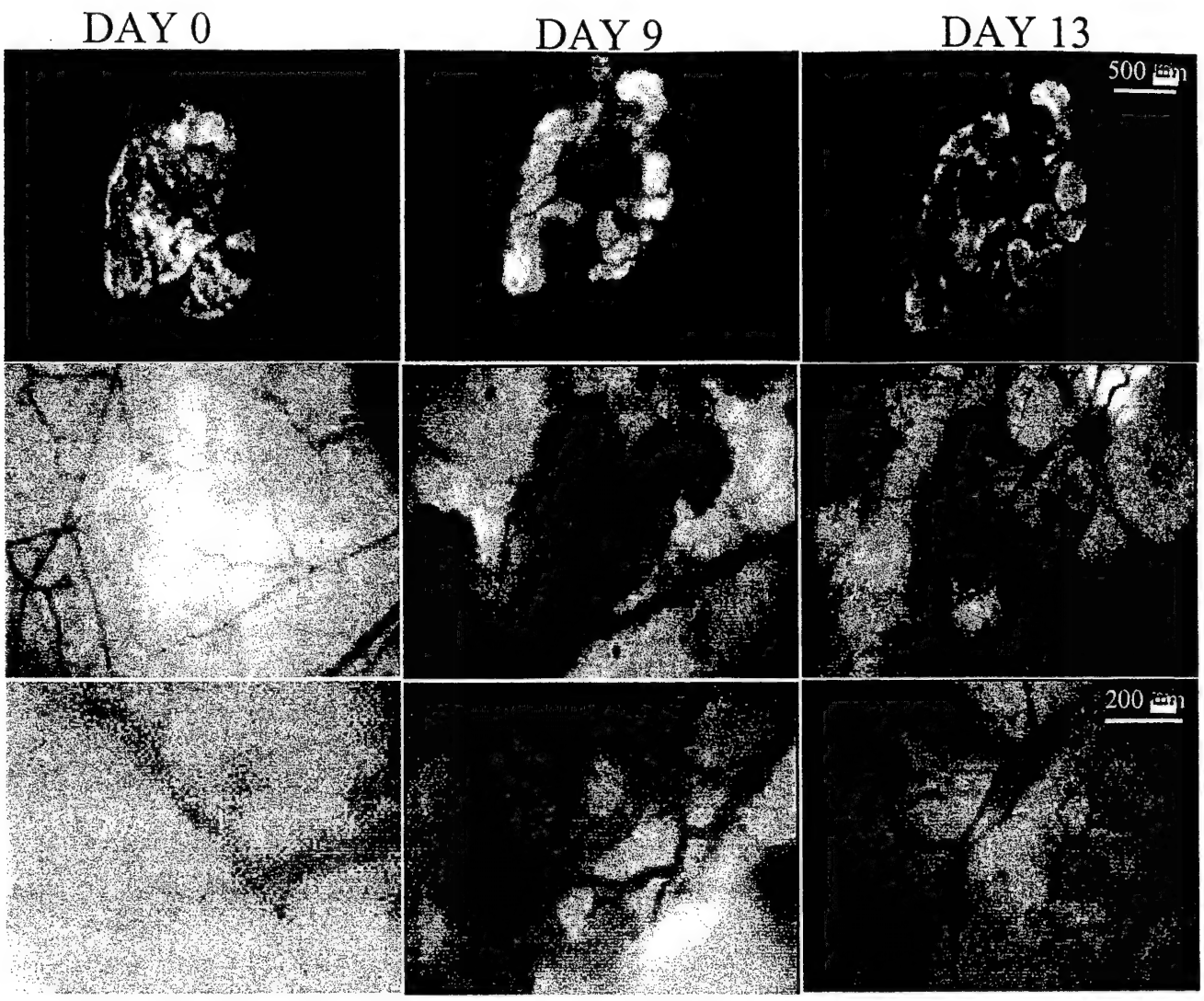

FIG. 3

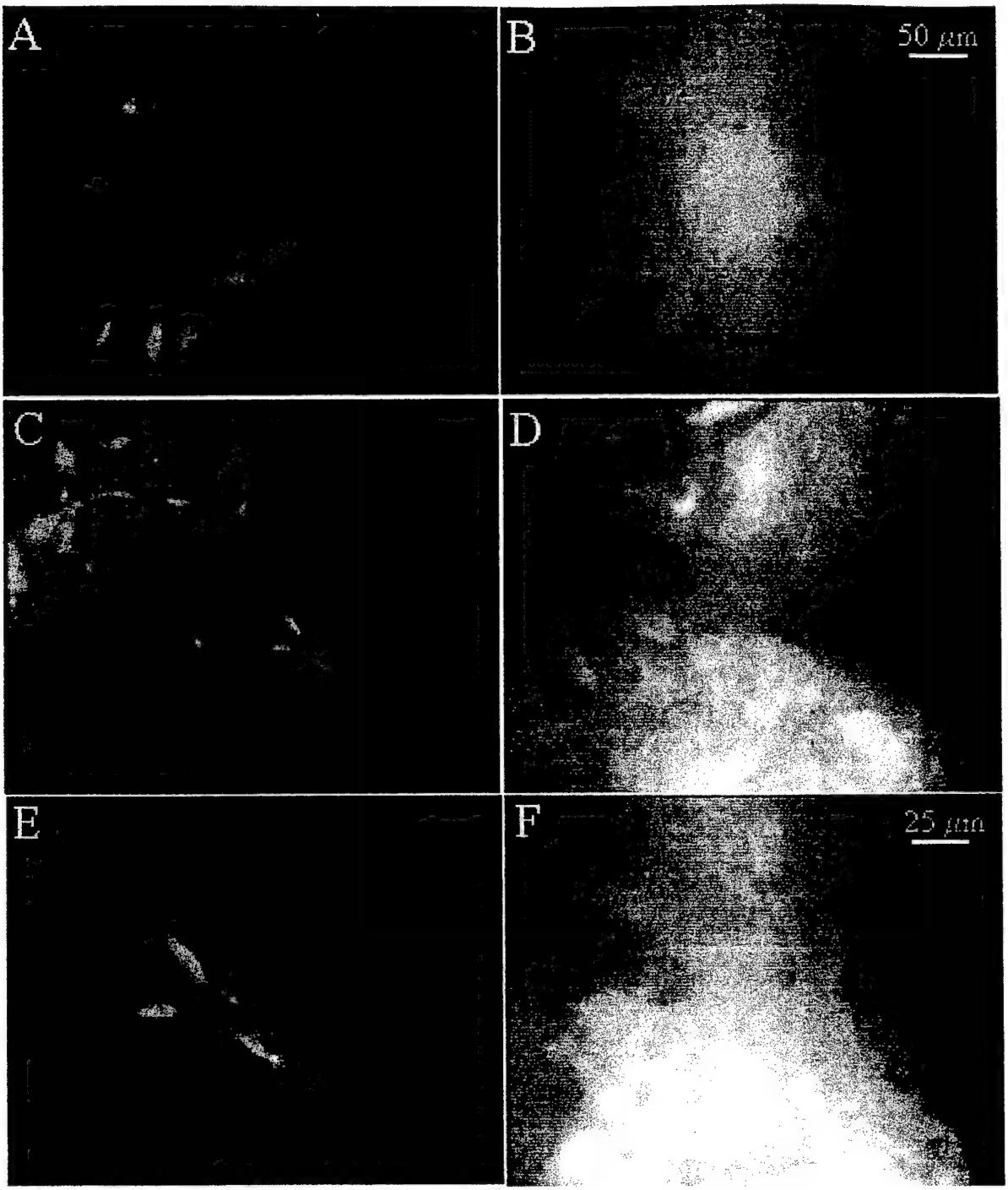

FIG. 4

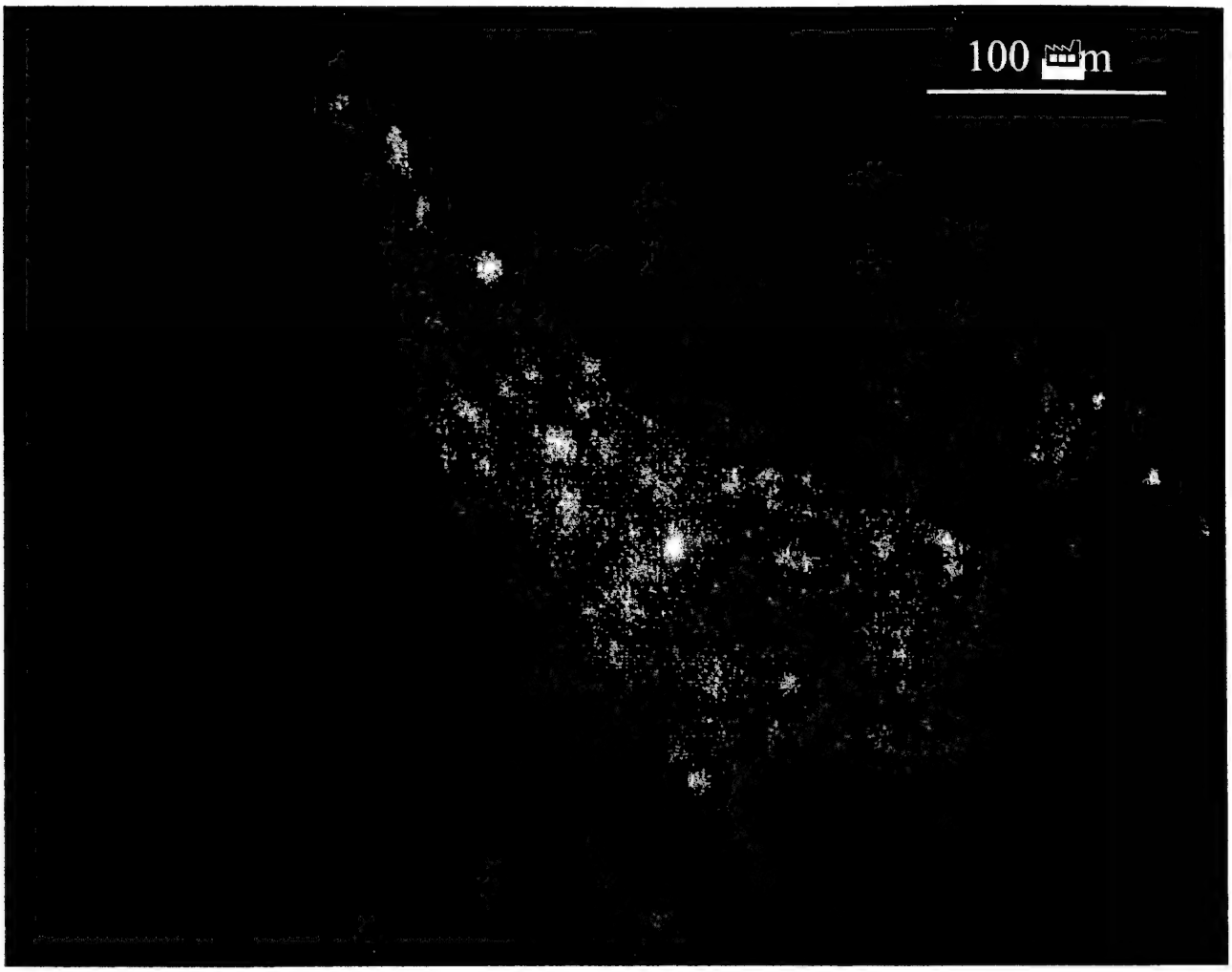

FIG. 5

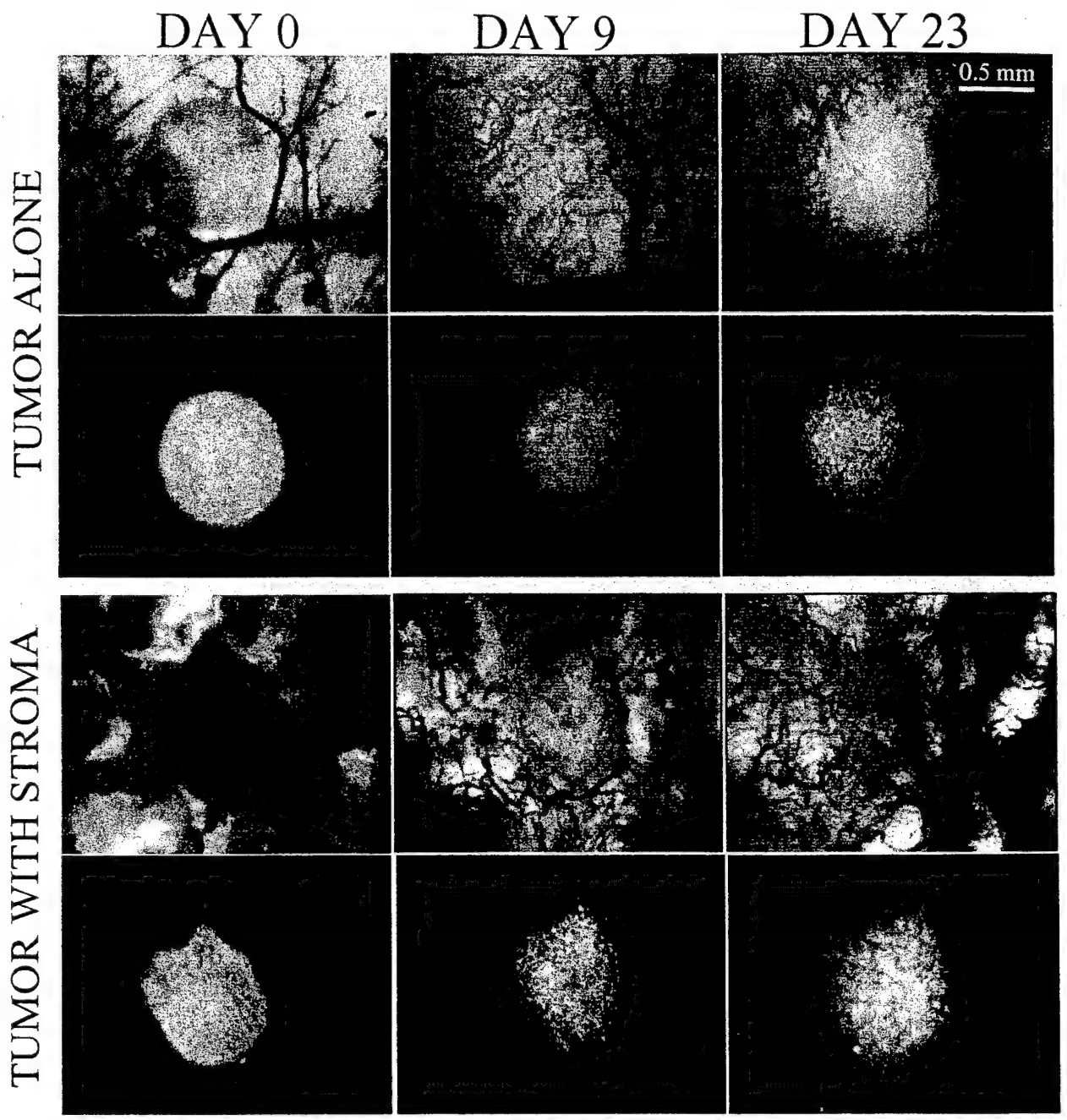

FIG. 6.

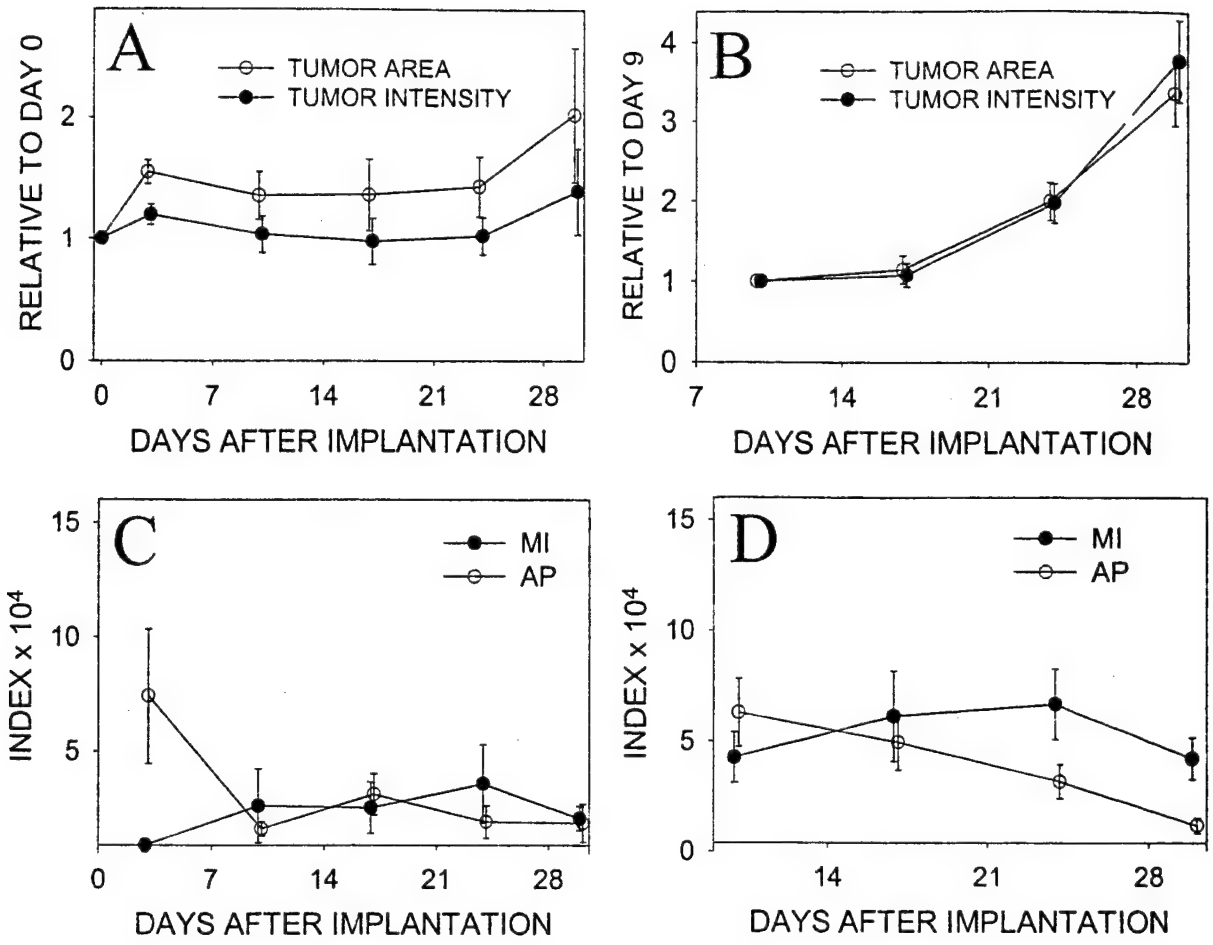
A
TUMOR AREA
TUMOR INTENSITY
RELATIVE TO DAY 0
DAYS AFTER IMPLANTATION
B
TUMOR AREA
TUMOR INTENSITY
RELATIVE TO DAY 9
DAYS AFTER IMPLANTATION
C
MI
AP
INDEX x 10^4
DAYS AFTER IMPLANTATION
D
MI
AP
INDEX x 10^4
DAYS AFTER IMPLANTATION

FIG. 7

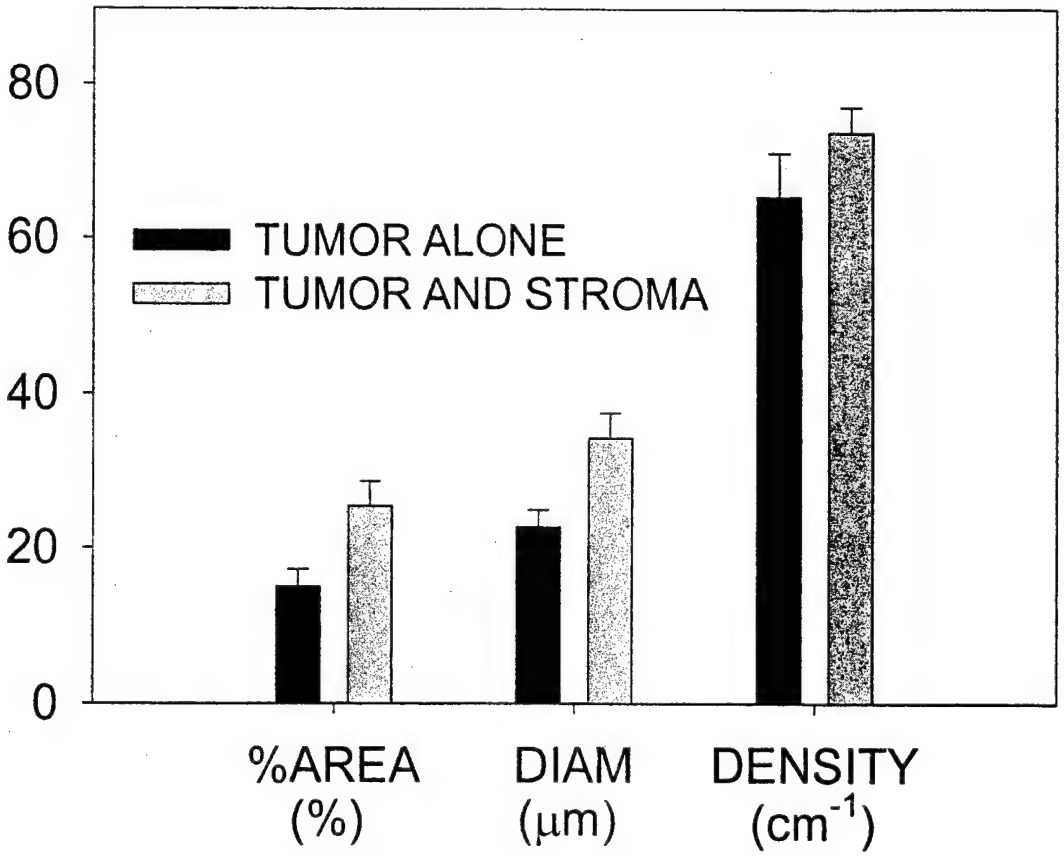
80
60
40
20
0
TUMOR ALONE
TUMOR AND STROMA
%AREA
(%)
DIAM
(μm)
DENSITY
(cm-1)

FIG 8

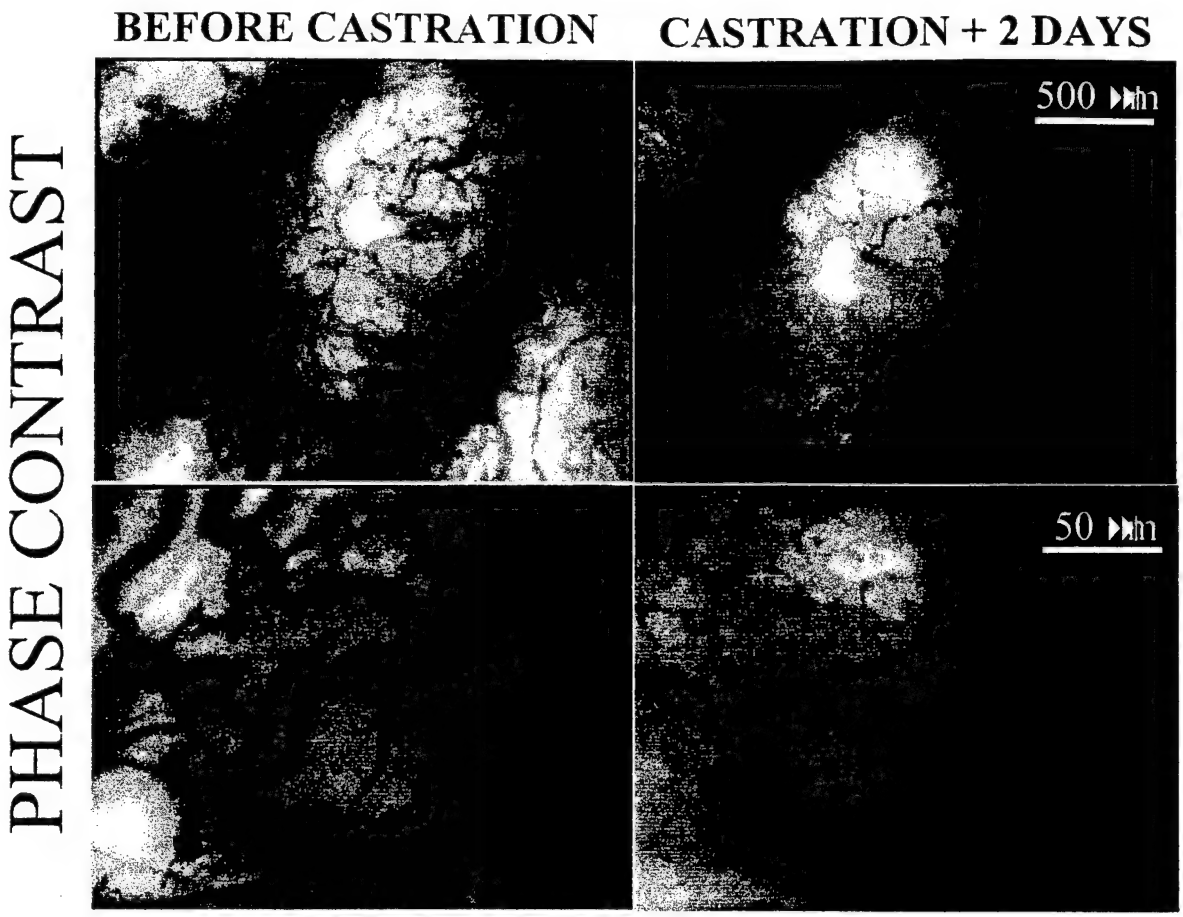
BEFORE CASTRATION
CASTRATION + 2 DAYS
PHASE CONTRAST
500 µm
50 µm

FIG. 9

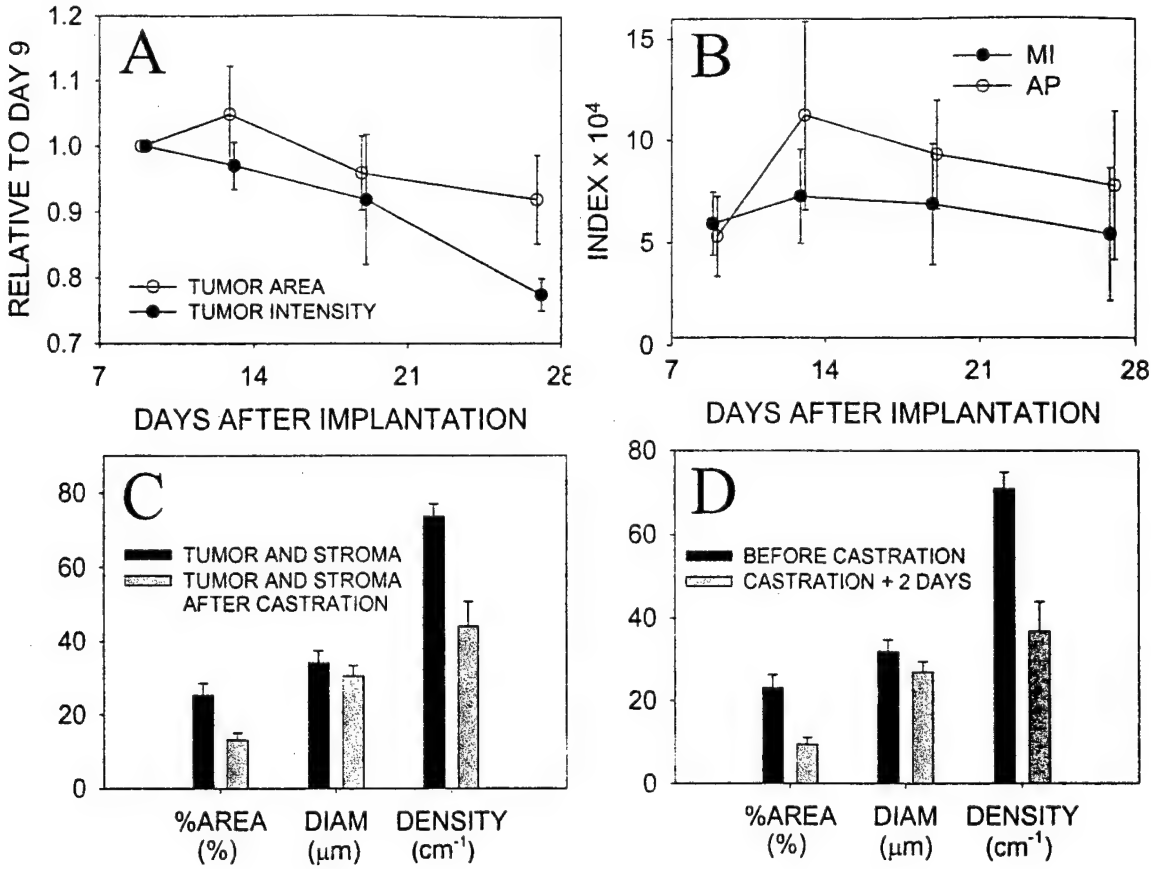
A
RELATIVE TO DAY 9
1.2
1.1
1.0
0.9
0.8
0.7
TUMOR AREA
TUMOR INTENSITY
7
14
21
28
DAYS AFTER IMPLANTATION
B
INDEX x 10⁴
15
10
5
0
MI
AP
7
14
21
28
DAYS AFTER IMPLANTATION
C
80
60
40
20
0
TUMOR AND STROMA
TUMOR AND STROMA AFTER CASTRATION
%AREA (%)
DIAM (μm)
DENSITY (cm⁻¹)
D
80
60
40
20
0
BEFORE CASTRATION
CASTRATION + 2 DAYS
%AREA (%)
DIAM (μm)
DENSITY (cm⁻¹)

FIG. 10

THE ROLES OF EPITHELIAL MESYNCHYMAL INTERACTIONS AND THE INNATE IMMUNE RESPONSE ON THE TUMORIGENICITY OF HUMAN PROSTATE CARCINOMA CELL LINES GROWN IN IMMUNO-COMPROMISED MICE

Gregory I. Frost, Brigitte Dudouet, Joseph Lustgarten, and Per Borgström

Sidney Kimmel Cancer Center, 10835 Altman Row, San Diego, CA 92121

Correspondence: Per Borgström, Sidney Kimmel Cancer Center, 10835 Altman Row, San Diego, CA 92121
Phone: (858) 450 5990 ext 353, E-mail: **pborgstrom@skcc.org**,
E-fax: 305-768-4602

ABSTRACT

Few examples of human prostate cancer micrometastatic growth in immuno-compromised mice exist. In the present study, the growth and angiogenic potential of three human prostate tumor cell lines (DU145, PC3, and LnCAP) were examined using an intravital microscopy system based upon the dorsal skinfold chamber in nude mice. Tumor cells were transduced *in vitro* with a novel Histone H2B-GFP fusion protein to permit measurement of tumor size as well as mitotic and apoptotic indices *in vivo*. Microtumors of the androgen dependent cell line, LNCAP, regressed completely in all animals within seven days post implantation. Such microtumors were poorly angiogenic, undergoing massive apoptosis within 24 hours post implantation with undetectable mitotic indices. Microtumors of the androgen independent cell line, PC3, regressed at a slower rate than LNCAP, with little angiogenesis and high levels of apoptosis, though considerably lower than LNCAP. DU145 microtumors regressed the slowest, demonstrating substantial angiogenic activity, considerably lower apoptotic rates, and measurable mitoses. This pattern was found on both beige nude XID and $^{nu/nu}$ animal backgrounds, ruling out NK cells or xenoantibodies as a host derived mediator of this phenomenon. Mitotic activity and suppression of apoptosis in some of these prostate cancer cell lines could be partially rescued by incorporation of prostate stroma within the tumor spheroids. Nevertheless, increases in tumor mass could not be maintained. Compared to other highly tumorigenic cell lines used in this model, a common feature of the prostate cancer cell lines was poor encapsulation post implantation. Paradoxically, this artifact of tumor xenografts appears to be a prerequisite for the successful growth of microtumors within the chamber system. Syngeneic tumors and human carcinoma

biopsies are frequently infiltrated by tumor associated macrophages (TAMs), yet tumorigenic xenografts in this model excluded the innate immune response. Surprisingly, the growth of poorly encapsulated human prostate carcinoma microtumors could be rescued by systemic administration of dextran, an α1,3, 1-6 linked glucose polymer phagocytosed by macrophages. Our data suggests that the inability to effectively exclude the innate immune system by encapsulation is the principal hurdle to the survival of small micro-tumor xenografts. The complex interactions between tumor cells and TAMs which are pivotal in carcinogenesis, are clearly perturbed by human tumor cells implanted in immunodeficient mice.

INTRODUCTION

Animal models of prostate cancer are crucial to further our understanding of the progression of this disease. Many groups have worked to isolate human prostate tumor cell lines representative of the human disease. Unfortunately, the limited number of prostate tumor cell lines and representative *in vivo* prostate tumor models has considerably hampered research in this field.

We have developed an intravital microscopy model based upon the dorsal skin fold chamber technique in nude mice. This system permits continuous measurement of the growth and angiogenesis of micrometastases. We have used this model system to evaluate therapeutic interventions to various mouse and human cancer cell lines (1). In such studies, a rhodamine-based dye (CMTMR) was utilized to calculate tumor growth. Unfortunately the CMTMR labeling lasted for at most for two weeks, preventing longer studies of tumor growth. Moreover, macrophages that phagocytosed xenografted tumor cells became fluorescent as well, making the true tumor area difficult to calculate.

Green fluorescent protein, GFP, is a spontaneously fluorescent protein isolated from coelenterates, such as the Pacific jellyfish, Aequoria victoria (2). When expressed in mammalian cells, fluorescence from wild type GFP is typically distributed throughout the cytoplasm, but is excluded from the nucleolus and vesicular organelles ([3]). However, highly specific intracellular localization including the nucleus (4), mitochondria (5), secretory pathway (6), plasma membrane (7) and cytoskeleton(8) can be achieved via fusions both to whole proteins and individual targeting sequences. The enormous flexibility as a noninvasive marker in living cells allows for numerous other applications

such as cell lineage tracing, reporting of gene expression and as a potential measure of protein-protein interactions (9).

Kanda et al. (10) recently developed a highly sensitive method for observing chromosome dynamics in living cells. A fusion protein between Histone H2B and eGFP was transfected into human HeLa cells to generate a stable line constitutively expressing H2B-GFP. This H2B-GFP fusion protein was effectively incorporated into chromatin without affecting the cell cycle.

We subcloned this H2B-GFP fusion protein into an LXRN cassette, and by retroviral transduction, introduced H2B-GFP into a number of human prostate cancer cell lines (LNCAP PC3M, and DU145). Following pooled drug selection and/or FACs sorting, homogeneous populations of H2B-GFP expressing tumor cell lines were obtained.

The purpose of the present study was to implement human prostate carcinoma cell lines transduced with the H2B-GFP fusion protein into our dorsal skinfold chamber model system, to simultaneously measure tumor growth, angiogenesis, and mitotic and apoptotic indices in response to therapeutic interventions.

METHODS

Animal model and surgical techniques: The dorsal skinfold chamber in the mouse was prepared as described previously (11). Male mice (25-35 g body weight) were anesthetized (7.3 mg ketamine hydrochloride and 2.3 mg xylazine /100 g body weight, i.p.) and placed on a heating pad. Two symmetrical titanium frames were implanted into a dorsal skinfold, so as to sandwich the extended double layer of skin. A 15 mm full thickness layer was excised. The underlying muscle (M. cutaneous max.) and subcutaneous tissues were covered with a glass cover slip incorporated in one of the frames. After a recovery period of 2-5 days, tumor spheroids were carefully placed in the chamber.

Preparation of tumor spheroids. Histone H2B-GFP kindly provided by Dr Teru Kanda (Salk Institute La Jolla CA) was subcloned into the LXRN retroviral vector (Clontech, Palo Alto CA). The resultant H2B-GFPLXRN vector was cotransfected with VSVG into GP-293 cells (Clontech) and viral supernatants harvested 48 hours post transfection. Retroviral supernatants were concentrated by centrifugation at 50,000xg and stored at –80°C until use. LNCAP-PC, PC3-M, (kindly provided by Dr Dan Mercola, SKCC) and DU145 cells (obtained from ATCC) were transduced with VSVG pseudotyped H2BGFP LXRN virus stocks for 48 hours with 5ug/ml polybrene and selected in 300μg/ml G418 for 2 weeks. Pooled H2BGFP expressing tumor cells as determined by fluorescent microscopy and FACs analysis were expanded and used for *in vivo* experiments. Cells were passaged in DMEM 4.5 gm/L glucose supplemented with pyruvate, glutamine, non essential amino acids, and gentamicin (50μg/ml) and maintained in a humidified 5% CO_2 atmosphere at 37 °C. Cells were routinely tested for mycoplasma

contamination with the Genprobe mycoplasma detection kit. Suspensions of trypsinized monolayers were washed with fresh complete medium viability tested with trypan blue exclusion, and diluted to a final volume of 250,000 tumor cells/ml. The tumor cell suspensions were dispersed 100ul/well into 96 well round bottom plates coated with 1.0 % agarose for a liquid overlay. The spheroids were allowed to compact for 48 hours followed by washing in serum free media for implantation into chambers.

Preparation of hybrid anterior prostate/ prostate carcinoma cell spheroids. Anterior prostate from a donor mouse was excised, minced into small <1mm pieces and digested with Collagenase (Sigma Chemicals) for 30 min at room temperature, followed by digestion with 0.25% trypsin for 15 min with agitation and pipetting. The resultant mixture of epithelium and stroma was washed 3x with complete media. Viability was tested with trypan blue exclusion followed by labeling with CMTMR for Rhodamine counter-label for 15min in serum free media. Labeled prostate was then washed and diluted to 100ul wet pellet per ml complete media (~200ul anterior prostate/mouse) with 1x 10^{-8}/M DHT followed by dilution 1:1 with trypsinized tumor cells to a final volume of 250,000 tumor cells/ml. The tumor cell prostate hybrid suspensions were dispersed 100ul/well into 96 well round bottom plates coated with 1.0 % agarose for a liquid overlay. The spheroids were allowed to compact for 48 hours followed by washing in serum free media for implantation into chambers.

Human Prostate fibroblasts: Peritumor stromal cells were derived from fine needle biopsies of patients with histologically confirmed prostatic carcinoma (kindly provided by Dr. Warren Kessler, Department of Urology, Scripps Mercy Hospital, San

Diego, CA). Explants were grown in DMEM 10% FBS, 10^{-8}M DHT. Stromal cells predominated in these explanted cultures and were used between passages 3-5.

Intravital microscopy : Fluorescence microscopy was performed using a Mikron Instrument Microscope (Mikron Instrument, San Diego, CA) equipped with epi-illuminator and video-triggered stroboscopic illumination from a xenon arc (MV-7600, EG&G, Salem, MA). A silicon intensified target camera (SIT68, Dage-MTI, Michigan City, IN) was attached to the microscope. A Hamamatsu image processor (Argus 20) with firmware version 2.50 (Hamamatsu Photonic System, USA) was used for image enhancement and to capture images to a computer. A Leitz PL1/0.04 objective was used to obtain an over-view of the chamber and for determination of tumor size. A Zeiss long distance objective 10/0.22 was used to capture images for calculation of vascular parameters. A Zeiss Achroplan 20X/0.5 W objective was used for capturing images for calculation of mitotic and apoptotic indices.

Image analysis: For each spheroid, video recordings were used to calculate length, area and vascular density of the neovasculature induced by the implanted tumor spheroids. Vasculature was analyzed off-line from the video recording using a photodensitometric computer software (Image-Pro Plus, Media Cybernetics, MD).

Mitotic and apoptotic indices: At each time point, two peripheral and two central X20 fields of the tumor were captured with a FITC filter using Image-Pro Plus software and an integrated frame grabber. Only mitotic figures from anaphase through early telophase were included in the mitotic index to exclude potential artifact of nuclear membrane distortion. Pyknotic/Apoptotic nuclei were defined by H2B-GFP labeled nuclei with a cross sectional area $<30uM^2$. Nuclear karyorrhexis, easily identified by the vesicular

nuclear condensation and brightness of the H2BGFP was included within this index. Values were expressed as number of figures/mm^2.

Statistical Analysis: Statistical analysis was made using a statistical software package (SigmaStat, Jandel Scientific). Statistical analysis was made using both analysis of variance and multiple comparison tests. For all tests, p values smaller than 5% were considered significant. Data was presented as MEAN ± STD.

RESULTS

We initially reasoned that the rich vascular supply of the skeletal muscle capillary bed would provide a suitable environment for the growth of prostate carcinoma microtumors, as was found with many other cell lines grown in the chamber model **(XXXrefs)**.

In a first series of experiments we implanted tumor spheroids derived from the androgen dependent cell line LNCAP, transduced *in vitro* with an H2B-GFP retrovirus. As illustrated in Figure-1, LNCAP-H2BGFP microtumors demonstrated poor growth, poor angiogenic activity and massive apoptosis following implantation into the dorsal skinfold chamber of $^{nu/nu}$ mice. By 72 hours post-implantation, no mitotic figures could be found and the number of apoptotic/pyknotic nuclei had increased to >300 cells/mm^2.

One plausible explanation for the poor growth of the implanted LNCAP-H2BGFP tumor cells was toxicity due to the ectopic expression of H2BGFP. In other cell lines, the H2BGFP fusion protein generated by Kanda et al. (13) did not alter cell cycle parameters nor viability. In agreement with these findings, we found no obvious *in vitro* changes in the growth rate of the LNCAP H2BGFP variant compared to parental lines (data not shown). For comparison spheroids of the parental LNCAP cell line were labeled with the rhodamine-based dye CMTMR, and were implanted into the chamber model. As shown in figure 1-C, the parental cell line labeled with CMTMR also regressed rapidly following implantation and lacked significant angiogenic activity. The growth data presented in figure-1D illustrates similar regression of tumors from the parental cell line.

Another androgen dependent cell line, LAPC4, was also labeled with CMTMR and demonstrated similar rapid regression *in vivo* (Figure 1D).

The third cell line examined was the androgen independent cell line, PC3-M, transduced with the H2B-GFP virus. Photomicrographs from these experiments (Figure 2A, upper panels) illustrate the lack of growth in the dorsal skinfold chamber, with poor angiogenesis, massive apoptosis, and very few mitotic figures. The compilation of this data is presented in panel B. One common feature of these poorly tumorigenic prostate carcinoma lines was the lack of encapsulation, compared to other human cell lines that grow very effectively in the dorsal skinfold chamber system. Unlike most syngeneic tumors and human tumor biopsies, apoptotic indices were much higher in the periphery of the microtumors than in the center (panel B), suggesting cell death was occurring from the outside in. This finding would also seem to rule out death due to a lack of angiogenesis within the central tumor mass.

The forth cell line to be tested was the androgen independent DU145 (transduced with H2B-GFP). As illustrated in Figure 2A, the DU145 H2BGFP cells survived longer than the other cell lines, with higher angiogenic activity and lower apoptotic and higher mitotic indices. Nevertheless, the DU145 tumors were still unable to maintain positive growth *in vivo*. An interesting finding was that DU145 tumor spheroids grew more encapsulated than the other cell lines. Cell death still occurred from the outside in, as demonstrated from higher apoptotic indices in the periphery, and mitotic plates were confined to the center of the tumor.

One plausible explanation for the poor growth of the human prostate carcinoma cell lines in our chamber model could be the implantation on skeletal muscle connective

tissue. To examine whether the poor tumor growth was simply due to the lack of appropriate tumor-mesenchymal interactions, we co-implanted tumor cells with ectopically implanted murine prostate tissue. Hybrid tumor-prostate tissue spheroids were generated by mixing excised anterior prostate tissue from donor nu/nu mice labeled with CMTMR (rhodamine) and mixed with 25,000 H2B-GFP PC3 M cells. Hybrid spheroids were implanted into chambers as before.

Representative photomicrographs from Figure 3 (A) demonstrates the inability of these tissue to permit prostate microtumor survival. Despite the addition of prostate stroma (upper panels), PC3 M tumors continued to regress. The compiled data from these experiments (B), suggested that even though the addition of murine prostate stroma does enhance tumor growth, tumors were still unable to survive in the chamber model.

Photomicrographs obtained from these experiments (Figure 4) illustrates the invasive behavior of tumor cells into the stroma (A and B), and the high angiogenic response induced by the implanted prostate tissue (C and D). Despite the supplementation with murine prostate, hybrid spheroids still displayed very high apopototic indices in the periphery of the tumor and remained poorly encapsulated (E, F, G, and H). However, the stroma did increase tumor cell proliferation in the center of the tumor.

As the tumors still regressed in the presence of murine prostate stroma, we next examined whether human prostate stroma could support growth of the human prostate cancer cell lines. We therefore cultured early passage human prostate fibroblast cultures generated from thin needle biopsies of human prostate carcinoma patients. The fibroblasts were mixed with the prostate cancer as hybrid spheroids prior to implantation

in the dorsal skinfold chamber. As seen in Figure 5, the introduction of human fibroblasts significantly improved the growth of the human cell lines by decreasing apoptosis mainly in the periphery of the tumor (Fig 5). Unfortunately, tumor spheroids still regressed and were unable to maintain positive growth.

As the DU145 cell line demonstrated the slowest regression in our system (Fig. 6), and we therefore decided to further compare the behavior of H2B GFP DU145 cells combined with the human prostate fibroblasts. In these experiments, two tumor spheroids were implanted in each chamber. As shown in Figure 6, the addition of human prostate cancer fibroblasts significantly enhanced tumor growth. Underlying this enhanced tumor cell growth we found increased tumor cell proliferation, mostly confined to the center of the tumors. However, despite the addition of the fibroblasts, we eventually still encountered massive apoptosis mainly confined to the periphery of the tumors (K).

Interestingly, the introduction of human prostate stromal fibroblasts labeled with CMTMR, revealed a massive infiltration of phagocytic host cells engulfing the human fibroblasts, as determined from a large number of CMTMR labeled vacuoles in the vicinity of the tumor spheroid (Fig. 6, panel I). The enhanced growth of the hybrid human stroma/DU145 spheroids was temporary, such that by seven days post implantation, few viable CMTMR positive fibroblasts could be found at the tumor site and the growth of the DU145 cells subsided.

Surprisingly, fibroblasts implanted alone did not cause significant phagocyte infiltration as determined by vesicular CMTMR staining, suggesting a dominant phagocytic recruitment to the spheroids by the tumor cells. The introduction of human

fibroblasts obtained from prostate cancer tissue thus could not resolve the poor growth *in vivo* of the human prostate cancer cell lines.

Tumors are frequently infiltrated by numerous cells of the monocytic lineage, commonly referred to as tumor associated macrophages (TAMs). Such cells can be found within the tumor mass and surrounding the tumor in human tumor biopsies and in syngeneic tumor models. These TAMs are postulated to exert diverse effects, including neovascularization, growth, inflammation and stroma formation.

One plausible explanation why the human prostate tumor cells failed to grow in our chamber system was that TAMs encountering the foreign human cancer cells participated in a T-cell independent innate antitumor response against the human tumor xenografts. The massive apoptosis in the periphery thus could be a result of such an innate immune response.

Many other human cell lines grow successfully in this system labeled with H2B GFP (HT1080, A673, MDA-231). One common characteristic of these cell lines is that they become encapsulated, effectively excluding infiltration of macrophages. One common characteristic of the human prostate cell lines tested in the chamber model was that they never become encapsulated. As demonstrated in Figure 7, vast differences in encapsulation were found between the highly tumorigenic human fibrosarcoma cell line HT1080 and the prostate carcinoma lines. Such encapsulation could effectively exclude macrophages from the tumor site, whereas the poorly encapsulated PC3 M tumor cells are exposed to the infiltrating innate immune cells, which engulf the slowly dividing cells.

To visualize the phagocytic cells, 100 µl of 2% FITC Dextran 500,000 was injected i.v., 24 hours prior to the observation, so that phagocytic cells that engulfed the FITC dextran could be visualized (Panels A, E, and F). Panel A in figure 8 illustrates the abundance of phagocytes labeled with FITC present in the chamber. Such phagocytes having engulfed the CMTMR labeled fibroblasts also become labeled with rhodamine (Panels B, C, and D). As shown in panels B, C, and D, rhodamine fluorescent macrophages could be found in the vicinity of a PC3 M tumor mixed with CMTMR labeled fibroblasts. Panels E and F demonstrate FITC-labeled phagocytes engulfing tumor cells.

We found that injection of Dextran (MW 500,000) injected repeatedly i.v. for 48 hours prior to implantation dramatically inhibited the phagocytototic activity towards tumor cells. Phagocytotic activity is checked by subsequent injection of FITC-dextran, and the absence of fluorescent macrophages suggests that macrophages have become saturated by the dextran.

In an attempt to test our hypothesis that the human prostate tumor cells failed to grow in our chamber system because of the tumorcidal TAMSs, we pretreated the mice with dextran. The mice received 200 µl dextran for two days prior to implantation, 200 µl at the day of implantation, followed by 10 daily injections of 100 µl all given i.v.

In these series of experiments, we had two groups of untreated nude mice (controls). The first group was implanted with tumor spheroids obtained from H2B GFP PC3 cells, and the second group was implanted with tumor spheroids obtained from a mixture of the PC3 cells and cultured human prostate fibroblasts. A third group of mice were implanted with the PC3 fibroblast mixture, and treated with dextran as described

above. Figure 9 illustrates the pronounced effect of pretreatment with dextran on tumor growth, whereas the addition of fibroblasts only marginally and transiently enhances tumor growth. Panel B depicts mitotic and apoptotic indices obtained from these experiments 5 and 10 days after implantation, illustrating significantly lower apoptotic as well as significantly higher mitotic indices in tumors of dextran treated mice.

DISCUSSION

In the present study we demonstrate that tumor spheroids obtained from human prostate carcinoma cell lines regress when implanted in the dorsal skinfold chambers of immunodeficient mice. The androgen dependent cell lines LNCAP and LAPC4 displayed rapid regression, with tumor spheroids being absent within 7 days post implantation. These cells were poorly angiogenic, and displayed massive apoptosis and very low mitotic indices. The androgen independent cell line PC3 regressed slower than LNCAP cells, had a weak angiogenic response, and displayed a high apoptotic rate, though considerable lower than LNCAP. DU145 cells regressed the slowest of the three cell lines, possessed higher angiogenic activity, considerably lower apoptotic rates, and measurable mitotic rates

The effects of subverting peritumor phaogocytes in the chamber through administration of a poorly catabolized polymer on the ability of prostate tumor cells to survive in the chamber model explained the ability this group to grow prostate tumors in the chamber previously. FITC labled dextran was administered in animals to visulize the tumor vasculature throughout the course of tumor growth. When a change was made to using H2B GFP tumors, FITC dextran was excluded from our protocol due to the wavelength overlap between the GFP and FITC dextran. When tumors failed to grow following H2B GFP transduction, the first assumption was that the H2B GFP toxicity was effecting tumor survival. However, after a careful dissection of the lack of tumor growth, it became apparent that the dextran was what apparently enabled the prostate tumors to grow in the chamber system. The subcutaneous space is occupied by a high density of macrophages, which presumably play a role in the innate defense against

pathogens that have breached the epidermis. While some studies have shown orthotopic models to support the growth of prostate carcinoma cells at a low inoculum, most subcutaneous studies use much larger numbers of tumor cells. It is possible that the inoculation of a high number of tumor cells sub cutaneously serves a similar function to the dextran in flooding the phagocytic cells with material. The tumor cells that remain are thus capable of propagation by outnumbering the local phagocyte population. Alternatively, the wound response generated by the chamber model promotes a higher density of marophages in the peritumor site and thus generate a greater challenge for human tumor xenografts. In either case, the ability of some tumor cells to form effective capsules and grow within the chamber site suggests that the innate immune response can be overcome in many circumstances by other human tumor cell lines as well as syngeneic tumors.

These studies point to the difficulty in study micrometastatic growth in xenograft systems when large numbers of phagocytic cells are present. As Beige Nude XID cells were also unable to support growth, a dominant role of NK cells or xenoantibodies could be largely excluded. The ability of systemic dextran treatement to divert the attention of phagocytes from the microtumors is a feasible strategy, but again raises question to the validity of xenograft studies grown in the subcutaneous space. While transplantation of murine prostate tissue into the chamber did not rescue the prostate tumor cells, it is possible that the surrounding chamber macrophages were still able to attack the tumor mass.

Data currently available suggests that in solid tumors, the TAMs can in fact induce immune suppression of host defenses in situ, through release of suppressive

specific cytokines, prostanoids and other humoral mediators. Converslely, TAMs can also participate in the immunologic anti-tumor defense mechanism through cytotoxic activities, such as direct cellular cytotoxicity and the release of cytokines and reactive oxygen species.

There is substantial evidence that tumor-mesenchymal interactions, are critical for prostate cancer progression (Fig 10). The reactive stroma in prostate cancer demonstrates elevated stromal cell proliferation, altered expression of matrix components, elevated expression of TGF beta-1, neovascularization, and expression of several common stromal markers([14]). Recent data also demonstrate that androgens, indirectly enhance prostate growth via up-regulation of VEGF in the surrounding stroma ([15]).

The poor angiogenic response and tumor growth in our system of human prostate cell lines could thus in part be attributed to lack of mesenchymal-epithelial interactions. We tested this hypothesis using both murine and human prostate mesenchyme. We utilized murine prostate as well as human prostate cancer fibroblast spheroid hybrids.

An interesting finding from these experiments was that grafted prostate tissue induced a very strong angiogenic response alone even without tumor cells being present. However, the introduction of murine prostatic stroma did only transiently enhance the growth of the human prostate cancer cell lines and we still observed very low mitotic and very high apopototic indices. In subsequent experiments we cultured human prostate fibroblasts at low passage obtained from a thin needle biopsy from a human prostate carcinoma patient. The introduction of human fibroblasts did significantly improve the

growth of the human cell lines. However, the introduction of fibroblasts which were labeled with CMTMR revealed massive infiltration of phagocytic host cells, and such cells engulfed the human fibroblasts, as evidenced from a large number of CMTMR labeled macrophages in the vicinity of the tumor spheroid. Consequently, the enhanced growth of the human prostate cells was only temporary, and when no live fibroblasts remained the proliferative response of the tumors ceased and tumors regressed.

Tumors are frequently infiltrated by numerous tumor associated macrophages (TAMs), which can be found within the tumor mass or surrounding the tumor. The TAMs excert diverse effects, including neovascularization, growth stimulation, and stroma formation. In solid tumors, TAMs can induce immune suppression of host defenses *in situ*, through release of specific cytokines, prostanoids and other humoral mediators. However, such TAMs can also participate in the innate rejection through cytotoxic activities. It is likely that the complex interactions between tumor cells and TAMs which are pivotal in tumor biology, could be perturbed when "foreign" human tumor cells are implanted in immunodeficient mice.

This concept is supported by earlier findings illustrating very different macrophage behavior in connection with human xenographs in immunodeficient mice as opposed to the growth of syngeneic murine tumors.

Bucana et al., ([16]) studied the distribution pattern of TAMs in murine and human neoplasms growing subcutaneously in nude mice. The TAMs were studied immunohistochemically by the use of several antibodies, including the macrophage-specific F4/80. The pattern of TAM distribution differed dramatically and consistently between mouse and human tumors. Regardless of histologic classification, TAMs were

uniformly distributed throughout murine neoplasms growing in syngeneic or nude mice. In tumorigenic human neoplasms however, TAMs were restricted to the periphery of the lesions and in association with fibrous septae.

Lapis et al. ([17]) also studied the effect of macrophages on tumor progression using human colorectal tumors transplanted in immune-suppressed mice and metastasizing Lewis lung carcinoma. Such results indicated that the activity of macrophages influences markedly the tumor progression, even in hosts with a damaged T-cell population.

Our data demonstrate that TAMs participate in the innate defense mechanism rather than facilitating the tumor progression, resulting in high numbers of apoptotic cells in the periphery of the prostate tumors and mitotic cells in the center characteristics which are not representative of tumor biology. However, the relevance of these findings in light of the role TAMS appear to play in syngeneic environments make these anti tumor effects appear more an artifact of xenografting.

In the past, we have successfully grown various other human cell lines in our system (HT1080, A673, MDA231). One common characteristic of these cell lines was that they became effectively encapsulated, and excluded infiltration of macrophages. A characteristic of all of the human prostate cell lines we have tested in the present paper, is that they are very invasive and do not become encapsulated. Thus, they are exposed to infiltrating TAMs which are able to eliminate the foreign cells, perhaps through recognition of foreign proteins or carbohydrates on the human tumor cell surface. The results from our experiments where we inhibited the phagocytotic activity of the TAMs by pretreatment of the mice with dextran, lend strong support to our hypothesis that the human prostate tumor cells failed to grow in our chamber system because of a strong

innate antitumor response to the human tumor xenografts. The success of inoculations with large numbers of human prostate tumor cells as occurs in most sub-cutaneous models may be due to the fact that the tumor cells effectively "outnumber" the innate immune response and permit tumor survival after effective encapsulation occurs. Interestingly, it has been reported that human prostate tumors grown subcutaneously grow encapsulated ([18]).

In conclusion, we provide evidence that the poor angiogenic activity and lack of growth of human prostate carcinoma cell lines ectopically implanted in immunodeficient mice partly can be explained by the lack of tumor-mesenchymal interactions, but more importantly because of the human prostate carcinoma cell lines being unable to repel the innate immune responses.

AKNOLEDGEMENT

We thank Dale Winger for his excellent assistance in the preparation of the dorsal skinfold chamber.

This work was supported by research grants from NCI (XX), and from DOD (XX).

LEGENDS

FIG. 1. Photomicrographs illustrating the poor growth, poor angiogenic activity, and massive apoptosis of LNCAP cells tranduced with H2B-GFP, implanted in dorsal skinfold chambers in nude mice (A). Compiled data from LNCAP tumor spheroids in nude mice demonstrating rapid regression, tumors disappear within 1 week after implantation, without inducing more than at most early budding. Behind the rapid regression there is massive apototosis, and very low mitotic activity (B). Photomicrographs demonstrating that the parental LNCAP cell line has similar growth characteristics as the H2B-GFP clone, suggesting the the poor growth is not due to the H2B-GFP tranduction (C). Compiled data demonstrating that the parental LNCAP cell line labeled with CMTMR, has similar growth characteristics as the H2B-GFP clone. Also the androgen dependent cell line LAPC4 displayed similar growth characteristics, and tumor spheroids disappeared within a week after implantation (D).

FIG. 2. The upper panels in A show photomicrographs obtained from an experiment where tumor spheroids of PC3M H2B-GFP cells were implanted in chambers of nude mice, again demonstrating very poor angiogenic activity and tumor regression The lower panels in A show photomicrographs from experiments where tumor spheroids from the androgen independent DU145 cell line were implanted in chambers in nude mice. These photos illustrate that the DU145 spheroids are much firmer, has a tendency

towards encapsulation, and has much higher angiogenic activity than LNCAP and PC3 cells. Compiled data demonstrating that androgen independent PC3M spheroids regressed slower that LNCAP, and spheroid remnants were still present 10 days after implantation, which could be attributed to somewhat lower apoptotic indices. There were statistically higher apoptotic indices in the periphery for both day 4 and 10 (B). Photomicrographs illustrating that PC3M tumor spheroids contained numerous apoptotic bodies. Interestingly, there were much higher apoptotic indices in the periphery of the tumors than in the centers, i.e., the tumors were dying from the outside in (C). Compiled data from DU145 spheroids illustrating a slower regression rate than for PC3M, a much higher angiogenic activity, regular vascular networks being formed within 10 days after implantation. DU145 cells also had much lower apoptotic indices than PC3M cells, and the DU145 cells even displayed some measurable mitotic indices, mostly confined to the center of the tumors (D).

FIG. 3. Photomicrographs showing growth characteristics of hybrid anterior prostate/ PC3M prostate carcinoma cell spheroids**.** The upper panels show H2B-GFP labeled tumor cells, the middle panel shows CMTMR labeled prostate stroma, and the lower panels demonstrate the high angiogenic activity possessed by the hybrid spheroids (A). Compiled data from an experiment where we had three groups of animals, implanted with spheroids obtained from PC3M cells alone, prostate PC3M hybrid spheroids, and spheroids obtained from a mixture of prostatic fibroblasts (obtained from a thin needle biopsy from a human prostate carcinoma) and PC3M cells. The figure demonstrates that PC3M prostate spheroids regressed slower than the PC3M fibroblasts mixture, however

none of the groups showed actual growth. At day 4, PC3 + prostate tumors were significantly larger than tumors from PC3 cells alone (B).

FIG. 4. Photomicrographs from PC3M hybrid spheroids, which more in detail illustrate that tumor cells invade the stroma (A and B), and the intense rapid re-vascularization of the hybrid spheroids (C and D). The lower panels photomicrographs illustrate the large number of apoptotic bodies in the tumor periphery, and the presence of mitotic plates in the tumor center, suggesting that also the hybrid spheroids dye from the outside in.

FIG. 5. Apoptotic indices in the periphery of the tumors show a significant reduction in apoptotic indices in tumors obtained from PC3 cells mixed with either prostate or fibroblasts compared to tumors obtained from PC3 cells alone.

FIG. 6. Photomicrographs from experiments where two sets of spheroids were implanted per chamber; DU145 spheroids, and a mixture of prostatic fibroblasts (obtained from a thin needle biopsy from a human prostate carcinoma) and DU145 cells. The upper panels (A, B, C) indicate that the mixture regresses slower than the pure DU145 spheroids. The middle panels (D, E, F) obtained from a mixed spheroid demonstrate that even though these spheroids were quite compact, there are still a large number of apoptotic cells in the periphery of the tumors. These experiments revealed a massive infiltration of macrophages (MOs), which became fluorescent after engulfing the CMTMR labeled fibroblasts (I). Compiled data revealing that the mixed spheroids initially (first 3 days)

actually showed positive growth, where-after they started to regress. The regression coincided with infiltration of Mos (J). Apoptotic and mitotic indices obtained from DU145 spheroids and the fibroblast DU145 mixture spheroids. Pure DU145 spheroids had massive apoptosis mostly confined to the periphery of the tumors, and unmeasurably low mitotic indices. The mixed spheroids had significantly lower much lower apoptotic indices in the periphery, and also mitotic indices where significantly higher, being in the order of 5-10 per mm^2 (K).

Fig 7. A common feature of the three human prostate carcinoma cell lines investigated in the present study was very poor encapsulation, with the fasted regressing cell line displaying the least encapsulation. Other human cell lines which grow well in the dorsal skinfold chamber have one thing in common, as exemplified in the lower panels by the fibrosarcoma cell line HT1080, very tight encapsulation.

FIG. 8. Photomicrographs illustrating macrophage interaction with tumor cells and fibroblasts in a mixture of prostatic fibroblasts (obtained from a thin needle biopsy from a human prostate carcinoma) and PC3 M cells. FITC Dextran (2%, 100 µl, i.v.) was injected 24 hours prior to the observation, and macrophages which have phagocytozed the dextran are fluorescent. Panel A illustrates the abundance of FITC fluorescent macrophages present at the tumor site (TAMs). The fibroblasts were prelabeled with the rhodamine based CMTMR in vivo dye, and panels B, C, and D show macrophages which are rhodamine fluorescent after phagocytozing fibroblasts. Panels E and F show macrophage killing tumor cells.

FIG. 9 Compiled data from experiments with implantation of spheroids obtained from PC3M cells alone and spheroids obtained from a mixture of prostatic fibroblasts (obtained from a thin needle biopsy from a human prostate carcinoma) and PC3M cells. Two groups were used as controls, and received no treatment (PC3 ALONE, and PC3 + FB). A third group which was implanted with the tumor cell fibroblast mixture was pretreated two days prior to implantation with 200 µl 10% dextran 500,000, followed by daily treatments with 200 µl for ten days, all given i.v. The figure demonstrates regression of tumor spheroids in both control groups, but a positive growth in mice being treated with dextran. At day 15, the tumors in mice treated with dextran were significantly larger compared to tumors of both control groups (A). Apoptotic and mitotic indices from spheroids obtained from PC3 cells alone and spheroids obtained from a mixture of prostatic fibroblasts and PC3 cells. Two groups were used as controls, and received no treatment (PC3 ALONE, and PC3 + FB). A third group which was implanted with the tumor cell fibroblast mixture was treated with dextran i.v., according to above. Tumors in untreated mice displayed massive apoptosis mostly confined to the periphery of the tumors, and very low mitotic indices. The mixed spheroids in mice treated with dextran had significantly lower apoptotic indices, but also significantly higher mitotic indices being in the order of 5-10 per mm^2 (B).

FIG. 10. Evidence is accumulating demonstrating that tumor-mesenchymal interactions, are of great importance in prostate cancer. One example is that androgens, indirectly enhance prostate growth via up-regulation of VEGF from the surrounding stroma. In the

absence of stroma, it's very likely that poor growth, and poor angiogenesis will result. Tumors are frequently infiltrated by numerous monocytes/macrophages (TAMs), which can be found within the tumor mass or surrounding the tumor. The TAMs excert diverse effects, including neovascularization, growth rate, and stroma formation. We hypothesize that in a xenograph, TAMs are reprogramed to participate in the immunological antitumor response.

[1] Borgstrom P, Gold DP, Hillan KJ, Ferrara N Importance of VEGF for breast cancer angiogenesis in vivo: implications from intravital microscopy of combination treatments with an anti-VEGF neutralizing monoclonal antibody and doxorubicin. Anticancer Res 1999 Sep-Oct;19(5B):4203-14

[2] Morin, J. and Hastings, J., 1971. Energy transfer in a bioluminescent system. J. Cell Physiol. 77: 313-8.

[3] Cubitt, A., Heim, R., Adams, S., Boyd, A., Gross, L. and Tsien, R., 1995. Understanding, improving and using green fluorescent proteins. TIBS. 20: 448-55

[4] Kanda T, Sullivan KF, Wahl GM. Histone-GFP fusion protein enables sensitive analysis of chromosome dynamics in living mammalian cells. Curr Biol 1998 Mar 26;8(7):377-85

[5] Rizzuto, R., Brini, M., De Giorgi, F., Rossi, R., Heim, R., Tsien, R. and Pozzan, T., 1996. Double labeling of subcellular structures with organelle-targeted GFP mutants in vivo. Curr. Biol.6: 183-188.

[6] Kaether, C. and Gerdes, H., 1995. Visualization of protein transport along the secretory pathway using green fluorescent protein. FEBS Lett. 369: 267-271.

[7] Marshall, J., Molloy, R., Moss, G., Howe, J. and Hughes, T., 1995. The jellyfish green fluorescent protein: a new tool for studying ion channel expression and function. Neuron. 14:211-215.

[8] Kahana, J., Schapp, B. and Silver, P., 1995. Kinetics of spindle pole body separation in budding yeast. Proc. Natl. Acad. Sci., USA. 92: 9707-9711.

[9] Mitra, R., Silva, C. and Youvan, D., 1996. Fluorescence resonance energy transfer between blue-emitting and red-shifted excitation derivatives of the green fluorescent protein. Gene. 173: 13-7.

[10] Kanda T, Sullivan KF, Wahl GM. Histone-GFP fusion protein enables sensitive analysis of chromosome dynamics in living mammalian cells. Curr Biol 1998 Mar 26;8(7):377-85

[11] Lehr H; Leunig M; Menger MD; Messmer K. Dorsal skinfold chamber technique for intravital microscopy on striated muscle in nude mice. Am. J. Pathol. 143,1055-1062, 1993.

[12] Morin, J. and Hastings, J., 1971. Energy transfer in a bioluminescent system. J. Cell Physiol. 77: 313-8.

[13] Kanda T, Sullivan KF, Wahl GM. Histone-GFP fusion protein enables sensitive analysis of chromosome dynamics in living mammalian cells. Curr Biol 1998 Mar 26;8(7):377-85

[14] Rowley DR. What might a stromal response mean to prostate cancer progression? Cancer Metastasis Rev 1998-99;17(4):411-9

[15] Levine AC; Liu XH; Greenberg PD; Eliashvili M; Schiff JD; Aaronson SA; Holland JF; Kirschenbaum A. Androgens induce the expression of vascular endothelial growth factor in human fetal prostatic fibroblasts. Endocrinology, Nov, 139:11, 4672-8 1998.

[16] Bucana CD, Fabra A, Sanchez R, Fidler IJ. Different patterns of macrophage infiltration into allogeneic-murine and xenogeneic-human neoplasms growing in nude mice. Am J Pathol 1992 Nov;141(5):1225-36

[17] Lapis K, Kopper L, Timar J, van Hanh T, Hegedus C. Effect of macrophages on the growth of syn- and xenogeneic tumors. Arch Geschwulstforsch 1981;51(6):475-9

[18] Bucana CD, Fabra A, Sanchez R, Fidler IJ. Different patterns of macrophage infiltration into allogeneic-murine and xenogeneic-human neoplasms growing in nude mice. Am J Pathol 1992 Nov;141(5):1225-36

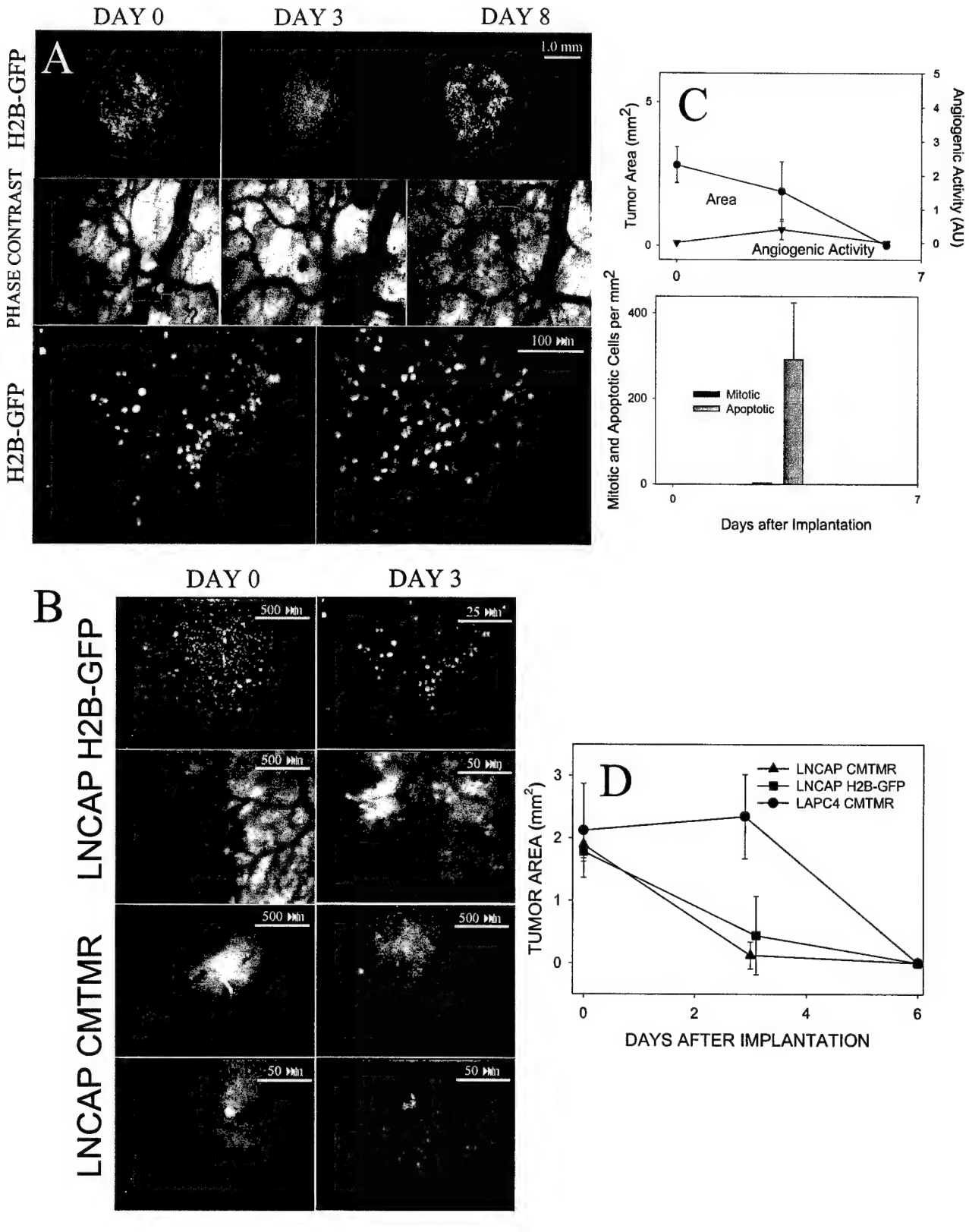
DAY 0
DAY 3
DAY 8
A
1.0 mm
H2B-GFP
PHASE CONTRAST
H2B-GFP
100 μm
C
Tumor Area (mm2)
Angiogenic Activity (AU)
Area
Angiogenic Activity
Mitotic and Apoptotic Cells per mm2
Mitotic
Apoptotic
Days after Implantation
B
DAY 0
DAY 3
LNCAP H2B-GFP
LNCAP CMTMR
500 μm
25 μm
50 μm
D
LNCAP CMTMR
LNCAP H2B-GFP
LAPC4 CMTMR
TUMOR AREA (mm2)
DAYS AFTER IMPLANTATION

FIG 1

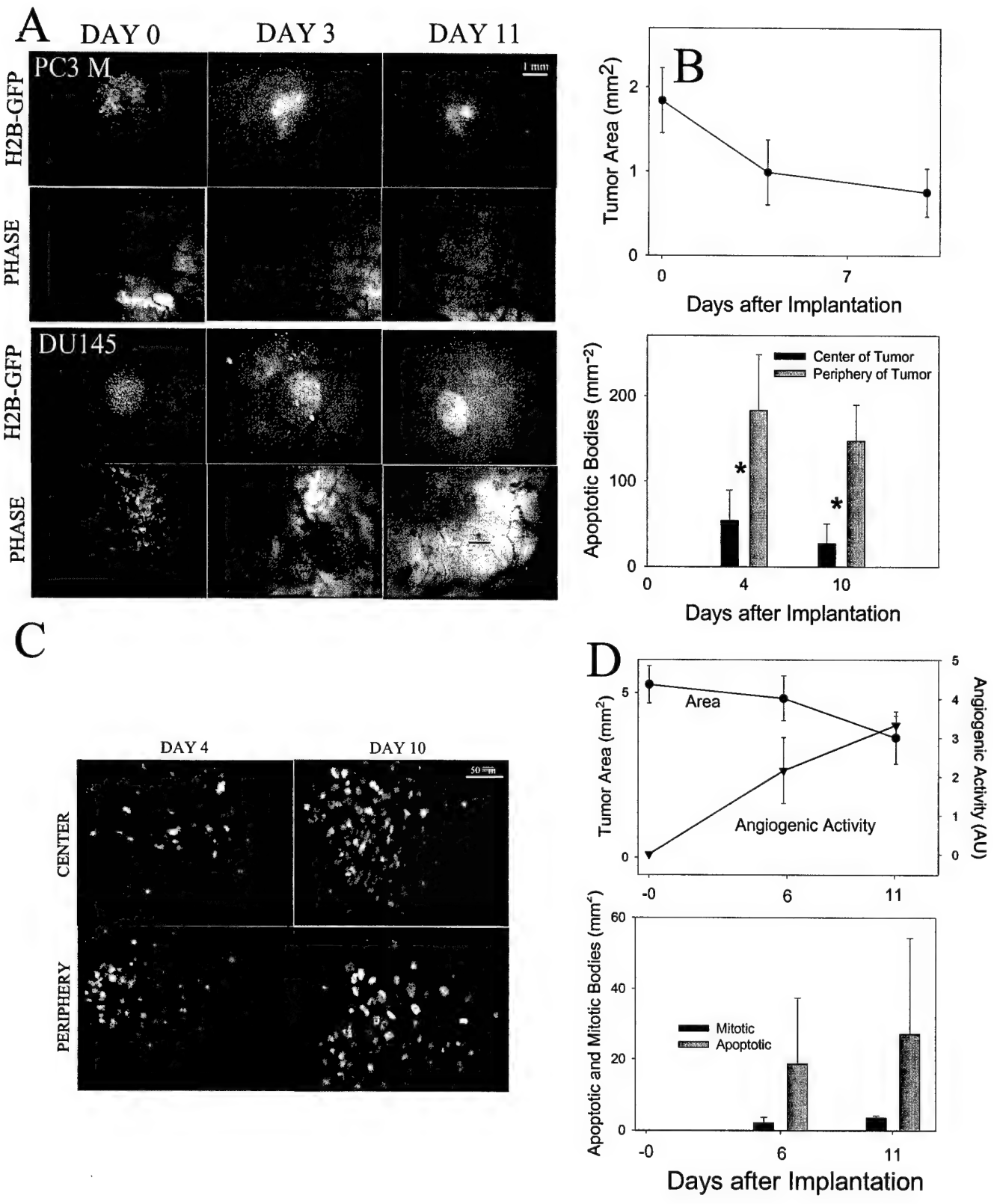
A
DAY 0
DAY 3
DAY 11
PC3 M
1 mm
H2B-GFP
PHASE
DU145
H2B-GFP
PHASE
B
Tumor Area (mm2)
2
1
0
0
7
Days after Implantation
Apoptotic Bodies (mm-2)
Center of Tumor
Periphery of Tumor
200
100
0
*
*
0
4
10
Days after Implantation
C
DAY 4
DAY 10
50 μm
CENTER
PERIPHERY
D
Tumor Area (mm2)
Area
Angiogenic Activity
Angiogenic Activity (AU)
5
0
-0
6
11
Apoptotic and Mitotic Bodies (mm-2)
60
40
20
0
Mitotic
Apoptotic
-0
6
11
Days after Implantation

FIG 2

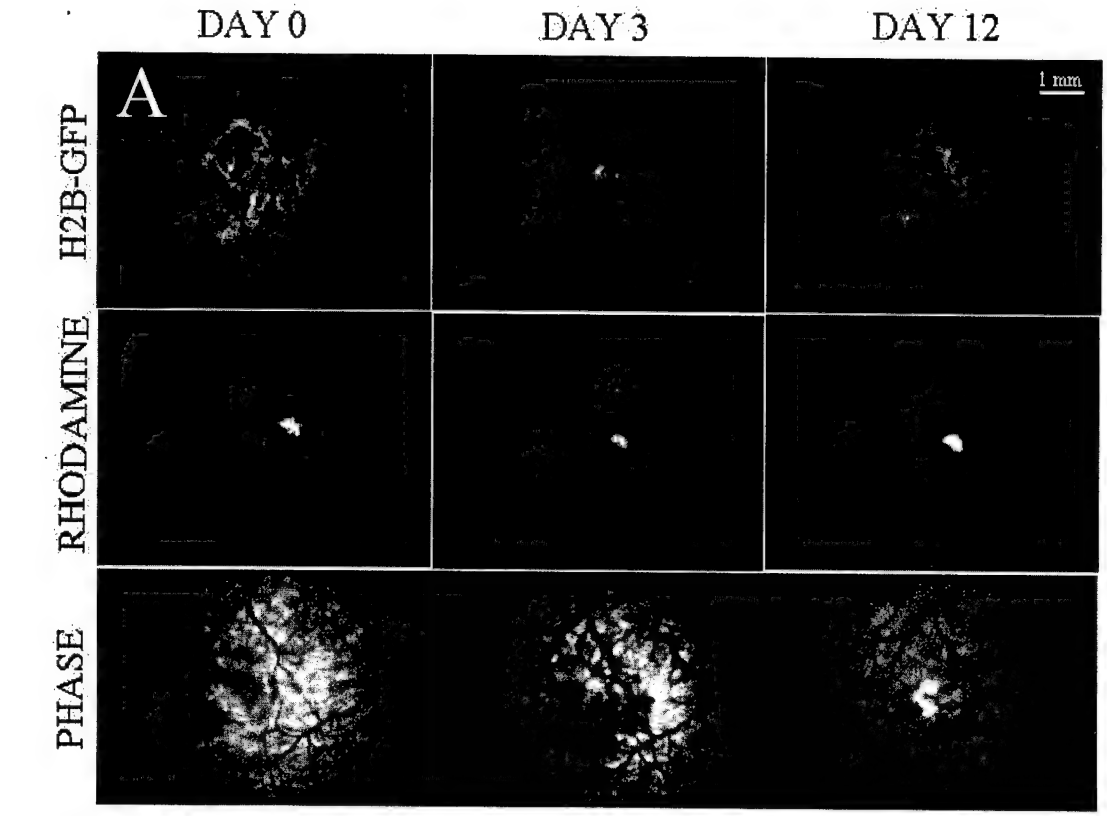
DAY 0
DAY 3
DAY 12
A
1 mm
H2B-GFP
RHODAMINE
PHASE

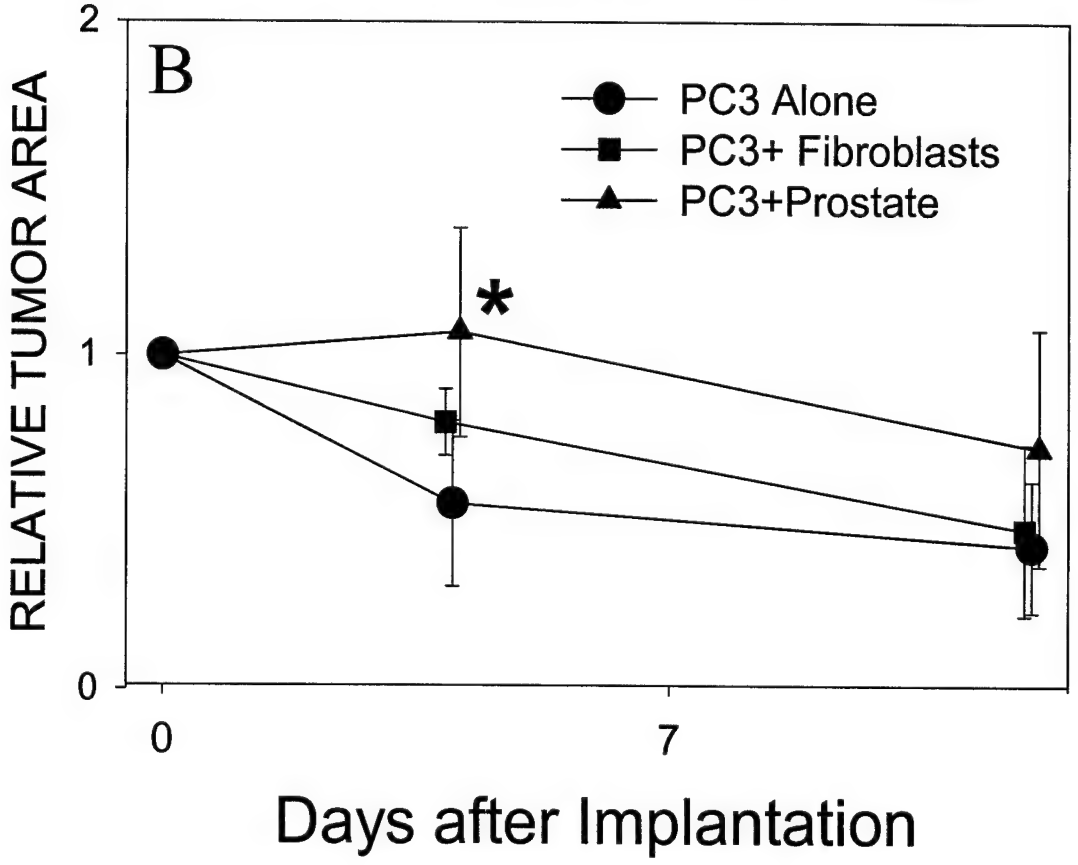
B
PC3 Alone
PC3+ Fibroblasts
PC3+Prostate
*
RELATIVE TUMOR AREA
2
1
0
0
7
Days after Implantation

FIG 3

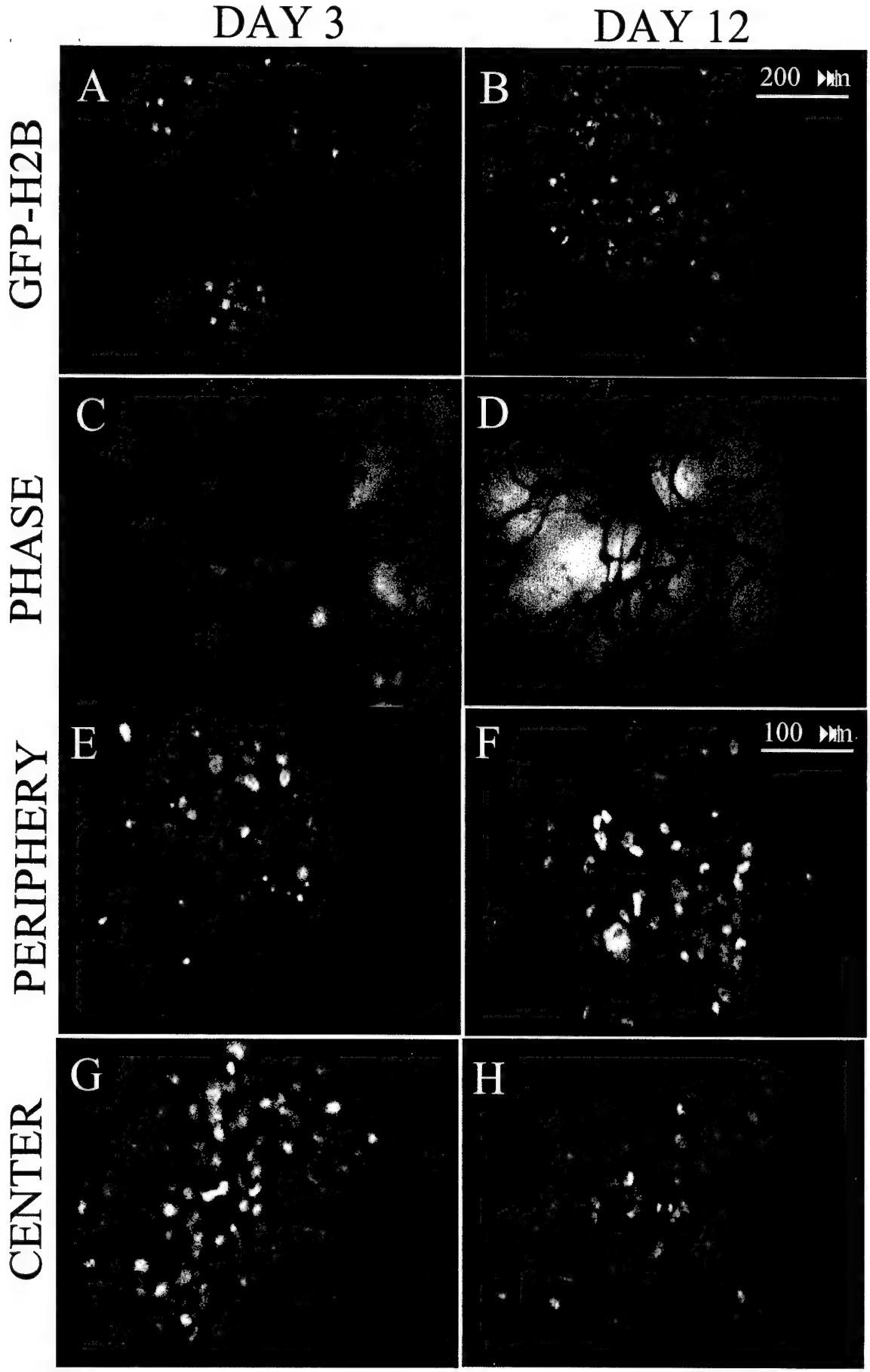
DAY 3
DAY 12
GFP-H2B
PHASE
PERIPHERY
CENTER
A
B
200 μm
C
D
E
F
100 μm
G
H

FIG 4

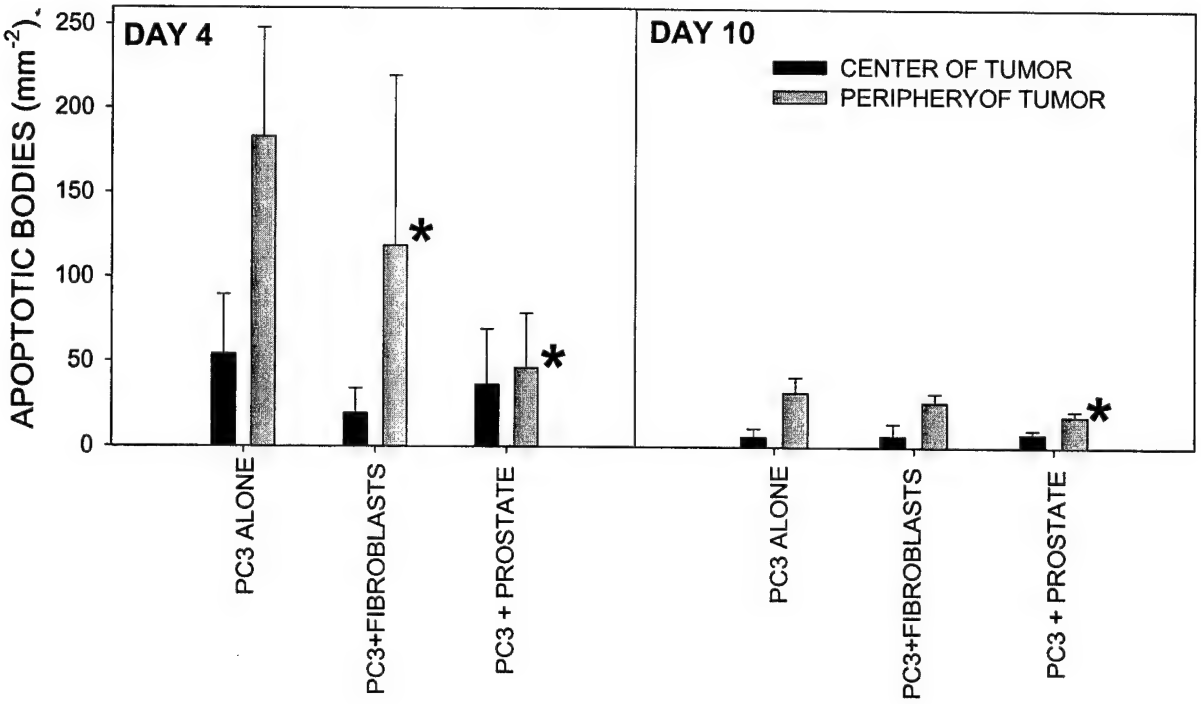
APOPTOTIC BODIES (mm-2)
250
200
150
100
50
0
DAY 4
DAY 10
CENTER OF TUMOR
PERIPHERYOF TUMOR
*
*
*
PC3 ALONE
PC3+FIBROBLASTS
PC3 + PROSTATE
PC3 ALONE
PC3+FIBROBLASTS
PC3 + PROSTATE

FIG 5

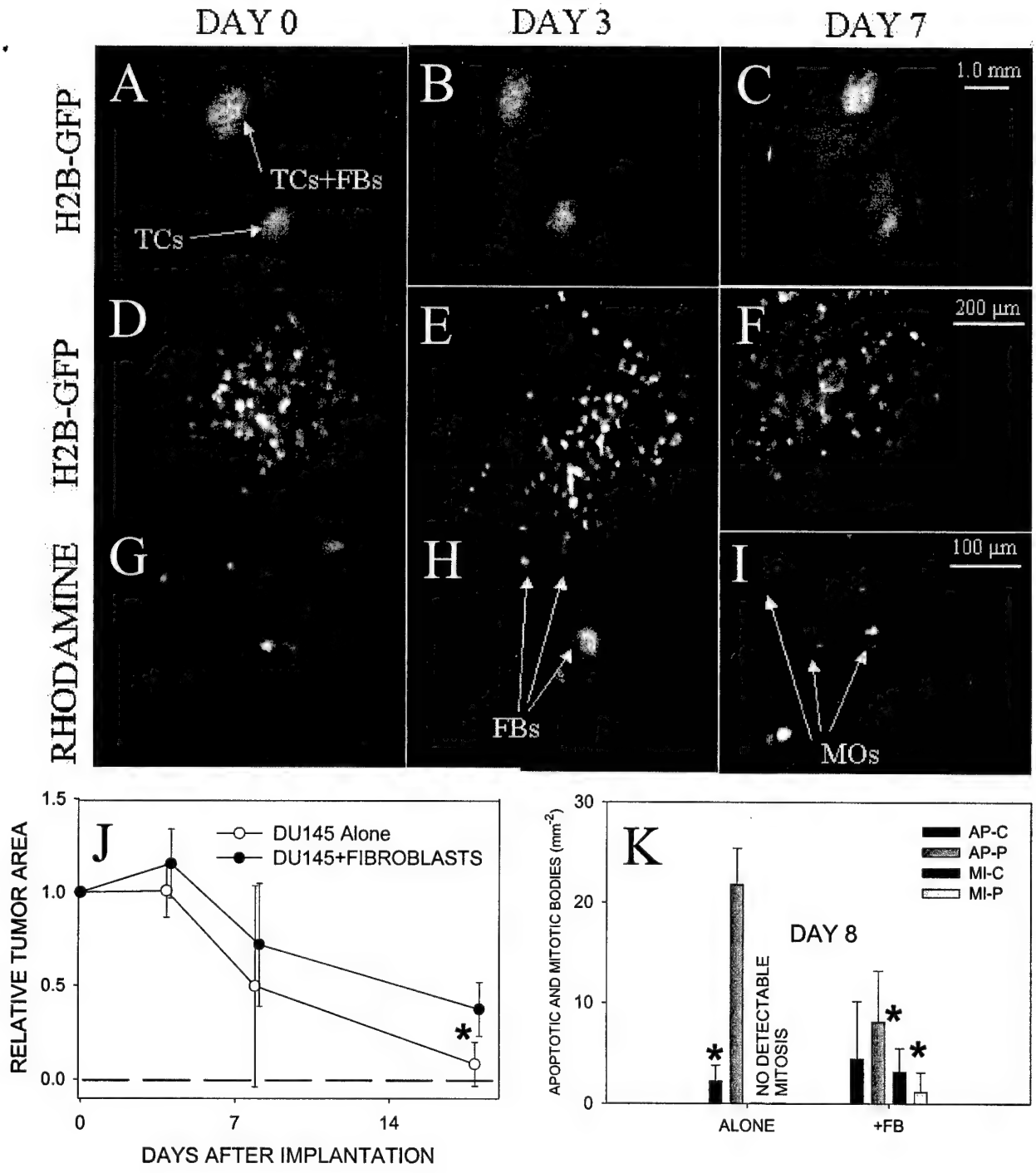
DAY 0
DAY 3
DAY 7
H2B-GFP
H2B-GFP
RHODAMINE
A
B
C
D
E
F
G
H
I
TCs+FBs
TCs
FBs
MOs
1.0 mm
200 µm
100 µm
J
DU145 Alone
DU145+FIBROBLASTS
RELATIVE TUMOR AREA
DAYS AFTER IMPLANTATION
K
AP-C
AP-P
MI-C
MI-P
DAY 8
NO DETECTABLE MITOSIS
APOPTOTIC AND MITOTIC BODIES (mm-2)
ALONE
+FB

FIG 6

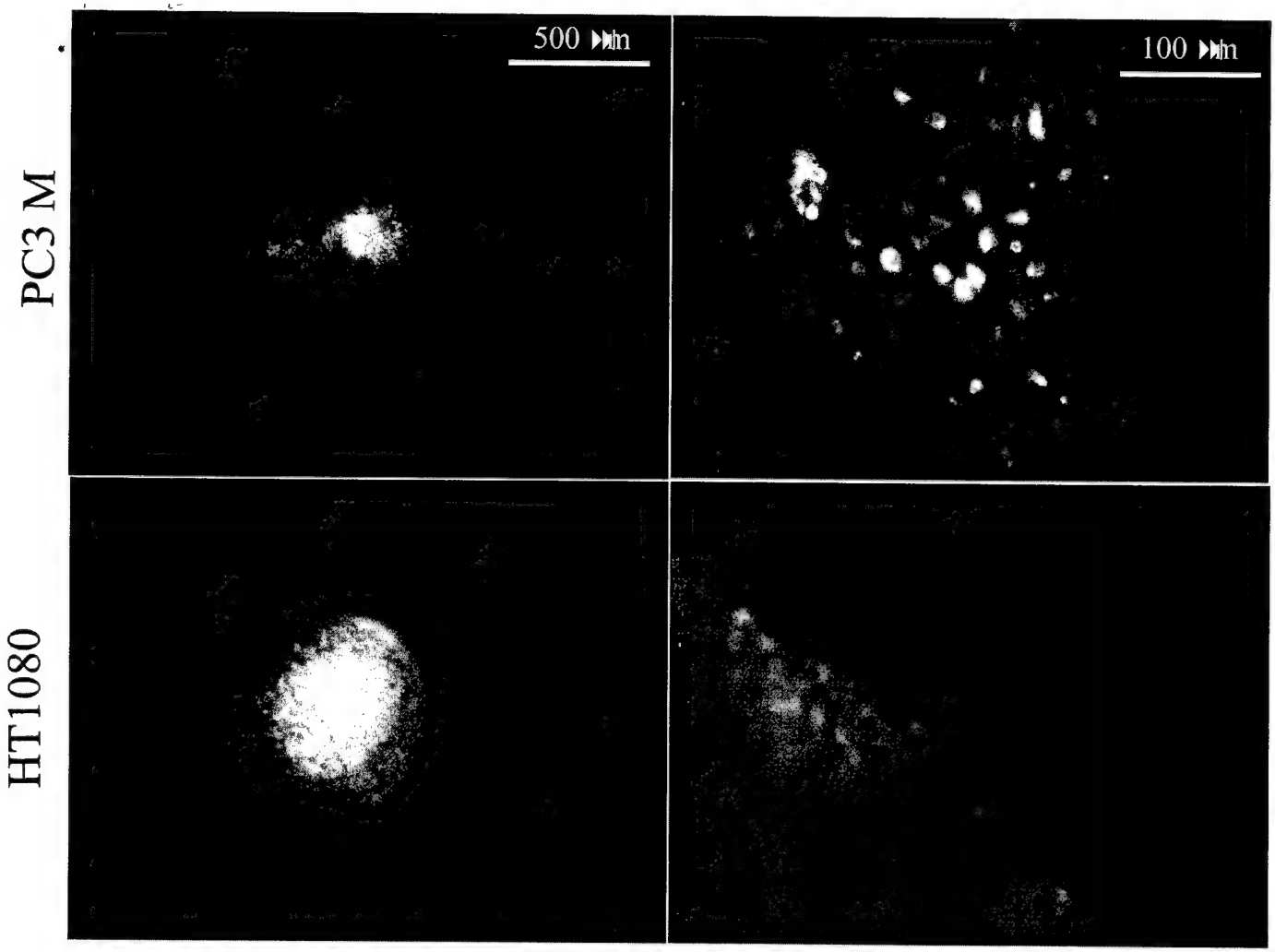

FIG 7

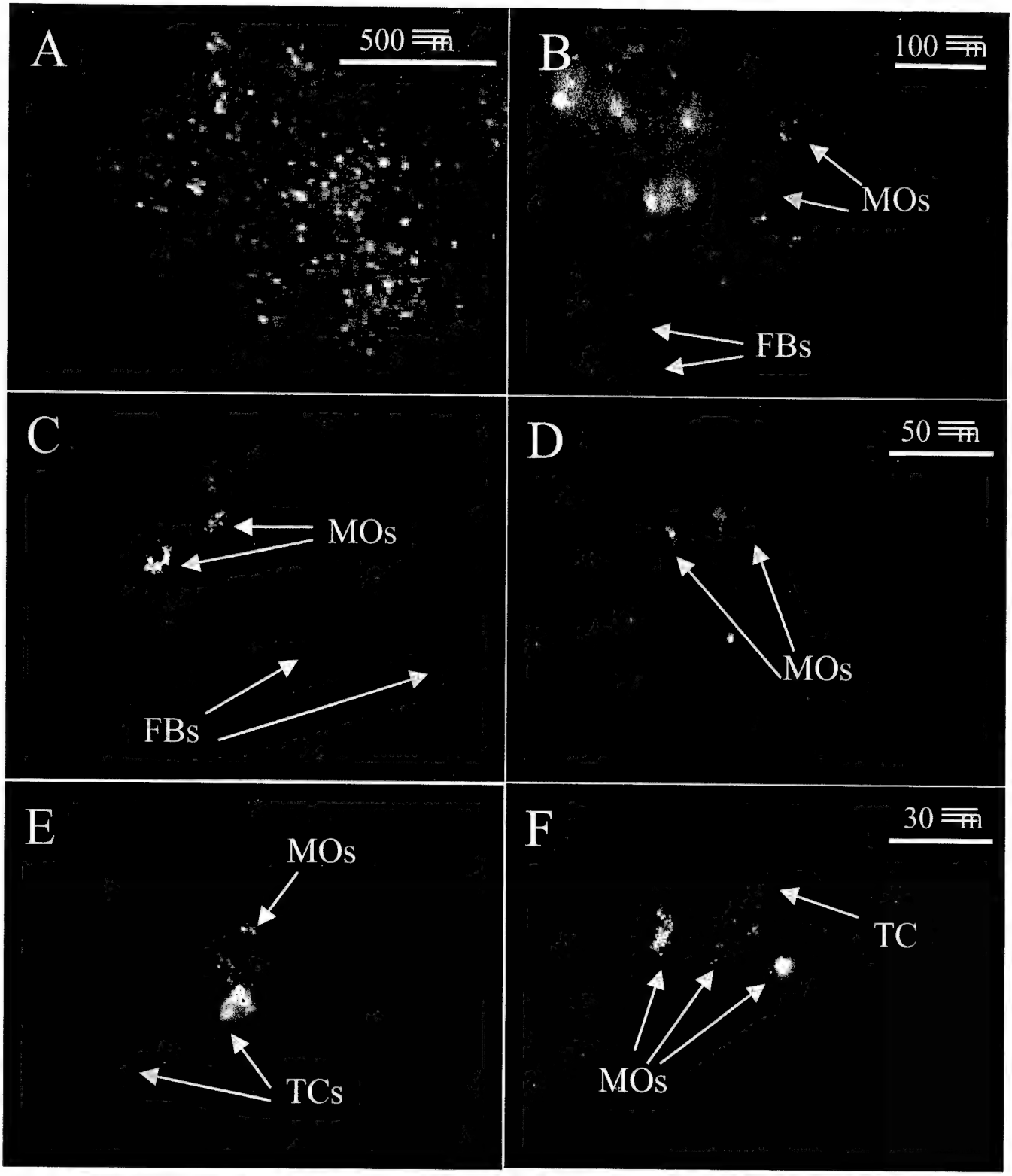
A
500 μm
B
100 μm
MOs
FBs
C
MOs
FBs
D
50 μm
MOs
E
MOs
TCs
F
30 μm
TC
MOs

FIG 8

A

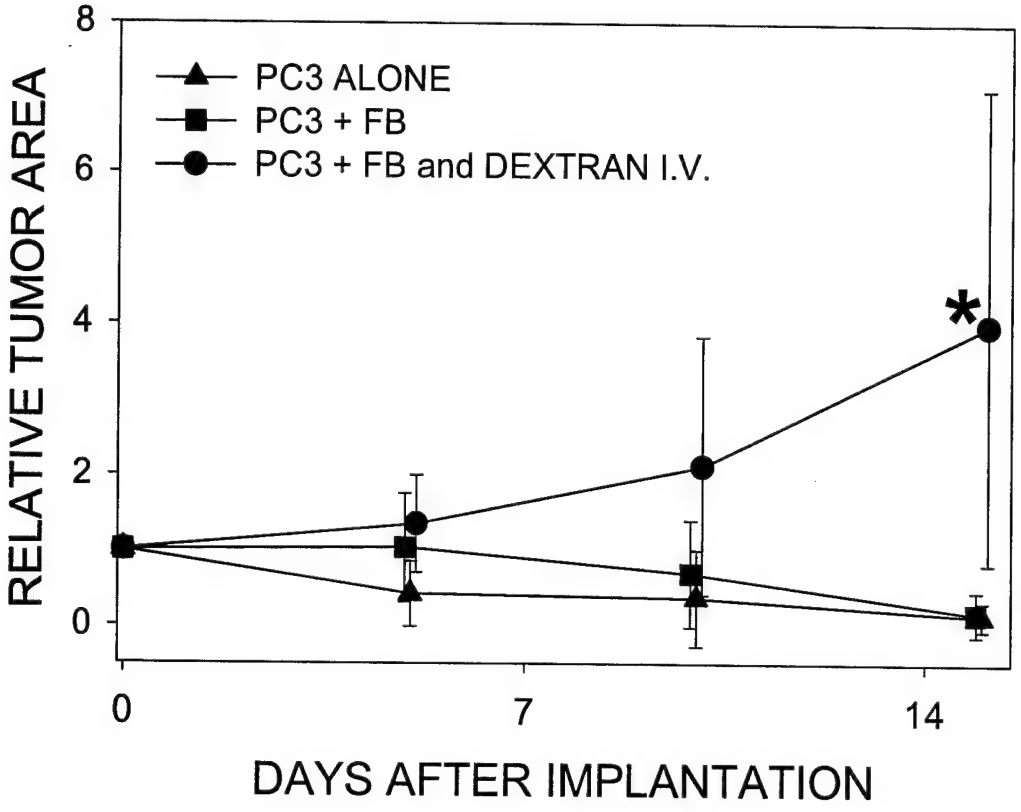
PC3 ALONE
PC3 + FB
PC3 + FB and DEXTRAN I.V.
RELATIVE TUMOR AREA
8
6
4
2
0
*
0
7
14
DAYS AFTER IMPLANTATION

B

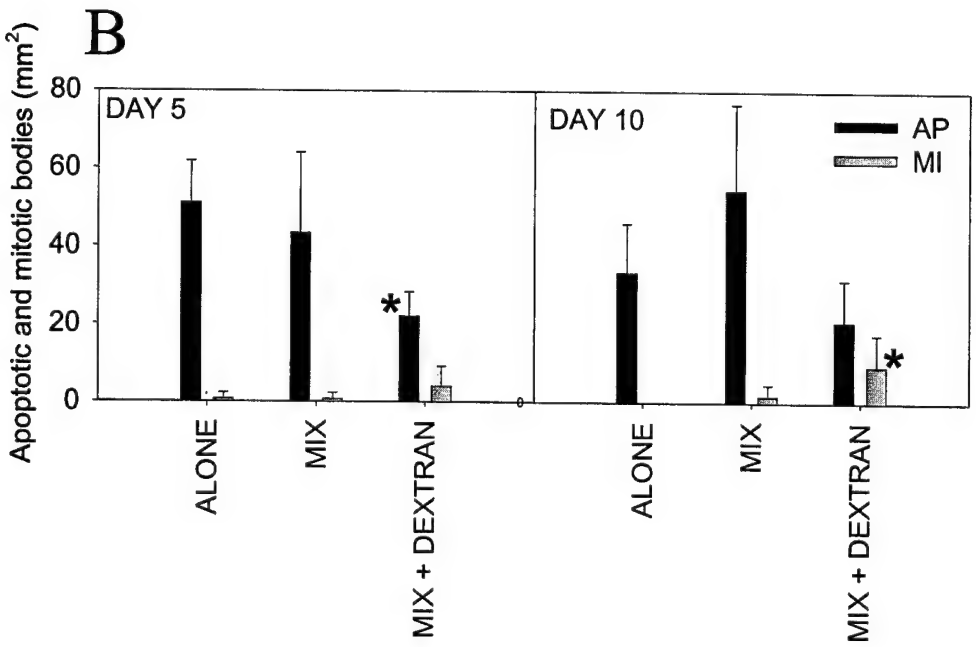
Apoptotic and mitotic bodies (mm²)
80
60
40
20
0
DAY 5
DAY 10
AP
MI
*
*
ALONE
MIX
MIX + DEXTRAN
ALONE
MIX
MIX + DEXTRAN

FIG 9

REAL TIME *IN VIVO* QUANTITATION OF TUMOR ANGIOGENESIS

By

Gregory I. Frost and Per Borgström

INTRODUCTION

Animal models are crucial to further our understanding of tumor biology. For many years, observation chambers, implanted in various animal species, have been used for intravital microscopy of tumor microcirculation. As far back as 1943, Algire described the adaptation of the transparent chamber technique to the mouse (1). From the introduction of a subsequent paper by Algire et al. (2) the following paragraph is quoted: "*Recently, in vivo techniques have been developed which make it possible to make microscopic observations of the development of the blood supply of tumor transplants in the mouse. It has also been possible to obtain a quantitative expression of the morphological changes as they occur over a prolonged period.*" In that paper, Algire et al concludes: "*The results presented indicate (1) that the rapid growth of tumor transplants is dependent upon the development of a rich vascular supply, and (2) that an outstanding characteristics of the tumor cell is its capacity to elicit continuously the growth of new capillaries.*" Algire thus concluded in 1945 that tumors were angiogenesis dependent. Subsequent reports, using intravital microscopic techniques are very sporadic. In 1965, Goodall et al. described a transparent chamber model inserted in the cheek pouch of the hamster (3). Yamura et al. developed a transparent chamber in the rat skin ([4]). In a study by Wolf and Hubler in 1975 ([5]), a transparent acrylic hamster cheek-pouch chamber was used to investigate the elaboration of a tumor angiogenic factor (TAF) by human cutaneous neoplasms, from which they concluded: "*Tumor angiogenic factor appears to induce direct stimulation of endothelial cell mitosis and may be essential for survival of nutritionally ravenous neoplastic tissues. The interference with TAF has therapeutic implications.*"

Transparent chambers have been instrumental in the understanding of tumor biology. With the development of molecular biology techniques such as spontaneously fluorescent proteins (GFP, RFP), and elaborate image analysis software, it is now much easier to generate quantitative data. Such systems can clarify tumor microcirculatory phenomena, and mechanisms underlying anti-angiogenic and anti–tumor activities that are poorly understood using traditional histopathology.

Multicellular tumor spheroids are being used with increasing frequency in various aspects of tumor biology, and there are many similarities in growth and cellular characteristics for different types of tumor cells grown as multicell spheroids. Cells cultured as spheroids present heterogeneity similar to that of tumors in vivo. In the spheroid peripheral layers, cells are proliferating with deeper cells are non-cycling, when in the aggregate center, cells form often a necrotic core. They are formed from monolayer tumor cells when these are grown by various in vitro methods (e.g. liquid-overlay, spinner flask and gyratory rotation systems). Because of the cellular organization in spheroids, they often recreate in vivo tumors much more closely than two-dimensional in vitro models (6).

We have developed an intravital microscopic model which is based on the dorsal skin fold chamber technique in mice. We use multicellular spheroids as the source for transplants (7). The use of tumor spheroids as the source of transplants, allows precise determination of tumor size to be implanted. Usually, spheroids are prepared from 25,000 to 50,000 tumor cells using liquid overlay techniques, which minimize variations within animals in the same groups. It also allows for preparations of hybrid spheroids, as exemplified by Fig 1, illustrating spheroids prepared from tumor cells from the human

prostate carcinoma cell line PC3, mixed with human fibroblasts cultured from a thin needle biopsy from a patient.

Our system allows continuous measurements of growth and angiogenesis of the small tumor spheroids. We used this system to evaluate various therapeutic interventions on various mouse and human cancer cell lines (8). In those studies, we used a rhodamine based in vivo dye (CMTMR) to determine tumor growth. However, we found that the CMTMR labeling lasted at most for two weeks. Moreover, macrophages which had engulfed tumor cells became fluorescent making it very difficult to assess the true tumor area.

Green fluorescent protein, GFP, is a spontaneously fluorescent protein isolated from coelenterates, such as the Pacific jellyfish, Aequoria victoria (9). When expressed in mammalian cells fluorescence from wild type GFP is typically distributed throughout the cytoplasm, but excluded from the nucleolus and vesicular organelles (10). However, highly specific intracellular localization including the nucleus (11), mitochondria (12), secretory pathway (13), plasma membrane (14) and cytoskeleton(15) can be achieved via fusions both to whole proteins and individual targeting sequences. The enormous flexibility as a noninvasive marker in living cells allows for numerous other applications such as a cell lineage tracer, reporter of gene expression and as a potential measure of protein-protein interactions (16).

Kanda et al. (17) developed a highly sensitive method for observing chromosome dynamics in living cells. They fused the human histone H2B gene to the gene encoding the (GFP) which was transfected into human HeLa cells to generate a stable line

constitutively expressing H2B-GFP. The H2B-GFP fusion protein was incorporated into chromatin without affecting cell cycle progression.

We have generated cDNA encoding a histone H2B-GFP fusion protein in an LXRN retroviral cassette, and introduced it into a number of human as well as murine cancer cell lines by retroviral transduction.

The use of well defined tumor spheroids also permits the introduction of stroma together with the spheroids. Tumor cells stimulate the formation of stroma that secretes various mediators pivotal for tumor growth, including growth factors, cytokines, and proteases, and especially in prostate cancer models, the "seed-soil" concept has been repeatedly explored (18). Direct tumor implantation into the prostate has resulted in a more accurate representation of the disease. In an attempt to create a "pseudo-orthotopic milieu" in our in vivo system, we have introduced tumor spheroids obtained from prostate carcinoma cells transfected to express the histone H2B-GFP fusion protein, mixed with anterior prostate tissue from donor mice (Fig. 2).

Using the murine TRAMP-C2 cell line which is derived from a spontaneous tumor from a TRAMP mouse (Transgenic Adenocarcinoma Mouse Prostate), we have shown more physiological growth characteristics as compared to implantation of TRAMP-C2 spheroids alone (FIG 3). The TRAMP is a transgenic mouse model, in which mice develop spontaneous prostate tumors. TRAMP mice develop a distinct pathology in the dorso-lateral epithelium of the prostate by 10 weeks of age. By 12 weeks they have widespread infiltration of the prostate and by week 24, mice exhibit well-differentiated prostate tumors (19).

The real advantage using the chamber technique, is that it allows the study of cancer in the context of the host (Fig 4). Tumors are frequently infiltrated by numerous tumor associated macrophages (TAMs), which can be found within the tumor mass or surrounding the tumor. Tumor associated macrophages (TAM) influence diverse processes such as angiogenesis, tumor cell proliferation, and metastasis during tumor progression. In a variety of tumor types, the amount of TAM has been associated with prognosis (20). Data currently available also suggest that in solid tumors, the TAMs can in fact induce immune suppression of host defenses in situ, through release of suppressive specific cytokines, prostanoids and other humoral mediators. However, TAMs can also participate in the immunologic anti-tumor defense mechanism through cytotoxic activities, such as direct cellular cytotoxicity and the release of cytokines and reactive oxygen species. To visualize the TAMs in our system we inject locally into the chamber 10 µl 1% RITC-dextran. Figure 5 illustrates the anti-tumor response encountered after implantation of tumor spheroids obtained from the human prostate carcinoma cell line PC3. In a recent study, we used our system to demonstrate that the inability to effectively exclude the innate immune system by encapsulation prevented the survival of small human prostate micro-tumor xenografts, suggesting that the complex interactions between tumor cells and TAMs which are pivotal in tumor biology, were extensively perturbed by "foreign" human tumor cells implanted in immunodeficient mice (21). The ability of our model to continuously assess mitotic and apoptotic indices, was an important feature to demonstrate that the tumors were dying "from the outside in", i.e., mitotic cells confined to the center of the tumor, and numerous apoptotic cells in the

periphery, instead of, a finding ruling out death due to a lack of angiogenesis within the central tumor mass (Fig. XX).

2. MATERIALS

All surgical procedures are performed in a sterile laminar flow hood. Dorsal skinfold chambers and surgical instruments are autoclaved before use. Saline used to keep tissue moist during surgical preparation is mixed with gentamicin (50 μl/ml). Small circular Band Aids are applied on the backside of the chamber after surgery to prevent scratching.

1. 7.3 mg ketamine hydrochloride and 2.3 mg xylazine /100 g body weight.
2. DMEM 4.5 gm/L glucose, supplemented with pyruvate, glutamine non essential amino acids, and gentamicin (50μg/ml)
3. Genprobe PCR mycoplasma detection kit
4. Rhodamine-B Isothiocyanate-dextran 70S
5. 96 well round bottom sterile tissue culture plates
6. Agarose
7. Angiogenic tumor cell line transduced with H2BeGFP

3. METHODS

Animal model and surgical techniques: The dorsal skinfold chamber in the mouse (Fig. 6) is prepared as described previously (22). Male mice (25-35 g body weight) are anesthetized (7.3 mg ketamine hydrochloride and 2.3 mg xylazine /100 g body weight, i.p.) and placed on a heating pad. Two symmetrical titanium frames are implanted into a dorsal skinfold, so as to sandwich the extended double layer of skin. A 15 mm full thickness layer is excised. The underlying muscle (M. cutaneous max.) and

subcutaneous tissues are covered with a glass cover slip incorporated in one of the frames. After a recovery period of 2-7 days, tumor spheroids are carefully placed in the chamber.

Generation of H2B-eGFPN1 Cell lines. Human Histone H2B-eGFP, a kind gift from Dr. Kanda (Salk Institute, La Jolla, CA) was excised from the Sal-I Not-I sites in the BOS H2BGFP-N1 vector. The H2B-eGFP retroviral vector was generated by cutting first with Not-I followed by Mung-Bean Nuclease digestion to remove the overhanging end. The fragment was gel purified followed by Sal-I digestion. The resultant Sal-I / blunt fragment was cloned into the Sal-I Hpa-I sites in the LXRN retroviral vector (Clontech, Palo Alto CA). VSVG pseudotyped retrovirus is generated by transfecting GP293 GagPol expressing 293 cells (Available from Clontech) in T75 flasks at 75% confluence with 5ug of this resultant L-H2BGFP-RN-L vector with 5ug VSV-G vector (Clontech) and harvesting viral supernatants 48 hours post transfection. Retroviral supernatants can be used immediately or concentrated by centrifugation and stored at –80°C until use. Tumor cells are transduced with VSVG peudotyped H2B-GFP LXRN viral supernatant for 48 hours in 8ug/ml polybrene followed by selection in 300μg/ml G418 for 2 weeks. Pooled H2B-GFP expressing tumor cells are usually heterogeneous as determined by fluorescent microscopy but can be FACS sorted if necessary for resistant cell lines such as Lewis Lung Carcinoma. Most cells used for chamber studies are passaged in DMEM 4.5 gm/L glucose supplemented with pyruvate, glutamine non essential amino acids, and gentamicin (50μg/ml) and maintained in a humidified 5% CO_2 atmosphere at 37 °C. Cells are routinely tested for mycoplasma contamination with the Genprobe mycoplasma detection kit.

Preparation of tumor spheroids. Liquid overlay plates are generated using 1% Molecular Biology grade Agarose melted in DMEM in a microwave. The melted agarose solution is plated into round bottom 96 well plates at 50ul/well and allowed to cool at room temperature. Tumor cells grown as pre confluent monolayers are trypsinized and diluted to a final volume of 250,000 tumor cells/ml. Viability should be determined using Trypan blue. The tumor suspensions are dispersed 100ul/well into the 96 well agarose coated round bottom plates. Spheroids are allowed to compact for 48 hours and picked from the plates with a pipette followed by transfer into serum free media immediately before implantation into chambers.

Intravital microscopy : Fluorescence microscopy is performed using a Mikron Instrument Microscope (Mikron Instrument, San Diego, CA) equipped with epi-illuminator and video-triggered stroboscopic illumination from a xenon arc (MV-7600, EG&G, Salem, MA). A silicon intensified target camera (SIT68, Dage-MTI, Michigan City, IN) is attached to the microscope. A Hamamatsu image processor (Argus 20) with firmware version 2.50 (Hamamatsu Photonic System, USA) is used for image enhancement and to capture images to a computer. A Leitz PL1/0.04 objective is used to obtain an over-view of the chamber and for determination of tumor size. A Zeiss long distance objective 10/0.22 is used to capture images for calculation of vascular parameters. A Zeiss Achroplan 20X/0.5 W objective is used for capturing images for calculation of mitotic and apoptotic indices.

Our system permits evaluation of the following parameters:

3.1 Parameters Related To Tumor Growth And Tumor Cell Motility

Tumor area (A_T) is defined as number of pixels with photo density above 75 (256 gray

levels), i.e.,

$$\mathbf{A_T} = \sum_{k=75}^{255} 3A_k,$$

Since TRAMP-C2 tumors are very heterogenous (Fig 7), changes in $\mathbf{A_T}$ per se do not directly reflect tumor growth. To take into account variations of tumor cell intensity, we define total intensity $\mathbf{I_T}$ as,

$$\mathbf{I_T} = \sum_{k=75}^{255} 3A_k * I_k,$$

and relative intensity, reflecting relative number of tumor cells at Day X as compared Day 0, is defined as,

$$\mathbf{(I_{REL})_{DAYX}} = (I_T)_{DAYX} / (I_T)_{DAY0}$$

Relative tumor cell density ($\mathbf{D_T}$) is defined as,

$$\mathbf{D_T} = I_T / A_T.$$

Calculation of these parameters permits evaluation of tumor growth/shrinkage (I_{REL}), as well as tumor cell motility (D_T). Thus, treatments resulting in an increase in A_T without corresponding increase in I_T reflect increased tumor cell motility rather than tumor growth.

3.2 Mitotic And Apoptotic Indices

At each time point, two peripheral and two central X20 fields of the tumor are captured with a FITC filter using Image-Pro Plus software and an integrated frame grabber. Only mitotic figures in telophase (MI) are included in the mitotic index to exclude potential artifact of nuclear membrane distortion. Apoptotic/Pyknotic nuclei are

defined as H2B-GFP labeled nuclei with a cross sectional area >30um^2. Nuclear karyorrhexis (NK), easily distinguishable by the vesicular nuclear condensation and brightness of H2BGFP, is included within this apoptotic index (Fig. 8).

3.3 Vascular Parameters

Image analysis: For each spheroid, video recordings are used to calculate length, area and vascular density of the neovasculature being induced by the implanted tumor spheroids. Vascular parameters are analyzed off-line from the video recording using a photodensitometric computer software (Image-Pro Plus, Media Cybernetics, MD). Photomicrographs obtained with the X10 objective (Fig. 9; Panel A), are "flattened" to reduce the intensity variations in the backround pixels (Panel B). The flattened photomicrograph is cropped to eliminate distorted areas, and the thresholding feature is used to segment the picture into objects and background (Panel C). This panel is used to calculate vascular area (A_V). Finally, the picture is skeletonized (Panel D), in order to calculate vascular length (L_V). From these parameters average tumor vessel diameter D_V is calculated as A_V/L_V, and vascular density (Δ_V) is calculated as L_V per tumor area.

REFERENCES

[1] Algire, GH. An adaptation of the transparent chamber technique to the mouse. J. Nat. Cancer Inst. $:1-11, 1943.

[2] Algire, GH Chakley HW. Vascular reactions of normal and malignant tissues in vivo. I. Vascular reactions of mice to wounds and to normal and neoplastic transplants.J. Natl Cancer Inst 6:73-85, 1945

[3] Goodall CM, Sanders AG, Shubik P. Studies of vascular patterns in living tumors with a transparent chamber inserted in hamster cheek pouch. J. Natl Cancer Inst 1965 Sep;35(3):497-521

[4] Yamura H, Suzuki M, Sato H. Transparent chamber in the rat skin for studies on microcirculation in cancer tissue. J Natl Cancer Inst 1968 Jul;41(1):111-24

[5] Wolf JE, Hubler WR. Tumor angiogenic factor and human skin tumors. Arch Dermatol 1975 Mar;111(3):321-7

[6] Mueller-Klieser W, Tumor biology and experimental therapeutics.
Crit Rev Oncol Hematol 2000 Nov-Dec;36(2-3):123-39.

de Ridder L; Cornelissen M; de Ridder D. Autologous spheroid culture: a screening tool for human brain tumour invasion.
Crit Rev Oncol Hematol 2000 Nov-Dec;36(2-3):107-22.

Desoize B; Gimonet D; Jardiller JC. Cell culture as spheroids: an approach to multicellular resistance. Anticancer Res 1998 Nov-Dec;18(6A):4147-58.

Santini MT; Rainaldi G; Indovina PL. Multicellular tumour spheroids in radiation biology. Int J Radiat Biol 1999 Jul;75(7):787-99.

[7] Torres et al XXX

[8] Borgstrom P, Gold DP, Hillan KJ, Ferrara N Importance of VEGF for breast cancer angiogenesis in vivo: implications from intravital microscopy of combination treatments with an anti-VEGF neutralizing monoclonal antibody and doxorubicin. Anticancer Res 1999 Sep-Oct;19(5B):4203-14

[9] Morin, J. and Hastings, J., 1971. Energy transfer in a bioluminescent system. J. Cell Physiol. 77: 313-8.

[10] Cubitt, A., Heim, R., Adams, S., Boyd, A., Gross, L. and Tsien, R., 1995. Understanding, improving and using green fluorescent proteins. TIBS. 20: 448-55

[11] Kanda T, Sullivan KF, Wahl GM. Histone-GFP fusion protein enables sensitive analysis of chromosome dynamics in living mammalian cells. Curr Biol 1998 Mar 26;8(7):377-85

[12] Rizzuto, R., Brini, M., De Giorgi, F., Rossi, R., Heim, R., Tsien, R. and Pozzan, T., 1996. Double labeling of subcellular structures with organelle-targeted GFP mutants in vivo. Curr. Biol.6: 183-188.

[13] Kaether, C. and Gerdes, H., 1995. Visualization of protein transport along the secretory pathway using green fluorescent protein. FEBS Lett. 369: 267-271.

[14] Marshall, J., Molloy, R., Moss, G., Howe, J. and Hughes, T., 1995. The jellyfish green fluorescent protein: a new tool for studying ion channel expression and function. Neuron. 14:211-215.

[15] Kahana, J., Schapp, B. and Silver, P., 1995. Kinetics of spindle pole body separation in budding yeast. Proc. Natl. Acad. Sci., USA. 92: 9707-9711.

[16] Mitra, R., Silva, C. and Youvan, D., 1996. Fluorescence resonance energy transfer between blue-emitting and red-shifted excitation derivatives of the green fluorescnet protein. Gene. 173: 13-7.

[17] Kanda T, Sullivan KF, Wahl GM. Histone-GFP fusion protein enables sensitive analysis of chromosome dynamics in living mammalian cells. Curr Biol 1998 Mar 26;8(7):377-85

[18] Rembrink K; Romijn JC; van der Kwast TH; Rubben H; Schroder FH. Orthotopic implantation of human prostate cancer cell lines: a clinically relevant animal model for metastatic prostate cancer. Prostate; 31(3):168-74 1997.

[19] Greenberg NM; DeMayo F; Finegold MJ; Medina D; Tilley WD; Aspinall JO; Cunha GR; Donjacour AA; Matusik RJ; Rosen JM. Prostate cancer in a transgenic mouse Proc. Natl. Acad.Sci. USA 92:3439-3443, April 1995.

[20] Lissbrant IF, Stattin P, Wikstrom P, Damber JE, Egevad L, Bergh A. Tumor associated macrophages in human prostate cancer: relation to clinicopathological variables and survival. Int J Oncol 2000 Sep;17(3):445-51

[21] Frost G.I., Dudouet B., Lustgarten J., Borgström P The Roles Of Epithelial Mesynchymal Interactions And The Innate Immune Response On The Tumorigenicity Of Human Prostate Carcinoma Cell Lines Grown In Immuno-Compromised Mice (Manuscript In Preparation)

[22] Lehr H; Leunig M; Menger MD; Messmer K. Dorsal skinfold chamber technique for intravital microscopy on striated muscle in nude mice. Am. J. Pathol. 143,1055-1062, 1993.

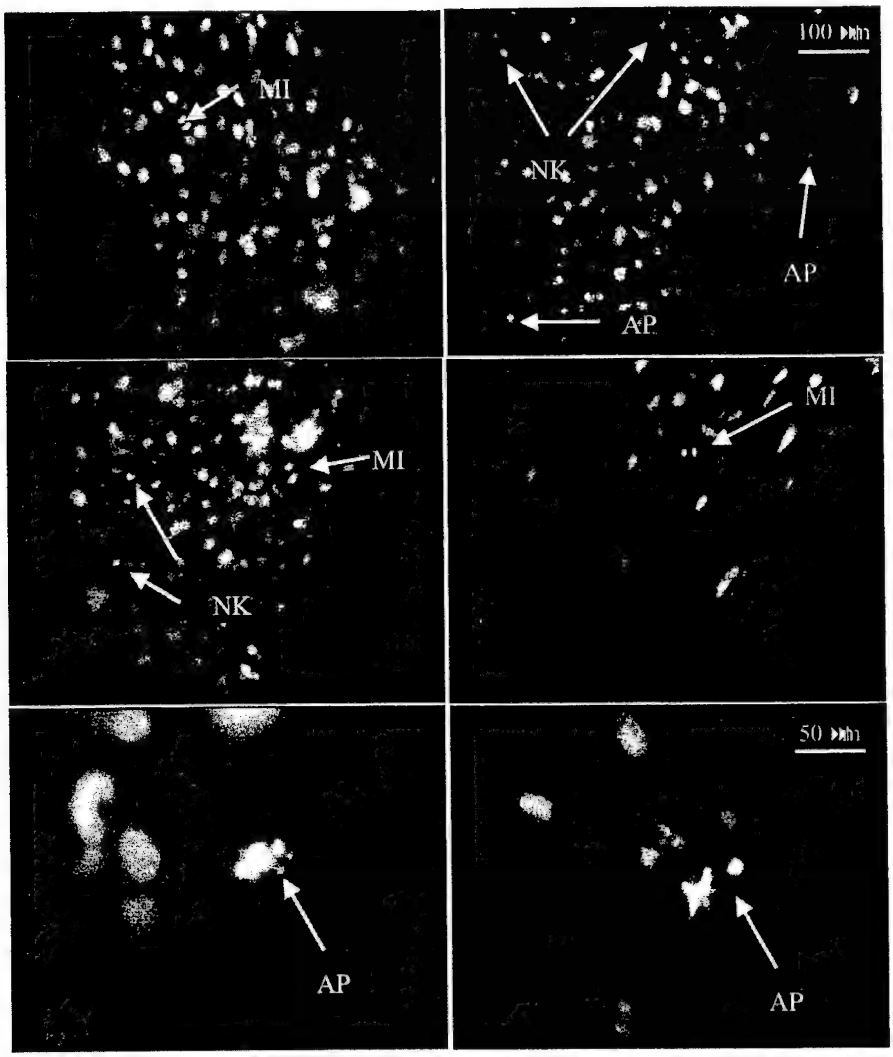
MI
100 μm
NK
AP
AP
MI
MI
NK
AP
50 μm
AP

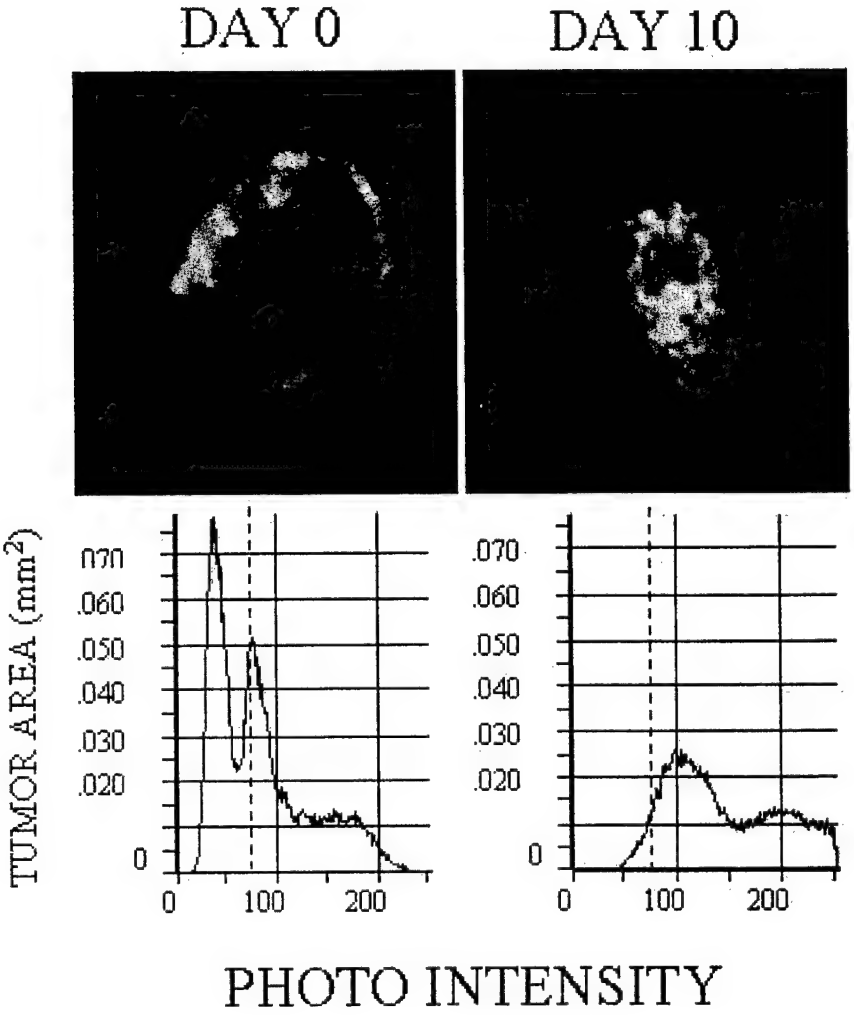
DAY 0
DAY 10
TUMOR AREA (mm²)
.070
.060
.050
.040
.030
.020
0
0
100
200
PHOTO INTENSITY

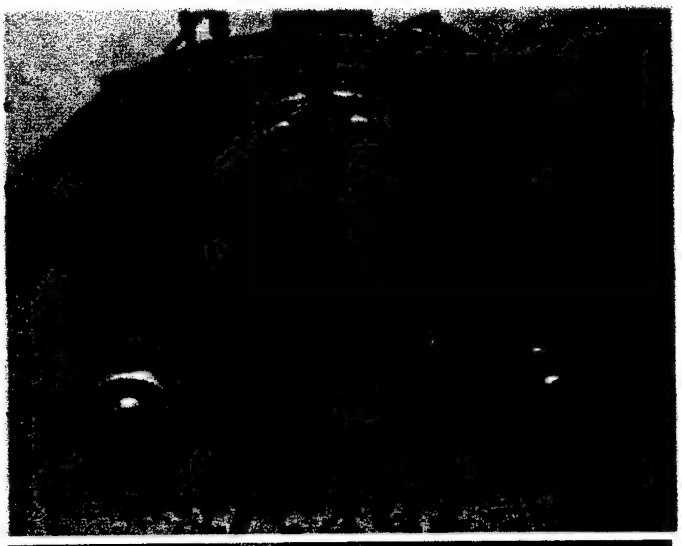

In Vivo Communication

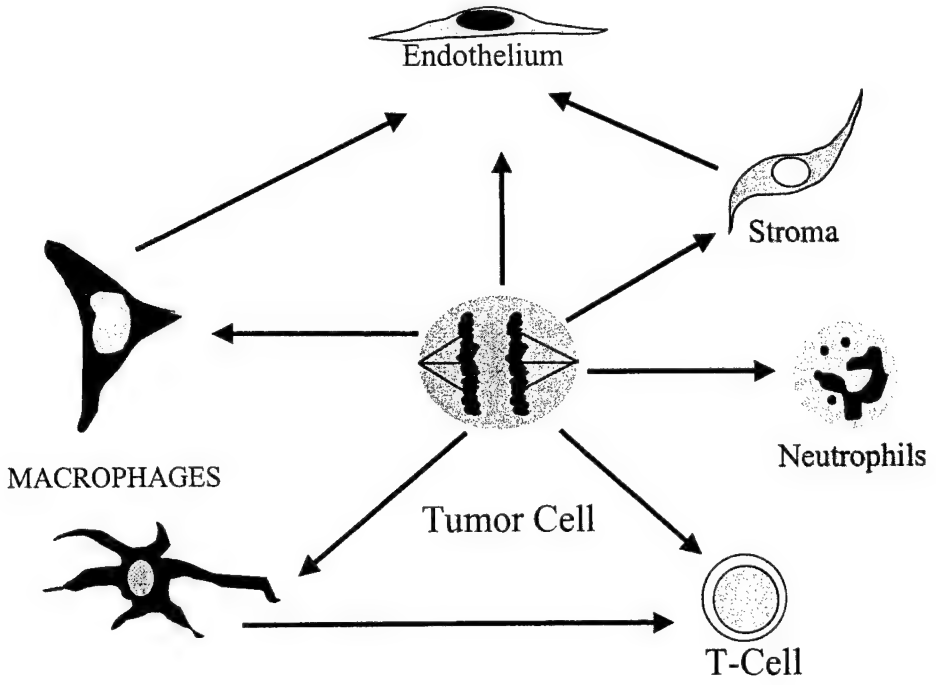

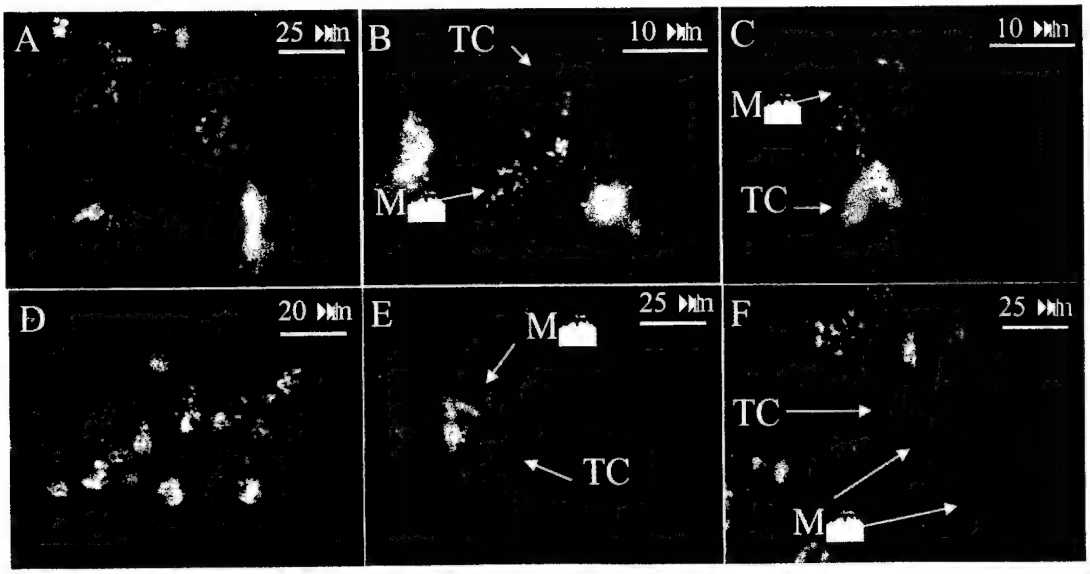

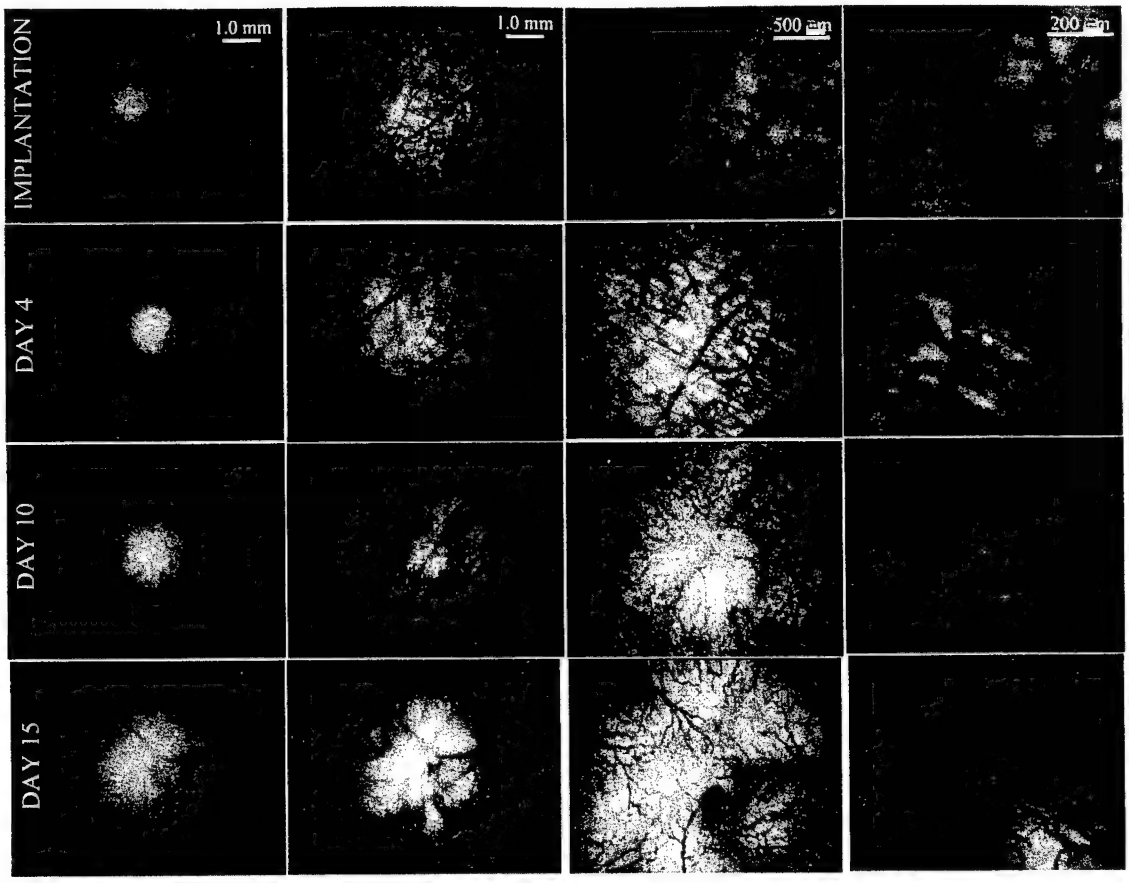
IMPLANTATION
DAY 4
DAY 10
DAY 15
1.0 mm
1.0 mm
500 μm
200 μm

Dendritic Cells Pulsed with Apoptotic Prostate Tumor Cells Induce Prostate Tumor Rejection *In Vivo*

Brigitte Dudouet, Gregory Frost, Joseph Lustgarten and Per Borgstrom

Sidney Kimmel Cancer Center
10835 Alman Row, San Diego, California 92121

Key words: Prostate Cancer, Dendritic Cells, Apoptotic Cells, Phagocytosis, Vaccine, Cancer Immunotherapy. TRAMP Model.

[1]This work was supported by the Department of Defense (DOD), Idea Development, Phase I Award.
[2] *Correspondence to: Brigitte Dudouet, Ph.D., Sidney Kimmel Cancer Center, 10835 Altman Row, San Diego, California 92121.

The abbreviations used are : DCs, dendritic cells; TRAMP, transgenic adenocarcinoma mouse Prostate; MHC, major histocompatibility complex; CD8+ and CD4+ ,T lymphocytes; GFP, green fluorescent protein; C57BL/6 mice, B6 mice.

ABSTRACT

BACKGROUND. Adoptive transfert of autologous dendritic cells(DCs) pulsed *ex vivo* with prostate tumor deriving antigen(s) may represent an appealing alternative therapy for hormone refractory metastatic prostate cancer. Recently, immature (DCs) have been described to internalize, process and present apoptotic tumor cells deriving antigens to naïve T in a highly efficacious manner, inducing a protective immune response against cancer.

METHODS. Using intravital microscopy in awake mice and a subcutaneous murine model for prostate cancer, we have investigated the efficiency of a cellular vaccine composed of autologous dendritic cells pulsed with the apoptotic established prostate carcinoma cells line (TRAMP-C2) to treat and eliminate transplanted growing prostate tumors.

RESULTS. We have shown that immature DCs internalized apoptotic prostate tumor cells (TRAMP-C2) with a great efficiency and exhibited phenotypic and functional changes corresponding to their maturation into potent antigen presenting cells (APC). In addition, immunization of mice with apoptotic tumor cells-pulsed DCs mediated an effective protection and successfully treated transplanted prostate tumors. Moreover, we have observed an important decrease of prostate tumor angiogenesis.

CONCLUSION. These findings suggest that autologous DCs pulsed with apoptotic tumor cells derived from an established tumor cell line or from resected tumors, may represent a powerful candidate for therapeutic application in patients afflicted with prostate cancer.

INTRODUCTION

Despite a sharp increase in detection of pre-clinical and early stage of prostate cancer, uncertainty still remains about the natural evolution of the disease. In particular, advanced hormone-refractory prostate cancer is a major problem of clinical research: initially treatable by androgen ablation, it ultimately escapes from hormonal control and relapses in chemo-resistant tumors. Therefore, the exploration of alternative or complementary therapies designed specifically for prostate cancer is justified. One such approach that continues to attract significant interest is the use of immunotherapy to treat prostate malignancies. It is now possible to manipulate immunological effector cells or APCs *ex vivo*, in order to induce an effective anti-tumor response. Among all APCs, DCs are the most effective and are pivotal players in the modulation of the immune response to many foreign and self-antigens (1,2). They are migratory cells broadly distributed within the body in lymphoid and non-lymphoid tissues. They are characterized by two stages of differentiation: immature and mature. Immature DCs strategically reside in non-lymphoid tissues such as epithelium in contact with the external environment or in intersticial tissues where they play a sentinel role. At this stage, they are characterized by a high capacity of Ag capture and processing and a low level of T cell stimulatory capacity. Inflammatory signals such as TNFα, IL-1, LPS or CD40 ligand induce their maturation, which corresponds to dramatic phenotypic and functional changes. Following maturation induction *in vivo*, DCs will migrate to the lymph node where they interact with and stimulate naïve T cells. At this stage, their endocytic activities are turned off, while their Ag presentation capabilities are considerably increased, a process that coincides with the up-regulation of cell surface MCH class I and class II, as well as costimulatory and adhesion molecules (3,4,5,6).

Current immunotherapeutic strategies for prostate cancer use DC-based vaccines targeting three tumor associated Ags: PSA (prostate specific antigen) (7), PSMA (prostate specific membrane antigen) (8) or prostatic acid phosphatase (PAP) (9). Some clinical trials, already have shown promising results (10,11) and confirmed that DCs-based vaccine may represent an alternative therapy for patients with advanced prostate cancer and/or in patients whose disease no longer responds to hormone therapy (12). However, DC-based adoptive transfer therapies are limited by their dependence on the identification and availability of appropriate tumor Ag(s). Cellular vaccines composed of autologous DCs that have engulfed apoptotic tumor cells may overcome

these limitations. Recent published data showed that immature DCs are able to phagocytose apoptotic cells via membrane scavenger receptors and integrins (13). Processing of phagocytosed apoptotic cells yields Ags that access the MHC class I pathway of engulfing DCs (14) and apoptotic body-derived epitopes are presented on MHC class II molecules as well (15). Moreover, *in vivo* immunization with DCs pulsed with apoptotic tumor cells can prime tumor-specific CTLs and confers protection against a tumor challenge (16). Thus, these observations suggest that DCs pulsed with apoptotic tumor cells, have the potential to stimulate immunity against numerous tumor Ag and can induce a synergistic protection through CD4+ and CD8+ T cell mediated immune responses.

Recently, Greenberg et al have created a transgenic mouse model called TRAMP (Transgenic Adenocarcinoma Mouse Prostate) in which mice develop spontaneous prostate tumors (17,18). Importantly, Greenberg has also derived and characterized three epithelial cell lines from a heterogeneous 32-week spontaneous tumor. Two of the three cell lines are tumorigenic in immune competent syngeneic C57BL/6 hosts: TRAMP-C1 and TRAMP-C2 (19). So far, few immunotherapeutic approaches for prostate cancer have been tested in the TRAMP mice or in syngeneic subcutaneous model. Kwon et al, have demonstrated that following vaccination with a B7-1 expressing TRAMP cell line, animals developed a T cell mediated immune response capable of rejecting tumors (20). Granziero et al, have shown that adoptive transfer of CTLs directed against the large T antigen, prevents the development of lethal clinical tumors in TRAMP mice (21). A metastatic prostate model with TRAMP-C2 cells transplanted into C57BL/6 mice has also been developped. In this system, the tumorigenic TRAMP-C2 cell line develops metastases in the lymph nodes and lung from the primary tumor. Following primary tumor removal, all mice relapse with metastases arising from micrometastases present at the time of the primary tumor resection. Interestingly, administration of immunotherapeutic treatment such as CTLA-4 blockade immediately after primary tumor resection can effectively prevent metastatic relapse (22).

Over the years, a system for non-invasive imaging study of tumor microcirculation in awake mice, using intravital video-microscopy (IVVM)) has been developed in Per Borgstrom's laboratory (Gregory Frost manuscript in preparation). IVVM is a technique of fluorescence video-microscopy that allows visualization of tissue of interest through a window (dorsal or cranial) providing direct observation and real time monitoring of steps in tumor growth and

tumor angiogenesis process). Visualization of tumor cells by IVVM requires that the cells carry a marker to distinguish them from the surrounding normal tissue for a long term observation in vivo. A life fluorescent reporter (A Histone H2B-GFP fusion protein) has been developed in the laboratory and introduced into TRAMP-C2 cells by retroviral transduction. H2B-GFP fusion protein incorporates into nucleosomes without affecting cell cycle progression allowing to evaluate not only tumor size and quantification of the motility of tumor cells but also mitotic and apoptotic indices of the implanted tumor spheroids. Under high magnification, the underlying mechanism behind immunotherapy mediated tumor regression (destruction of tumor by tumor antigens specific CTLs or by innate immunity effectors) can be distinguished. Moreover parameters such as vessel morphology (shape, length, diameter) and density, blood flow rate and white blood cells infiltration allows detailed quantitative evaluation of immunotherapeutic treatment effectiveness.

Using intravital microscopy and the subcutaneous prostate tumor model developed with syngeneic TRAMP-C2 cell transplanted in C57BL/6 male mice, we have evaluated the protective and therapeutic effect of a cellular vaccine composed of autologous DCs pulsed with apoptotic TRAMP-C2 cells which may represent a powerful candidate for therapeutic application in patients afflicted with prostate cancer.

MATERIAL AND METHODS

Animals

Six to 8 weeks old males C57BL/6 (denoted B6) mice were purchased from Jackson Laboratory and housed at the animal maintenance facility of the Sidney Kimmel Cancer Center.

Animal model and surgical techniques

The dorsal skinfold chamber in the mouse is prepared as described (G. Frost et al.manuscript in preparation) Male mice (25-35 g body weight) are anesthetized (7.3 mg ketamine hydrochloride and 2.3 mg xylazine /100 g body weight, i.p.) and placed on a heating pad. Two symmetrical titanium frames are implanted into a dorsal skinfold, so as to sandwich the extended double layer of skin. A 15 mm full thickness layer is excised. The underlying muscle (M. cutaneous max.) and

subcutaneous tissues are covered with a glass cover slip incorporated in one of the frames. After a recovery period of 2-7 days, tumor spheroids are carefully placed in the chamber.

Culture medium and reagents

Complete medium (CM) used for DC culture consisted of RPMI 1640 medium supplemented with 10% heat inactivated fetal bovine serum from hyclone, 2mM fresh L-Glutamine, 100microg/ml streptomycine 100 units/ml penicillin, from Gibco and 5x10 moins 5 M 2mercaptoethanol (Sigma). Cultured medium used for TRAMP-C2 cells was composed of RPMI-1640 supplemented with 2mM L-Glutamine, 5% Nu-serum IV (Collaborative Biomedical Products), 5% FBS (Hyclone), 5 microg/ml insuline (Sigma) 25 U/ml peniciline-streptomycine (Life Technology), 10 moins 8 dihydrotestosterone (DHT) in 10% ETOH (Sigma).

Cytokines

Recombinant murine granulocytes/macrophage colony-stimulating factor (GM-CSF) provided by Dr. Ralph Steinman laboratory was diluted in CM at the concentration of 1000 units /ml. TNFalpha was from Pharmingen and was added at 50ng/ml in DCs culture.

Tumors cells

The syngeneic tumor cell line, TRAMP-C2, established from a 32 weeks old prostatic adenocarcinoma from C57BL/6 male TRAMP- mouse was provided by Greenberg laboratory. The irrelevant epithelial cell line MC57 cells purchased in ATCC

Preparation of tumor spheroids

Tramp C2 cells transduced with a Histone H2B-GFP fusion protein in an LXRN retroviral vector have been generated as described : TRAMP-C2 H2BGFP cells to a final volume of 250,000 tumor cells/ml. The tumor cell prostate hybrid suspensions are then dispersed 100ul/well into 96 well round bottom plates coated with 1.0 % agarose for a liquid overlay. The spheroids are allowed to compact for 48hours followed by washing in serum free media for implantation into chambers.

Intravital video-microscopy

Fluorescence microscopy is performed (Greg Frost et al, manuscript in preparation) using a Mikron Instrument (Mikron Instrument, San Diego, CA) equipped with epi-illuminator and video-triggered stroboscopic illumination from a xenon arc (MV-7600, EG&G, Salem, MA). A silicon intensified target camera (SIT68, Dage-MTI, Michigan City, IN) is attached to the microscope. A Hamamatsu image processor (Argus 20) with firmware version 2.50 (Hamamatsu Photonic System, USA) is used for image enhancement and to capture images to a computer. A Leitz PL1/0.04 objective is used to obtain an over view of the chamber and for determination of tumor size. A Zeiss long distance objective 10/0.22 is used to capture images for calculation of vascular parameters. A Zeiss Achroplan 20X/0.5 W objective is used for capturing images for calculation of mitotic and apoptotic indices.

Image analysis

For each spheroid, video recordings are used to calculate length, area and vascular density of the neovasculature being induced by the implanted tumor spheroids. The vasculature is analyzed off-line from the video recording using a photodensitometric computer software (Image-Pro Plus, Media Cybernetics, MD).

Dendritic cells preparation

DCs have been prepared according to a protocol provided by Dr. Ralph Steinman (2). Briefly, bone marrow from C57BL/6 mice is depleted of lymphocytes and cultured in complete medium supplemented with 1000U/ml of GM-CSF. On day seven, DCs are harvested and tested for DCs specific markers cell surface expression (MHC class II, B7-2 and CD11c), by flow cytometry analysis. For effective engulfment of apoptotic tumor cells, it is essential that DCs be immature.Immature DCs display a high level of endocytic activity. To assess the stage of DCs maturation, we have quantitated endocytosis by flow cytometry using FITC-dextran and Lucifer yellow. We use DCs at their highest level of endocytic activity from day 6 to day 8.

Induction of apoptosis of the prostate tumor cell line, TRAMP-C2

We have determined that optimal apoptosis induction of parental TRAMP-C2 cells occurs following 1 minute of UVB irradiation (2mj/cm2/sec) and 16 hours of culture in medium without serum at 37°C, as assessed by Annexin-V FITC staining.

Preparation of TRAMP-C2 dendritic cells-based vaccine

Following UV irradiation and serum deprivation, apoptotic TRAMP cells are co-cultured with immature DCs (day 7) at a ratio of 1 DC for 2 apoptotic tumor cells. After 18 hours of co-culture at 37°C, the mixture of DCs/apoptotic TRAMP-C2 cells (we have determined that usually in these conditions, more than 70% of immature DCs have ingested apoptotic bodies) are treated with TNFα (50ng/ml) to ensure DCs maturation and capacity for antigen presentation. After 24 hours of incubation in presence of TNFα, the cell-mixture is harvested, washed in PBS and counted. One millions of DCs which have engulfed apoptotic tumor cells are then injected in mice.

Monoclonal antibodies

For fluorescence-activated cell sorter (FACs) analysis the following monoclonal antibodies Phycoerythrin (PE) labeled were used: anti MHC class II, anti-B7-2, anti CD11c (Pharmingen). For depletion *in vivo*, antibodies anti-CD4 and CD8 have been purchased from Pharmingen.

Phagocytosis assay

To evaluate phagocytosis of apoptotic TRAMP-C2 cells by immature DCs, we utilized flow cytometry. Viable TRAMP-C2 cells are labeled with aliphatic green fluorochrome PKH2-GL according to the manufacturer's instruction (Molecular Probes) prior to the induction of apoptosis. Following UV irradiation and serum deprivation culture, the apoptotic green fluorescent TRAMP-C2 cells are cocultured with immature DCs (day 7) at the ratio of 1 DCs for 2 apoptotic tumor cells. After 18 hours of coculture at 37 oC, the mixture of DCs/apoptotic TRAMP-C2 cells were harvested and and stained with Phycoerythrin (PE) labeled antibodies (Pharmingen) against MHC class II and B7-2 (CD86) for flow cytometry analysis. MHC class II and B7-2 are expressed specifically by DCs and not by TRAMP-C2 cells or MC57 cells.

Primary Immunization

Normal B6 mice were immunized s.c. in the right flank with 1 million of apoptotic TRAMP-C2 cells-pulsed DCs at 7 days of interval (day 0 and day 7). As a controls, additional groups of mice were vaccinated with unpulsed DCs, apoptotic TRAMP-C2 cells, DCs pulsed with an irrelevant apoptotic cell line MC57, or with PBS. All vaccinated mice were challenged 7 days after the last immunization with a lethal dose of viable TRAMP-C2 cells (2 millions) by s.c. injection in the left flank . Starting 2 weeks after tumor challenge, mice were inspected for palpable tumor masses. Survival has been determined.

Treatment of established micro-tumor in chamber model

One TRAMP-C2 H2B-GFP spheroid composed of 25 000 cells has been implanted per dorsal skinfold chamber on syngeneic B6 mice has been implanted as described above. Six days after implantation, animal were immunized s.c. near the inguinal lymph node with 1 million of DCs pulsed *in vitro* with apoptotic parental TRAMP-C2 cells. As controls other groups of mice have been vaccinated with DCs alone, apoptotic TRAMP-C2 cells, DCs pulsed with an irrelevant apoptotic cell line MC57, or with PBS. Using intravital microscopy, tumor size has been evaluated by day 7 after immunization.

Treatment of transplanted TRAMP-C2 tumor in syngeneic mice

Male C57BL/6 mice (6 per group) were challenged 7 to 10 days prior to vaccination by s.c. injection of $5x10^5$ viable TRAMP-C2 cells in the left flank. Vaccination with 10^6 irradiated DCs pulsed with apoptotic TRAMP-C2 cells were performed four times at 14-21 day intervals. Control groups received irradiated DCs alone, apoptotic TRAMP C2 cells, apoptotic MC57 cells-pulsed DCs irradiated, or PBS only. Repeated vaccination were performed if necessary. Mice were monitored every other day to evaluate tumor regression and survival.

In vivo determination of CD4+ and CD8+ role to protect against transplanted prostate tumor

To evaluate the contribution of each category of T cells to protection against tumor, we performed *in vivo* depletion of CD4+ and CD8+ T cells in the syngeneic murine tumor model -

TRAMP-C2 cells transplanted in C57BL/6 male mice - and in the spontaneous TRAMP model. CD4+ or CD8+ T cells were depleted by i.v. injection of anti-CD4 mAb (GK1.5) or anti-CD8 mAb (53-3.8) respectively prior to the first immunization. Treatment of mice with an irrelevant isotype matched mAb served as a control. Antibody treatment continued for 3,7, and 10 days after the first immunization to guarantee a chronic depletion of the desired cell type. The efficiency of the antibody depletion were analyzed by flow cytometry.

RESULTS

Several considerations must be taken into account to prepare DCs based vaccine. These include the maturation state of the DC being used, the conditions for apoptosis induction in the tumor cell component of the vaccine, and the ability to measure the uptake of the apoptotic tumor by the DC. To prepare bone marrow derived DCs we followed a published protocol provided to us by Dr. Ralph Steinman (2). The DC maturation state is critical for antigen uptake and processing. For effective engulfment of apoptotic tumor cells, it is essential that DCs be immature. Following uptake of apoptotic bodies, DCs undergo subsequent maturation. Immature and mature DCs can be distinguished by their endocytic capacities. To assess the stage of DC maturation, we quantitated endocytosis through the mannose receptor (MR) by flow cytometry using FITC Dextran uptake and macropinocytosis activity by Lucifer Yellow (LY) uptake (data not shown). Immature DCs displayed a high level of endocytosis of these two markers, while mature DCs showed a strong down regulation of FITC-DX and LY uptake. Using this technique, it was possible to conclude that DCs exhibited the highest level of endocytic activity from day 6 to day 8. To induce apoptosis of the TRAMP-C2 cell line, we have exposed tumor cells to UVB irradiation (60 watt UVB lamp) calibrated to provide 2mj/cm2/sec. Cells exposed to UV light for varying lengths of time were then cultured in medium deprived of serum for 16 hours at 37^0C. Apoptosis was assessed using an annexinV detection test. Following labeling with annexinV, cells were counter stained with propidium iodide (PI) and analyzed by flow cytometry. Using this protocol we have determined that optimal apoptosis induction of TRAM-C2 cells occurs following 1 minute of UVB irradiation. As a control cell line in this application,

we used the C57BL/6 derived fibroblast cell line, MC57. We determined that apoptosis induction of MC57 is optimal under the same conditions used for TRAMP-C2.

It is critical for each vaccine preparation to establish that maximal uptake of apoptotic cells by the immature DCs has occurred. To evaluate phagocytosis of apoptotic cells by immature DCs, we utilized flow cytometry. Viable TRAMP-C2 cells were labeled with the aliphatic green fluorochrome PKH2-GL according to the manufacturer's instruction prior the induction of apoptosis. Following UV irradiation and serum deprivation culture, the apoptotic green fluorescent TRAMP cells were co-cultured with immature DCs (day 7) at the ratio of 1 DC for 2 apoptotic tumor cells. After 18 hours of co-culture at 37°C, the mixture of DCs/apoptotic TRAMP-C2 cells were harvested and stained with Phycoerythrin (PE) labeled antibodies against MHC class II and B7-2 (CD86) for flow cytometric analysis. MHC class II and CD86 are expressed specifically on DCs and not on TRAMP-C2 or MC57 cells. As shown in Figure 1, greater than 72% and 68% of immature DCs engulfed apoptotic TRAMP and MC57 cells respectively. We observed that the ingestion of TRAMP-C2 apoptotic bodies triggered DC maturation. DC maturation upon phagocytosis of apoptotic TRAMP-C2 cells (or apoptotic MC57 cells) was assessed by flow cytometry based on the relative increase in cell surface expression of MHC class I and II and CD86. Inflammatory cytokines such as TNFα. are known to also promote DC maturation and were used as controls in these studies. However, in order to assure DCs maturation and the efficacy of the vaccine after uptake of apoptotic TRAMP-C2 cells, the coculture were exposed to the inflammatory cytokine during 24 hours before injection.

We first investigated the capacity of apoptotic TRAMP-C2 cells-pulsed DCs to induce tumor specific CTLs *in vivo* after immunization. Syngeneic naïve mice C57BL/6 were immunized s.c. with 10^6 irradiated apoptotic TRAMP-C2 cells-pulsed DCs without adjuvant. Seven days after immunization, spleen cells were restimulated *in vitro* with irradiated TRAMP-C2 cells and then assayed 5 days later for lytic activity against tumor targets. As expected, . mice immunized with the apoptotic TRAMP-C2 cells-pulsed-DCs vaccine developed a significant levels of CTLs activity against TRAMP-C2 cells and DCs pulsed with apoptotic TRAMP-C2 cells as well and did nor recognized the irrelevant cells line MC57 or DCs alone (Fig.2). In contrast mice vaccinated with PBS, or DCs alone, apoptotic TRAMP-C2 cells or DCs pulsed with apoptotic MC57 failed to result in the generation of CTLs (data not shown). These results demonstrate

that the immunization of syngeneic mice with apoptotic TRAMP-C2 cells-pulsed DCs elicited a response against TRAMP-C2 prostate tumor cells.

The efficiency of apoptotic tumor cells-pulsed DCs to induce anti-tumor immunity *in vivo* was assessed by vaccinating syngeneic immunocompetent transplanted C57BL/6 mice with viable parental TRAMP-C2 cells. In order to acquire quick preliminary informations about immunotherapeutic treatment effectiveness (dose and timing of vaccination accuracy) and to observe in real time the underlying mechanisms behind immunotherapy mediated tumor regression, we initially used IVVM. IVVM permitted direct assessment of tumor growth and tumor vascularization (vessels morphology and density) and white blood cells infiltration. The fluorescent reporter gene (H2B-GFP fusion protein) introduced into TRAMP-C2 cells helped evaluate the state of the implanted tumor spheroids by providing mitotic and apoptotic indices. Spheroids composed of $25x10^{4}$ TRAMP-C2 H2B-GFP cells were implanted into dorsal skinfold chamber in syngeneic C57BL/6 male mice). Six days after implantation, animals (6 per group) were immunized s.c. with 10^{6} DCs pulsed *in vitro* with apoptotic parental TRAMP-C2 cells, DCs alone, apoptotic TRAMP-C2 cells or DCs pulsed with apoptotic MC57 cells. Tumor regression was observed as shown in figure 3 (C2) by day 12 post immunization (day 18 after implantation), while no tumor regression was observed in controls (Fig.3:A2). In addition we observed a high number of tumor cells undergoing apoptosis in animal treated with the vaccine while animals untreated exhibited a high level of cells division within the tumor. Tumor spheroids in chambers of animal untreated were extremely dense as shown in Figure 3 (A3 a A4) meanwhile the tumors were loose and not compact in animal injected with the vaccine (Fig.3: C3 and C4) Tumor spheroid vascularization was disorganized and disrupted in animal treated (Fig. 3: D3, and D4) showing an important leukocyte infiltration of the tumor (Fig.3: D3) . In contrast, microvasculature was dense, intact and extremely organized in tumor spheroids of control animals with no sign of leukocytes infiltration (Fig.3: B3 and B4) . We observed that the best dose for the vaccine was 10^{6} DCs pulsed with apoptotic TRAMP-C2 cells and that vaccine administration everytwo weeks was the more appropriate schedule.

We then investigated the protective effect of the vaccine on a larger tumor burden in subcutaneous model. Cohort of mice were immunized s.c. with autologous DCs pulsed with apoptotic TRAMP-C2 cells, prior to challenge with viable parental TRAMP-C2 cells. The

vaccine elicited a strong protective response against TRAMP-C2 tumor growth. Mice remained tumor free for at least 100 days postumor challenge (Fig.3). In contrast, control groups of mice either left untreated or immunized with unpulsed DCs alone or apoptotic TRAMP-C2 cells or DCs pulsed with apoptotic irrelevant cell line MC57 harbored large tumors by day 30 after tumor challenge and died within 55 to 75 days.

We next studied whether apoptotic TRAMP-C2 cell-pulsed DCs administration could mediate a therapeutic benefit on established prostate tumors. Treatment of TRAMP-C2 tumors bearing C57BL/6 male mice with DCs pulsed with apoptotic TRAMP-C2 cells resulted in a strong immune response against TRAMP-C2 subcutaneous tumors (50% of mice remained alive for at least 140 days). Control groups of mice armored larger tumors and succumbed within 45 to 65 days after challenge. (Fig.4). Selective depletion of $CD8^+$ or $CD4^+$ T cells subset by specific mAb administration prevented the effective immune priming by a DCs pulsed with apoptotic TRAMP-C2 cells. All depleted mice of either CD4+ or CD8+ T cells succumbed to progressive TRAMP-C2 tumor growth on challenge. Figure 5 shows that depletion of either CD4 or CD8 positive cells completely abrogates the survival of mice that were preimmunized with apoptotic TRAMP-C2 cell-pulsed DCs. This indicates that both $CD4^+$ and $CD8^+$ T cells are essential in the effector phase, suggesting that upon tumor challenge, tumor specific T helper cells are required for prompt activation of CD8 positive effector cells.

DISCUSSION

For prostate cancer, conventional adjunct therapies including chemotherapy and radiation therapy give little or no advantage over surgery alone. Therefore, the fact that one third of prostate cancer patients experience postchirurgical treatment failure due to progression of residual micrometastases is of particular concern. Moreover, when patients reach the stage of disseminated prostate cancer, the only treatment available is androgen ablation that may selectively trigger the growth of hormone independent forms of the disease. Based on the small volume of residual cancer after surgery, the ineffectiveness of conventional adjunct therapies and the temporary effect of hormone ablation, we think that immunotherapy might be an effective strategy when used as an adjunct treatment after surgery and to prevent and/or treat hormone independent prostate cancer relapse. Previously, the development and evaluation of various

immunotherapy treatments for prostate cancer have been hampered by the lack of syngeneic immunocompetent prostate cancer models. The transgenic model for prostate cancer TRAMP and deriving tumorigenic cell line TRAMP-C2 established by Greenberg et al (19), have opened many possibilities for immunotherapeutic studies on prostate cancer. We have developed two models to perform our experiments exclusively *in vivo* in order to study the biological protective effect of DCs based vaccine and the effector cells interaction with tumor tissue in its natural environment that cannot easily be mimicked in an *in vitro* setting. We have first used a syngeneic model for intravital microscopy by implantation of histone H2B-GFP transduced TRAMP-C2 spheroids in a skinfold chamber in awake mice in order to evaluate the efficiency of our vaccine formulation and timing of administration against prostate cancer *in vivo*. This method helped us evaluate *in vivo* mitotic and apoptotic indices of the prostate tumor cells, revealing the state of the tumor cells after treatment. Moreover, intravital microscopy allowed imaging of important physiological processes that are lacking *in vitro* such as angiogenesis influencing the tumor growth, the access of effector cells to the tumor and finally the metastatic spread to other tissues.

The second model has been obtained by subcutaneous injection of the parental cell line TRAMP-C2 in syngeneic C57BL/6 male host to test the effect of DCs based treatment on larger tumor scale and understand the role played by one or both subsets of T cells, CD4+ and CD8+, involved in tumor elimination. The use of apoptotic cells as a source of antigen(s), however, offers the advantage of potentially providing to the DCs multiple tumor-associated antigens in the form of both helper and CTL-defined epitopes for presentation to T cells, which could overcome tumor evasion by stimulating both arms of the cellular immune response. DCs are known to be able to both generate antigen-specific CTL from naïve T cells and can stimulate $CD4^+$ T cells to specific antigens in an MHC class I and class II manner (6). It has been shown recently that whole tumor lysate can serve as effective immunogens to stimulate CD8+ and $CD4^+$T cell reactivity *in vitro* and *in vivo* when processed and presented by murine Langherans cells or bone marrow derived-DCs (23,24,25,26). Moreover, earlier studies have demonstrated that MHC class I presentation of exogenous antigens can be achieved by professional APCs both *in vitro* and *in vivo* (27). DCs pulsed with tumor associated peptides or proteins have shown therapeutic efficacy *in vivo* (28)

In the current study, we have shown that immature bone marrow-derived DCs pulsed with apoptotic TRAMP-C2 cells generate both prostate tumor-specific cytolytic and proliferative T

cells *in vivo*. In addition, treatment of syngeneic mice with s.c injections of apoptotic TRAMP-C2-cell pulsed DCs could elicit effective immune priming which results in protection against prostate cancer and in regression of established transplanted prostate tumors (Fig. 2, 3 and 4). This *in vivo* antitumor effect was specific for TRAMP-C2 tumor; DCs pulsed with the irrelevant syngeneic cell line MC57 did not induce any protection. However we have observed a slight delay in the survival of animals vaccinated with apoptotic TRAMP-C2 cells that can be explained by the fact that some apoptotic bodies may have been uptaken by the host DCs that reside or have been recruited in the environment of the injection.

Some authors (29) have recently reported that uptake of apoptotic cells by human monocyte derived DCs may induce a peripheral tolerance due to the absence of DCs maturation, a step which is a cornerstone in the initiation of immunity. In contrast in immunocompetent syngeneic murine model, we have observed that bone marrow derived DCs upregulate molecules involved in antigen presentation and interaction with T cells, upon ingestion of apoptotic bodies and, as described in recent works (30) they are able to break tolerance. Moreover, to assure DCs maturation and differentiation into potent APCs, our vaccine has been treated with TNFalpha during 24 hours after apoptotic cells uptake.

One potential problem of this approach is a possible autoimmune reactivity might occur to self and to normal tissue antigens present in the apoptotic tumor-cells, which are processed by very effective APCs. It has been reported that some patients bearing melanoma and undergoing immunotherapy can present vitiligo showing that normal tissues antigens can be the target of the immune response (31). Although the potential exists for inducing autoimmunity by immunization with apoptotic cells-pulsed CDs, most of the recent studies using crude tumor-cell membrane, total tumor-cell RNA or tumor cell lysates did not report any pattern of autoimmunity (25,26,32). However, the behavior and biology of syngeneic tumors obtained by transplantation of tumor cells in C57BL/6 host is totally different from the comportment of spontaneous tumor growing in transgenic animal model for prostate cancer such as TRAMP (ref).

Our next step will be to test the therapeutic potential of our vaccine in condition of tolerance in the transgenic animal model TRAMP for prostate cancer. Both murine prostate cancer models, subcutaneous and transgenic, offer a potential clinical application for immunotherapy of human prostate cancer.

CONCLUSION

The use of DCs after uptake of apoptotic prostate tumor cells is particularly appealing since the procedure is rapid and does not require antigen identification and production, reducing considerably the interval between the tumor excision and the beginning of the immunotherapeutic treatment. Moreover, this approach is patient specific and can be applied to multiple cancers.

Upon successful completion of these studies in tolerant conditions in TRAMP mice, we believe it would be possible to rationally design human clinical trial using as source of Ag apoptotic bodies derived from patient resected tumor.

REFERENCES

1. Banchereau, J., and R,M. Steinman. 1998. Dendritic cells and the control of immunity. Nature. 392:245-251.

2. Inaba, K, N. Romani H.Aya, M.Deguchi, S. Muramatsu, and R.M. Steinman. 1992.Generation of large number of dendritic cells from mouse bone marrow culture supplemented with granulocyte/macrophage colony-stimulating factor. J.Exp.Med.176: 1693-1702.

3. Sallusto F and A.Lanzavecchia.(1994) efficient presentation of soluble antigen by cultured human dendritic cells is maintained by granulocyte/macrophage colony stimulating factor plus interleukine 4 and down regulated by tumor necrosis factor α. *J.Exp. Med.***179**: 1109-2889.

4. Sallusto and A.Lanzavecchia. (1995). Dendritic cells use macropinocytosis and the mannose receptor to concentrate macromolecules in the major histocompatibility complex Class II compartment: down regulation by cytokines and bacterial products. J.Exp.Med. **182**:389-400.

5. Cella, M, Federica Sallusto and Antonio Lanzavecchia (1997) Origin, maturation and antigen presentation function of dendritic cells. *Current opinion in immunology.* **9:** 10-16

6. Steinman Ralph, Maggie Pack and Kayo Inaba.(1997) Dendritic cells in the T cell areas of lymphoid organs. *Immunological reviews.* Vol.156:25-33

7. Peehl, D.M., Prostate specific antigen role and function. *Cancer.* **75**:2021. 1995.

8. Leek, J., Lench, N., Marag, B., Bailey, A., Carr, I.M., Andersen, S., Cross, J., Whelan, P.,MacLennan, K.A., Meredith, D.M., and Markham, A.F. Prostate-specific membrane antigen:evidence for the existence of s second related gene. *British Journal of Cancer,* **72**: 583. 1995

9. Jacob, E., Haskell, C. Clinical use of tumor markers in oncology. *Curr. Probl. Cancer.* **15**:299. 1991.

10. Tjoa, B.A., erickson,S.J., Bowes, V.A., Ragde, H., Kenny G.M., Cobb, O.E., Ireton, R.C.,Troychak, M.J., Boynton, A.L. and Murphy, G.P. Follow-up evaluation of prostate cancer patients infused with autologous dendritic cells pulsed with PSMA peptides. *Prostate.* 1997. September 1; **32**(4):272-8

11. Murphy, G., Tjoa, B., Ragde, H., Kenny, G. and Boynton, A. Phase I clinical trial: T-cell therapy for prostate cancer using autologous dendritic cells pulsed with HLA-AO201-specific peptides from prostate-specific membrane antigen. *Prostate.* 1996. December; **29**(6):317-80

12. Murphy, G.P., Tjoa, B.A., Simmons, S.J., Jarisch, J., Bowes, V.A., Ragde, H., Rogers, M., Elgamal, A., Kenny, G.M., Cobb, O.E., Ireton, R.C., Troychak, M.J., Salgaller, M.L. and Boynton, A.L. Infusion of dendritic cells pulsed with HLA-A2-specific prostate-specific membrane antigen peptides: a phase II prostate cancer vaccine trial involving patients with hormone-refractory metastatic disease. *Prostate.* 1999.January 1;**38**(1):73-8.

13. Albert L. Matthiew, Frieda A. Pierce, Loise M. Francisco and Nina Bhardwaj.(1998) Immature dendritic cells phagocytose apoptotic cells via αvβ5 and CD36 and cross present antigens to cytotoxic T lymphocytes. *J.Exp.Med.* Vol.**188**:Number7. 1359-1368.

14. Albert M.L., Sauter, B. & Bhardwaj, N.(1998) Dendritic cells acquire antigen from apoptotic and induce class I-restricted CTLs.Nature **392**:86-69.

15. Inaba K, Truly S, Yammered F, Iyo T, Manhole K, Ina M, Pack M, Subklewe M, Sauter B, Sheff D, Albert M, Bhardwaj N, Mellman I, Steinman RM. Efficient presentation of phagocytosed cellular fragments on the major histocompatibility complex class II product of dendritic cells. *J. Exp. Med.* 1998 Dec 7; **188**(11): 2163-73.

16. Rovere, Patrizia, Vallinoto,Cristina, Bondanza, Attilio, Crosti, Maria Cristina, Rescigno, Maria, Ricciardi-Castagnoli, Paola, Rugarli, Claudio and Manfredi, Angelo A.
Cutting Edge: Bystander Apoptosis Triggers Dendritic Cell Maturation and Antigen-Presenting Function. *Journal of Immunol.,* 1998, **161**: 4467-4471

17. Gingrich, Jeffrey R., Barrios, Roberto J., Morton, Ronald A., Boyce, Brendan F., DeMayo, Francesco J., Finegold, Milton J., Angelopoulou, Roxani, Rosen, Jefrrey M.,
Greenberg, Norman M. Metastic Prostate Cancer in a Transgenic Mouse *Cancer Research* **56,** 4096-4102, September 15, 1996.

18 . Gingrich, Jeffrey R., Barrios, Roberto J., Kattan, Michael W., Nahm, Hyun S., Finegold, Milton J., Greenberg, Norman M. Androgen-independent Prostate Cancer Progression in the TRAMP Model *Cancer Research* **57**, 4687-4691, November 1, 1997.

19.. Foster, Barbara A., Gingrich, Jeffrey R., Kwon, Eugene D., Madias, Christopher, Greenberg, Norman M. Characterization of Prostatic Epithelial Cell Lines Derived from Transgenic

Adenocarcinoma of the Mouse Prostate (TRAMP) Model *Cancer Research,* **57**, 3325-3330, August 15, 1997.

20.Kwon, E.D., Hurwitz, A.A., Foster,B.A., Madias, C., Feldhaus, A.L., Greenberg, N.M., Burg, M.B. & Allison, J.P.(1997). Proc.Natl. Acad.Sci.USA 94, 8099-8103.

21. Granziereo, Luisa, Krajewski, Stanislaw, Farness, Peggy, Yuan, Lunli, Courtney, Michele K., Jackson, Michael R., Peterson, Per A., Vitiello, Antonella Adoptive immunotherapy prevents prostate cancer in a transgenic animal model *Eur. J. Immunol.* 1999, **29**: 1127-1138.

22. Kwon ED; Foster BA; Hurwitz AA, Madias C, Allison JP, Greenberg N; Burg MB. Elimination of residual metastatic prostate cancer after surgery and adjunctive cytotoxic lymphocyte- associated antigen (CTLA-4) blockade immunotherapy. PNAS, December 21,1999, vol.96, , N26.

23. R.C.Fields, K. Shimizu, and J.J. Mule. Murine dendritic cells with whole tumor lysate mediatepotent antitumor immune responses in vitro and in vivo. *Proc.Natl. Acad.Sci. 1998, Vol.95, Issue16, 9482-9487.*

24. Cohen, P. J., Cohen, P. A., Rosenberg, S. A., Katz, S. I. & Mule, J. J. (1994) *Eur. J. Immunol.* **24,** 315-319.

25.W. Herr, E. Ranieri, W.Olson, H. Zarour, L.Gesualdo and W. Storkus. Mature dendritic cells pulsed with freeze-thaw cell lysates define an effective in vitro vaccine designed to elicit EBV-specific CD4+ and CD8+ lymphocytes responses. *Blood,1September 2000, Vol.96,No.5,pp.1857-1864.*

26. F.Nestle,S.Alijagic, M.Gilliet, Y. Sun, S. Grabbe, R.. Dummer, G. Burg & D. Schadendorf. Vaccination of melanoma patients with peptide- or tumor lysate pulsed dendritic cells. *Nature Med.Vol 4.Number3. March 1998.*

27. Kovacsovics-Bankowski, Klark Benacerraf& Keneth Rock. Efficient major histocompatibility complex ClassI presentation of exogenous antigen upon phagocytosis by macrophages. *Proc. Natl.Acad. Sci.USA 90, 4942-4946 (1993).*

28. Nestle, F.O. et al. Human dermal dendritic cells process and present soluble protein antigens. *J.Invest.Dermatol. 110 (5): 762-6.*

29.R.Steinman,S.Turley, I.Mellman and k.Inaba. the induction of tolerance by dendritic cells that have captured Apoptotic Cells. *J.Exp.Med. Vol.191,Number3, February 7,2000, 411-416*

30. A. Ronchettiet al;immunogenicity of apoptotic cells in vivo: role of antigen load, antigen presenting cells and cytokines. *J.of Immunol, 1999, 163:130-136.*

31. Rosenberg SA; White DE. J. Immunother, 19, 81-84, 1996.

32. Vierboom MPM; Nijman HW; Offringa R; Van der Voort EIH; Van Hall T; Van den Broe L; Fleuren GJ; Kenemans P; Kast WM; Melief *C.J.M. 1997.*

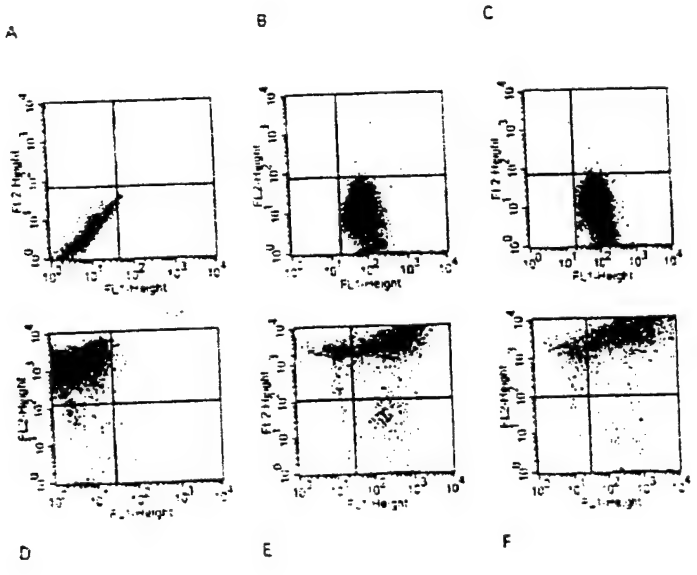

Figure 1. Phagocytosis of apoptotic cells by immature DCs assessed by flow cytometry: **A**: Negative control for dendritic cells (DCs) using isotype matched control Ab-PE. **B**: Negative control for apoptotic TRAMPC-2 cells dyed with PKH2-GL (green fluorescence) and stained with PE labeled antibodies against MHC class II and CD86. **C**: Same negative control for apoptotic MC57 cells dyed with PKH2-GL and stained with PE-labeled antibodies against MHC class II and CD86. **D**: Immature DCs stained with PE labeled antibodies against MHC class II and CD86. **E**: Coculture of immature DCs and apoptotic TRAMP-C2 cells dyed with PKH2-GL. The coculture was harvested and stained with PE- labeled antibodies against MHC class II and CD86. Double positive cells indicate uptake of the apoptotic TRAMP-C2 cells by immature DCs. Percentage of phagocytosis was calculated based on the number of double positive cells (72%) **F**: Same experiment as described above for the coculture: immature DCs pulsed with apoptotic MC57 cells. The percentage of phagocytosis reached in this case was 68%.

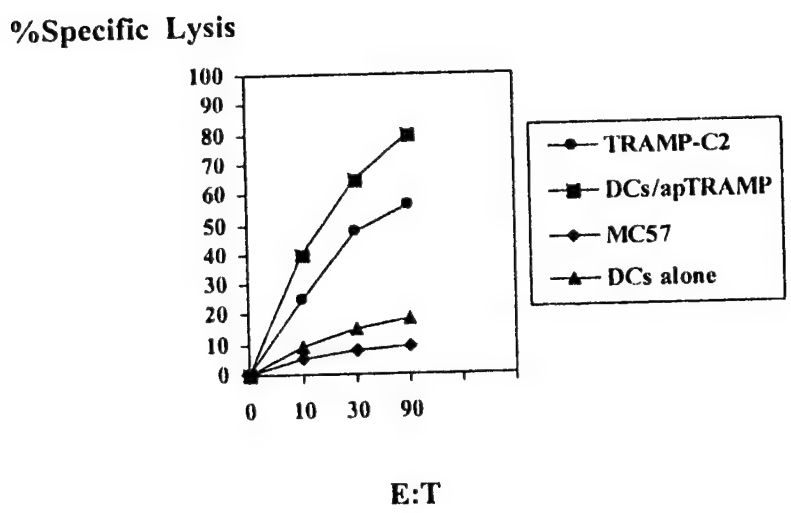

Fig.2: C57BL/6 TRAMP-C2 specific CTLs response after immunization with the vaccine DCs pulsed with apoptotic TRAMP-C2 cells

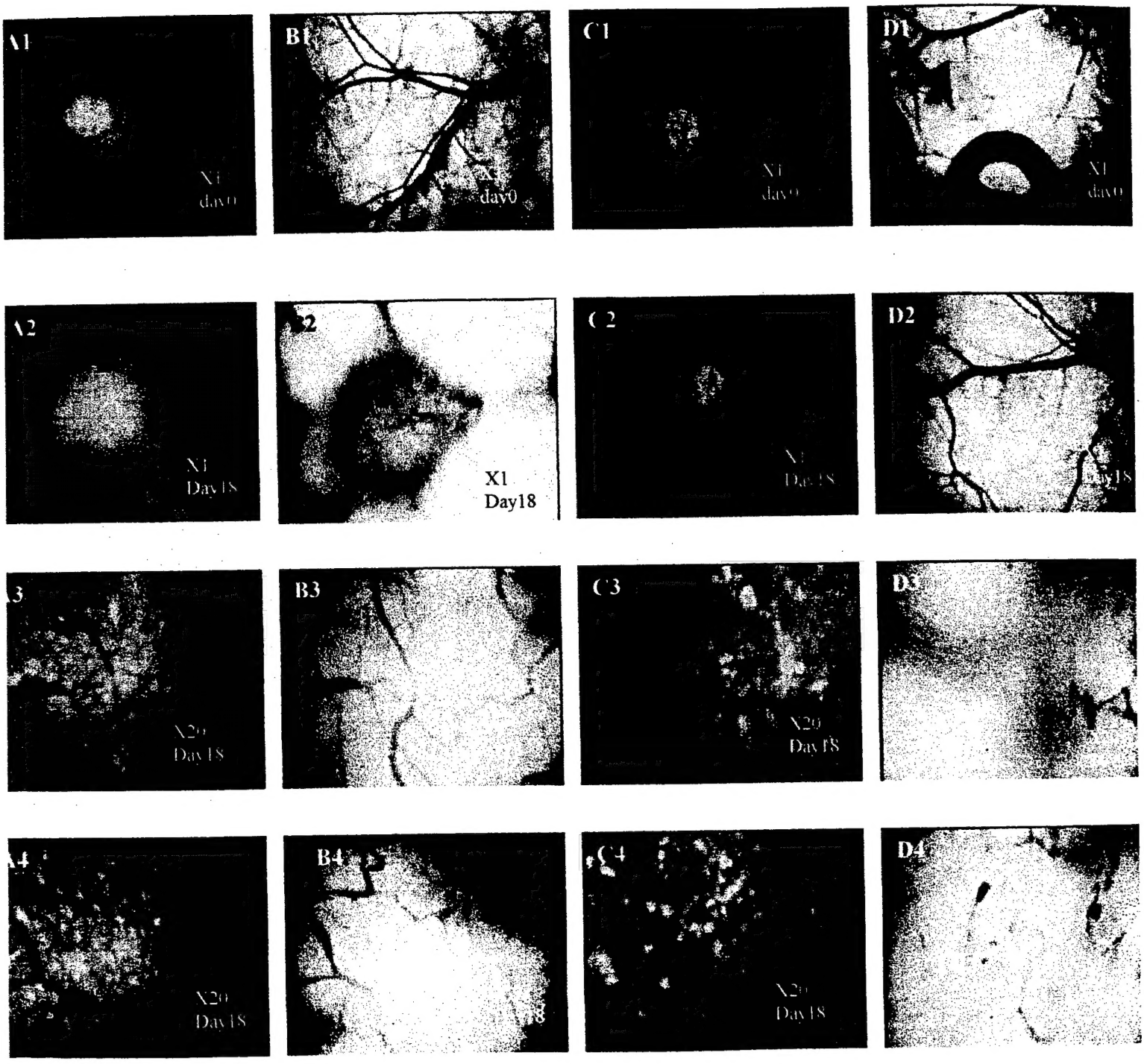

Fig. (3a) Subcutaneous vaccination with Ex-Vivo pulsed DCs with apoptotic TRAMP-C2 tumor cells (10^6) induces tumor regression of established tumors in chamber model. TRAMP-C2 H2B-GFP spheroids ($25x10^4$cells) were implanted into immunocompetent syngeneic C57/BL6 male mice on day 0. Animals were injected with apoptotic TRAMP-C2-pulsed DCs on day 6. tumor regression were observed on day 12 post immunization (day 18 after implantation.

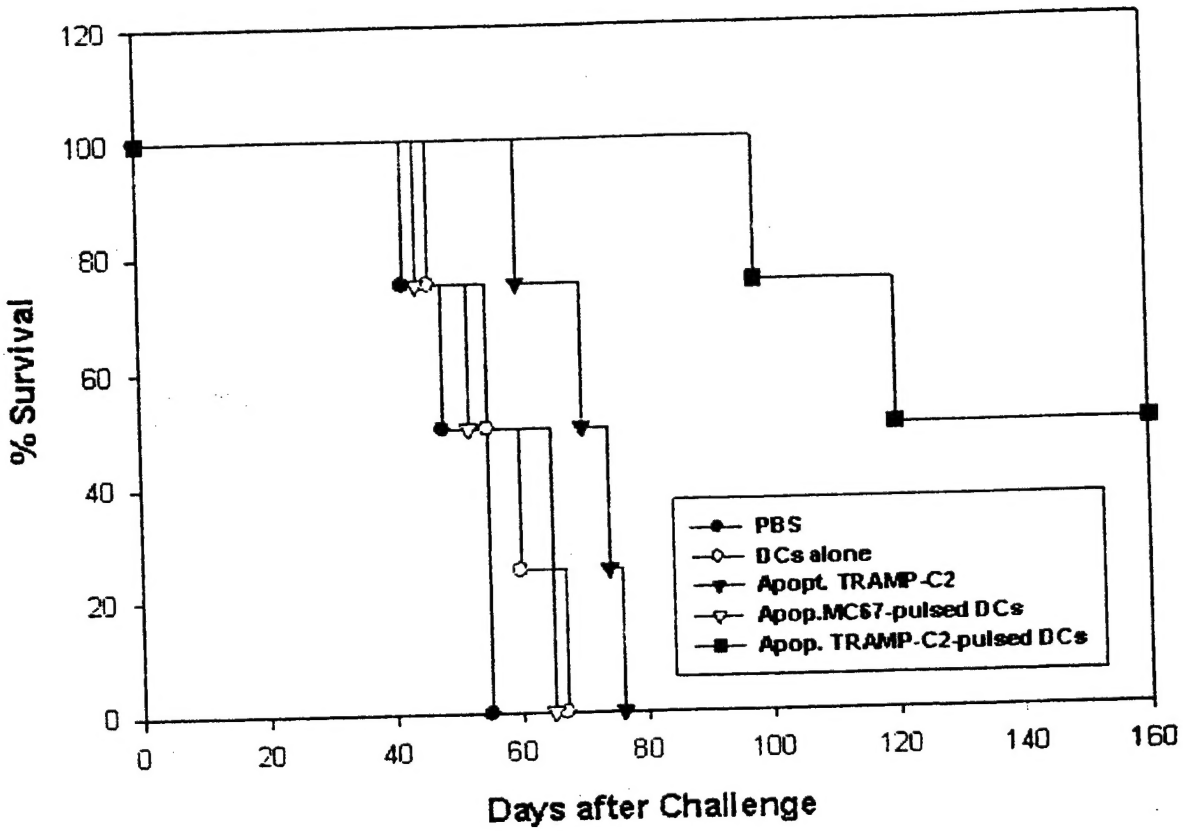

Fig. (3b) Survival of mice challenged with TRAMP C2 tumor cells following vaccination s.c. (day 0 and day 7) with apoptotic TRAMP-C2-pulsed DCs (1x10). As controls, additional groups of mice were vaccinated with unpulsed DCs, apoptotic TRAMP-C2 cells, DCs pulsed with an irrelevant apoptotic cell line MC57 or with PBS. All vaccinated mice were challenged 7 days after the last immunization with a lethal dose of 2x10 TRAMP-C2 cells by s.c. injection. Starting two weeks after tumor challenge, mice were inspected for palpable masses. Survival has been determined.

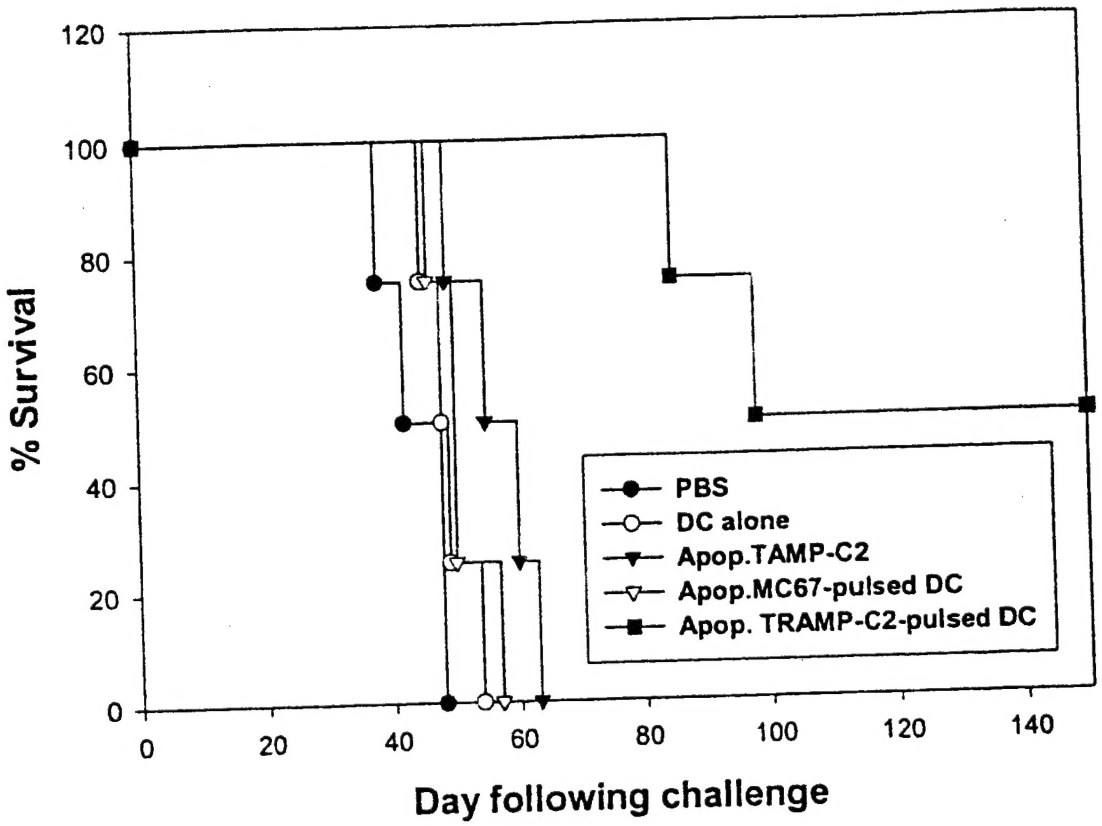

Fig.4: vaccination with apoptotic TRAMP-C2 cells-pulsed DCs increases long term survival of mices challenged with TRAMP-C2 tumor cells. B6 mice were challenged with 2 millions of TRAMP-C2 cells, s.c., in the left flanck (day0). Days 7and day 28 after challenge, B6 mice were vaccinated with 1 million od DCs pulsed with apoptotic TRAMP-C2 cells. Control groups received DCs alone, apoptotic TRAMP-c2 cells alone, apoptotic MC57 cells-pulsed DCs or PBS only.

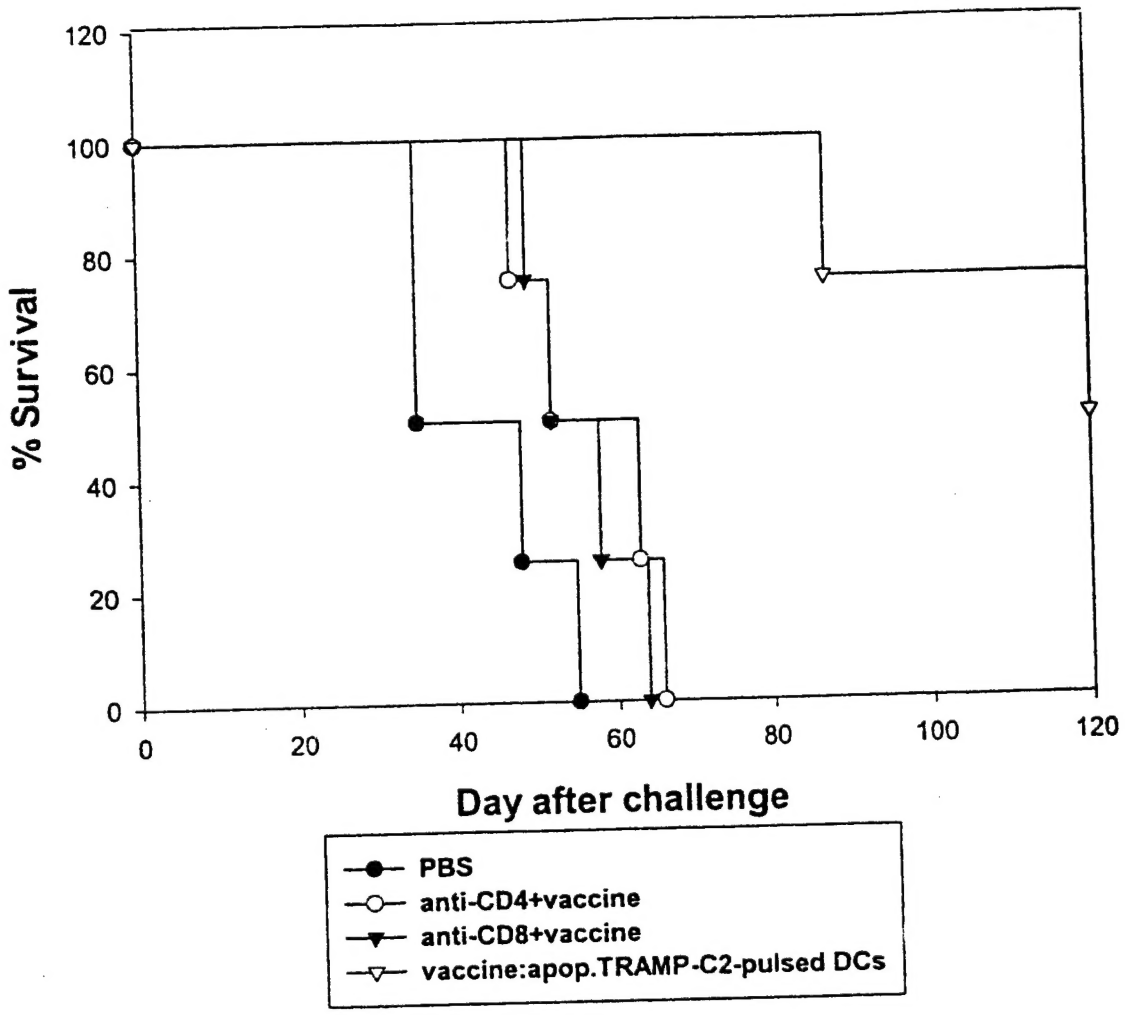

Fig.5: Both CD4+ and CD8+ T cells are involved in the protective mechanism B6 male mice were treated with anti-CD4+(GK 1.5) and anti-CD8+(53-3.8) monoclonal antibodies leading to selective depletion (<95%) of these T cells subsets.Mice were vaccinated s.c. in the right flank with 1 million of apoptotic TRAMP-C2 cells-pulsed DCs (day-14 and day -7) or as control with PBS. at day 0, 2 millions of TRAMP-C2 cells were injected s.c. in the left flank. Antibody treatments were administered day 0,3 and 7(100mg).